The Dissertation Committee for Hyewon Byun
certifies that this is the approved version of the following dissertation:

Function and Trafficking of the MMTV-encoded Rem Gene Product

Committee:

Jaquelin P. Dudley, Supervisor

Jon Huibregtse

David G. Johnson

Philip W. Tucker

Carla Van Den Berg

Function and Trafficking of the MMTV-encoded Rem Gene Product

by

Hyewon Byun, B. S.; M. S.

Dissertation

Presented to the Faculty of the Graduate School of

The University of Texas at Austin

in Partial Fulfillment

of the Requirements

for the Degree of

Doctor of Philosophy

The University of Texas at Austin

May 2011

To my family and friends

Acknowledgements

I really appreciate our Father for his great love. He has given me great opportunities to grow. Studying in the graduate program at UT is a turning point in my life.

I would like to express my gratitude to my advisor, Dr. Jaquelin Dudley, for providing me with the opportunity to study in her laboratory. Her dedication to science and her insightful guidance have always been a great inspiration to me. I would also like to extend my sincere thanks to the rest of my committee members; Dr. Jon Huibregtse, Dr. David Johnson, Dr. Phil Tucker, and Dr. Carla Van Den Berg for serving on my committee and for their constructive feedback and suggestions during my committee meetings.

I would like to acknowledge my colleagues in the Dudley Lab: Mary Lozano, Dr. Jenny Mertz, Dr. Sanchita Bhadra, Dr. Urmila Maitra, Rachel Lay, Almas Ali, Nimita Halani and Andrea Nash for their friendship and support on my project work. I would not have been able to accomplish the things described in this dissertation without all of them. A special thanks to Mary Lozano for helping me with efficient handling of all lab business and great patience with my English. I would also like to thank to all members of the Bose, Huibregtse, Payne, Sullivan and Tucker labs for sharing reagents, protocols and advice.

Finally, I could not have done this without the support of my family. I sincerely thank my parents, Colin, and the Gormley family for love, patience and encouragement. I also appreciate the friendship and support of all my friends here, my friends in Korea, and the UGAP folks. It is a great blessing for me to have everyone in my life.

Hyewon Byun

The University of Texas at Austin

May 2011

Function and Trafficking of the MMTV-encoded Rem Gene Product

Publication No._____

Hyewon Byun, Ph.D.

The University of Texas at Austin, 2011

Supervisor: Jaquelin P. Dudley

Mouse mammary tumor virus (MMTV), a member of the betaretrovirus family, primarily induces mammary carcinomas in mice. Like human immunodeficiency virus (HIV), MMTV is a complex retrovirus that encodes a viral regulatory protein, Rem. Rem is a 33 kDa glycosylated protein containing an unusually long ER signal peptide (SP). MMTV SP contains all of the functional motifs for the nuclear export of MMTV unspliced/genomic RNA. SP activity requires binding to MMTV RNA. To characterize the minimal Rem-responsive element (RmRE) that overlaps the 3' LTR, several deletion mutations were introduced in the MMTV-based reporter plasmid, pHM*Rluc*. Results from these mutants in transient transfections revealed a 476-nt RmRE at the junction of the envelope gene and the 3' LTR. RmRE function was not cell-type specific. The RmRE is predicted to have a complex secondary structure, similar to the Rev-responsive element (RRE) of HIV. Unlike the HIV RRE, the 3' LTR RmRE occurs in all MMTV mRNAs, and Rem does not increase the export of unspliced RNA of the pHM*Rluc* reporter vector. These results suggest that another RmRE near the 5'-end participates in

export of MMTV genomic RNA, whereas the RmRE overlapping the 3' LTR supports different Rem functions, such as translational regulation.

Recent research has shown that SP directs Rem translation to the ER where Rem is cleaved and released into the cytoplasm. Rem mutants with ER signal peptidase cleavage site mutations completely lost function, and mutant proteins were highly unstable and mislocalized. Dominant-negative AAA ATPase p97 and Derlin-1 proteins, which are involved in the ER-associated degradation (ERAD) pathway, inhibited Rem function. Therefore, Rem is a precursor protein that is processed by ER signal peptidases. Rem then manipulates the ERAD system to retrotranslocate SP to the cytoplasm prior to nuclear entry and MMTV RNA binding.

Unexpectedly, a commercial control shRNA expression vector, LK0.1, induced additional Rem, HIV-1 Rev and human T-cell leukemia virus type 1 Rex activity (called super-induction). Also, the LK0.1 vector increased protein expression levels of co-transfected genes, and the target of the shRNA was not critical. When the hairpin segment was deleted from LK0.1, the super-induction of Rem activity was greatly reduced. Deletion of *cis*-acting lentiviral segments also decreased protein expression levels. Although LK0.1 did not affect the levels of interferon-induced genes or eIF-2α phosphorylation, LK0.1 reduced the number of stress granules significantly. Therefore, LK0.1 may induce several cellular signaling pathways, leading to Rem super-induction.

This study characterizes the minimal RmRE overlapping the 3' MMTV LTR and reveals the unique processing of Rem and SP trafficking prior to nucleolar localization. Additional functions of MMTV Rem and other retroviruses may be discovered using studies of cellular events induced by LK0.1.

Table of Contents

List of Tables

List of Figures

1. INTRODUCTION

1.1. MOUSE MAMMARY TUMOR VIRUS (MMTV).

MMTV is a betaretrovirus in the Retroviridae family. As characterized by J.J. Bittner, MMTV is a milk-transmitted agent in mice responsible for a high incidence of breast cancer [21, 154]. MMTV primarily induces mammary carcinomas, but also causes T-cell lymphomas and other tumors at a lower frequencey [40, 144].

1.1.1 MMTV VIRION AND GENOME STRUCTURE.

Similar to other retroviruses, the mature MMTV virion is a spherical enveloped particle, usually about 100nm in diameter [26, 195]. The viral envelope is derived from a host plasma membrane by budding. The envelope contains the virally-encoded glycoproteins, surface protein (SU, gp52) and transmembrane (TM, gp36), which are linked by disulfide bonds. The viral matrix protein (MA) is located on the inner side of the envelope adjacent to the capsid. The capsid protein (CA), the major structural protein of MMTV, forms an icosahedral core that contains the viral RNA genome, which is a dimer, associated with the nucleocapsid (NC) protein. The virus encodes three enzymes, a protease (PR), an integrase (IN) and a reverse transcriptase (RT). Although the PR is located between the capsid and envelope, the IN and RT are located in the viral core. Cellular lysyl-tRNAs are localized in the viral core since they are required for the initiation of reverse transcription [27, 169].

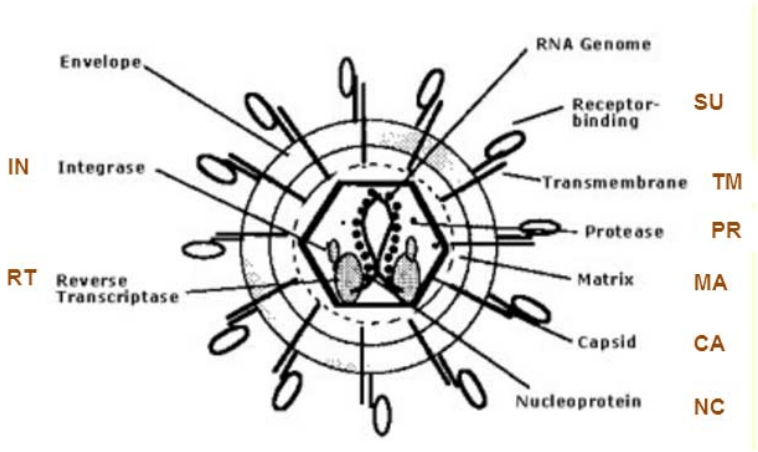

Figure 1.1: MMTV virion structure.

(http://www.stanford.edu/group/nolan/tutorials/ret_5_struct.html)

The MMTV genome is a single-stranded, positive-sense RNA of about 9 kb. Genomic RNA contains a methylguanosine cap structure at the 5'-end and is polyadenylated at the 3'-end [20, 186, 197]. Although the same short direct repeat (R) sequence of 15 bp is located at both ends, unique sequence regions of 120 bp at the 5' end (U5) and 1200 bp at the 3' end (U3) are found internal to the R region. After reverse transcription of the viral genome in infected cells, the double-stranded viral DNA (provirus) is synthesized to generate the long terminal repeat (LTR) of U3-R-U5 at both ends. The LTR contains a mammary gland enhancer (MGE), negative regulatory elements (NREs) and a hormone-response element (HRE), all of which enable tissue-specific transcription to provide optimal virus production [145, 180, 249]. The MMTV genome encodes at least 6 viral genes following the U5 unique region: *gag* (group specific antigen), *dut* (dUTPase), *pro* (protease), *pol* (reverse transcriptase and integrase), *env* (envelope), *rem* (regulator of expression of MMTV mRNAs) and *sag* (superantigen).

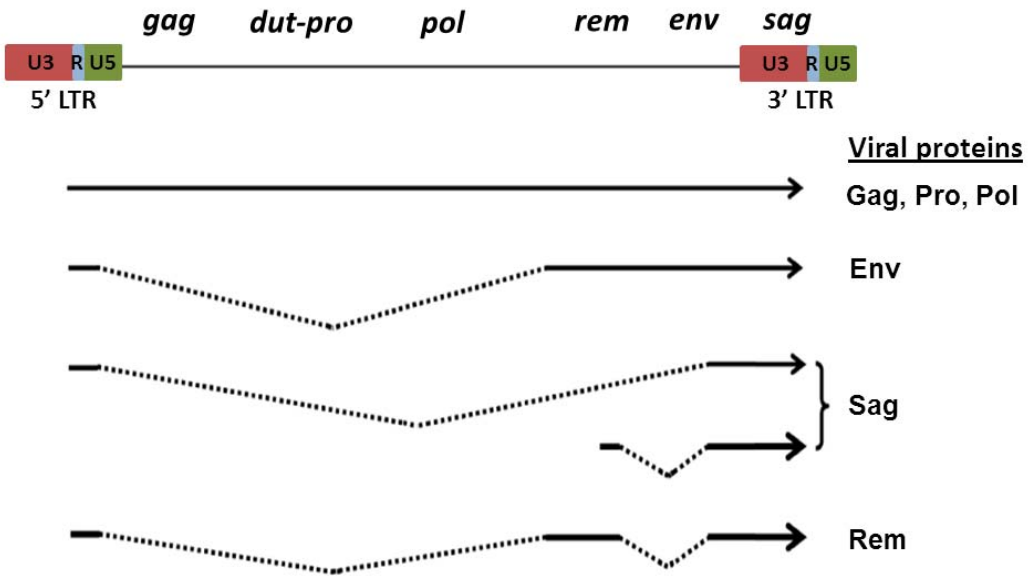

Figure 1.2: MMTV proviral genome and gene products.

Brown boxes represent viral LTRs. Solid and V-shaped dotted lines represent MMTV mRNAs and introns, respectively. Gag, Gag-Pro and Gag-Pro-Pol polyproteins are cleaved into functional viral proteins by viral protease. Adapted from Ross, S. [186].

At least five mRNAs are synthesized after integration of the MMTV provirus. MMTV DNA contains two primary promoters for transcription of viral mRNAs: the U3 promoter in the 5' LTR and an intragenic *env* promoter. From the U3 promoter in the 5' LTR, full-length unspliced MMTV RNA is transcribed. The full-length mRNA is translated into Gag, Pro, and Pol proteins. From a double ribosomal frameshift, three polyprotein precursors, Gag (Pr77), Gag-Pro (Pr110), and Gag-Pro-Pol (Pr160), are generated from the full-length mRNA. Gag is cleaved by the viral protease (PR, encoded by *pro*) to yield the MA protein (membrane-associated or matrix, p10), the CA protein (capsid, p27), and the NC protein (nucleocapsid, p14), as well as several proteins of

unknown function [82, 97, 196]. The Gag-Pro (Pr110) precursor is cleaved to yield the DU protein (dUTPase) and PR (protease). The dUTPase-encoding (*dut*) gene is found in non-primate complex retroviruses, such as equine infectious anemia virus (EIAV), but its role in virus infection or pathogenesis is not fully understood. The DU protein is a 30 kDa protein that degrades deoxyuridine triphosphate (dUTP) into deoxyuridine monophosphate (dUMP) and pyrophosphate. This protein prevents dUTP incorporation into viral DNA during replication and maintains cellular nucleotide pools. DU is believed to play an important role in retroviral replication in non-dividing cells [165, 186, 217]. RT (reverse transcriptase) and IN (integrase) are cleaved by PR from the Gag-Pro-Pol (Pr160) precursor, and both are involved in double-strand viral DNA production and integration into the host genome [186].

Another mRNA generated from the 5' LTR is the singly spliced *env* transcript encoding Env precursor protein (envelope glycoprotein). Env precursors are synthesized on the rough endoplasmic reticulum (rough ER) and processed into TM (transmembrane, gp36) and SU (surface, gp52) by host furin enzymes in the Golgi apparatus. Cellular protein trafficking delivers the SU/TM complex to the plasma membrane. Env proteins are assimilated into the viral envelope during virus budding from host cells. The SU contains the receptor binding site (RBS) for the specific host receptor, transferrin receptor 1 (TfR1), whereas the TM mediates envelope fusion with the cell membrane, a prerequisite for viral entry [186, 187].

MMTV encodes two additional genes from alternatively spliced mRNAs, Rem (regulator of export/expression of MMTV) and Sag (viral superantigen), which are required for efficient MMTV infection [186]. Rem is a 33 kDa protein encoded by a doubly spliced mRNA in the same reading frame as the *env* gene [142]. Rem is a human

immunodeficiency virus-1 (HIV-1) Rev-like protein that facilitates transport of unspliced MMTV mRNAs from the nucleus to the cytoplasm [95, 142]. Sag is a 36 kDa type II transmembrane protein, produced from two singly spliced mRNAs that are generated independently from the U3 promoter in the 5' LTR and the intragenic *env* promoter [33, 136]. The open reading frame of Sag is located in the 3' LTR. MMTV is one of the few retroviruses that utilizes an open reading frame within the U3 region. Sag protein is an immunostimulatory molecule that is critical for viral amplification in B cells, T cells and dendritic cells (DCs) [185, 186]. Sag is also important in the transmission of virus to mammary cells and dissemination of MMTV within the mammary gland [62, 186].

In addition to the canonical *gag*, *pol*, and *env* genes, MMTV additionally encodes the accessory and regulatory genes *dut, sag* and *rem.* Accessory genes (*dut* and *sag*) are believed to be dispensable for virus replication in tissue culture, whereas regulatory genes (*rem*) are required for efficient production of infectious virus. The translation of Rem as a viral RNA-export protein from a doubly spliced mRNA indicates that MMTV is the first example of a complex murine retrovirus.

1.1.2 MMTV INFECTION AND REPLICATION.

MMTV infection in mice primarily causes mammary adenocarcinomas following a long latency of 6 to 9 months. MMTV transmission is accomplished in two ways. Exogenous MMTV is transmitted through breast milk from infected mothers to newborn pups. Endogenous proviruses integrated in the host (mouse) genome are vertically transmitted through germline transmission following a Mendelian inheritance pattern. These endogenous proviruses are called *Mtv*s and more than 40 *Mtv*s have been identified in the common inbred mouse strains. Each strain contains an average of 2 to 8

endogenous *Mtv*s. Most *Mtv*s are replication-defective and thus do not produce infectious virion particles [115, 186]. However, it has been shown that *Mtv*s affect host susceptibility to exogeneous MMTV since an inbred mouse strain, *Mtv*-null, selected for the absence of endogenous proviruses, has been shown to be resistant to MMTV strains that cause breast cancer or T-cell lymphomas. This same strain also has displayed resistance to some bacterial pathogens, including *Vibrio cholerae* [17].

Infection of susceptible pups by ingestion of breast milk from infected female mice is the most common route for MMTV infection. Viral particles in ingested milk pass through the stomach and cross the intestinal epithelial layers through M cells. MMTV then infects dendritic cells (DCs) in the small intestine and Peyer's patches prior to infection of B and T lymphocytes [28, 62, 103]. Both the DCs and B cells are MHC class II-positive antigen-presenting cells that allow expression of MMTV-encoded Sag on the plasma membrane of infected cells.

Viral infection is initiated by the binding of the viral envelope SU protein with a specific cellular receptor, TfR1, on target cells [187]. MMTV then enters the cells via a late acidic endosomal compartment [186]. Reverse transcription from the viral RNA genome occurs in the cell cytoplasm to produce a DNA copy. Integration of the viral DNA into the host genome is presumed to occur during cell division, although the infection of dendritic cells suggests that the MMTV genome may allow integration in non-dividing cells.

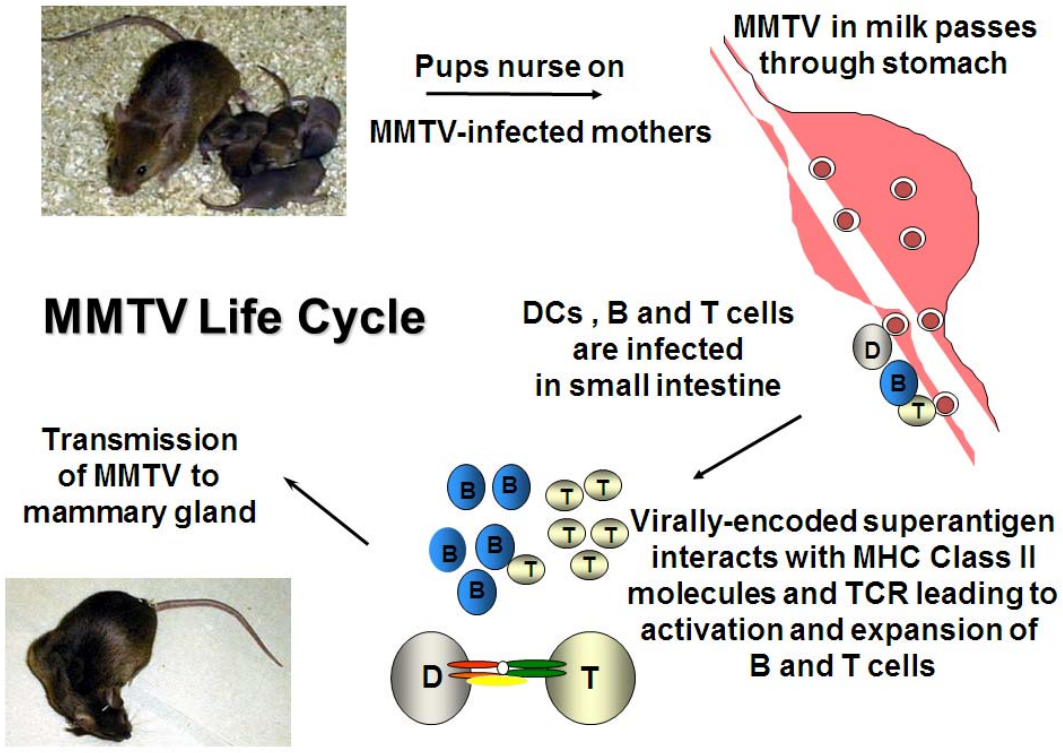

Figure 1.3: Life cycle of exogenous MMTV.

Exogenous MMTV is transmitted through breast milk of infected mothers. Viral particles in ingested milk pass through the stomach to infect immune cells in the small intestine. Infected dendritic cells (D) and B cells (B) present virally-encoded superantigen (Sag) on their surface in conjunction with MHC class II protein. This Sag-MHC complex is recognized by specific T-cell (T) subsets via T-cell receptor (TCR), leading to activation and expansion of B and T cells. Ultimately, the virus spreads to the mammary gland, where multiple proviral integrations lead to mammary carcinomas by insertional mutagenesis.

Infected DCs and B cells present MMTV Sag at the cell surface with major histocompatibility complex (MHC) class II proteins [33, 98, 113]. Sag-presenting cells interact with T cells expressing specific T-cell receptor (TCR) Vβ chains [233, 234]. The interaction of Sag with the TCR induces T-cell expansion and production of cytokines, leading to the amplification of additional DCs, B and T lymphocytes that can be infected by the virus. Infected lymphocytes spread the virus to the mammary gland, the ultimate target of MMTV [7, 62, 80]. In infected mammary epithelial cells, amplification of the virus is required for maximum virus production and induction of mammary carcinomas. MMTV is a non-acute tumorigenic retrovirus that does not encode a typical oncogene, although some reports have suggested that MMTV Env protein has transforming potential [106, 188]. Therefore, mammary tumors induced by MMTV are believed to be the result of integration near cellular proto-oncogenes, such as *Wnt1*. Since MMTV integration is not site-specific, many integration events are required in mammary epithelial cells. The increased viral production is necessary for MMTV tumorigenesis.

1.1.3 TISSUE SPECIFICITY OF MMTV.

MMTV replication is restricted in various cells [63, 90]. The highest level of viral replication occurs in alveolar epithelial cells of the mammary gland, whereas lower levels are detectable in lymphoid organs. One determinant of cell-specific targeting by MMTV is the availability of TfR1, a host surface receptor for MMTV. TfR1 is a type II glycoprotein that contains a single transmembrane domain and is the major receptor for iron uptake [187]. Although TfR1 is a ubiquitous receptor, higher expression levels of TfR1 have been reported in activated cells of the immune system and dividing mammary epithelial cells [24, 56, 200].

Regulation of MMTV transcription is a major determinant of tissue-specific viral expression. For example, the mammary gland enhancer (MGE) in the LTR acts primarily in mammary epithelial cells to upregulate transcription. The hormone responsive element (HRE) also is known to increase virus expression in mammary cells during pregnancy and lactation. Nevertheless, MMTV is not transcribed in many other cells that express glucocorticoid receptors [47]. A number of studies indicate that tissue-specificity of MMTV expression is due to negative regulation. At least two transcription factors, Cux1 and SATB1, have been shown to suppress MMTV transcription in non-mammary tissues [129, 249]. MMTV expression also is developmentally controlled in mammary tissues by the Cux1 protein. Low levels of transcription in the virgin mammary gland are correlated with reduced MMTV transcription. Cleavage of Cux1 during late pregnancy relieves MMTV transcription repression, allowing high levels of viral expression at a time when positive factors are available to increase virus production in milk [133].

1.2 RETROVIRAL EXPORT OF UNSPLICED RNA.

The nuclear transport of macromolecules is a highly regulated process. Many molecules can move only through nuclear pore complexes (NPC), channels that can expand from 10 nm to 25 nm [152]. Small molecules like water, ions and small proteins, whose size is less than 40 kDa, diffuse through the NPC, whereas bigger macromolecules, such as DNA, RNA, and proteins, need specific transport adaptor proteins to transverse the NPC [152, 207]. Major cellular mRNAs are transported by the Tip-associated protein (TAP)-p15 dependent pathway. Post-transcriptional modifications of cellular mRNAs occur in the nucleus, including capping of the 5' end, polyadenylation

of the 3'-end, and splicing [152, 153]. During splicing, the exon junction complex (EJC) binds to spliced mRNAs and some of its components, such as UAP56 and Aly/REF. Ultimately, the TAP-p15 heterodimer export receptor binds to REF in the EJC. Binding facilitates the transport of the RNA-protein complex and, once the transport is completed, the export factors are dissociated from mRNA. The EJC binds only to fully spliced mRNAs, facilitating their export [152, 207, 215]. On the other hand, rRNA, U snRNAs and some specific mRNAs, such as those encoding c-Fos and Cyclin D1, are transported from the nucleus by the chromosome region maintenance 1 protein (Crm1)-dependent pathway [152, 207]. Crm1 binds to adaptor proteins that have a nuclear export signal (NES) [92, 152, 207]. Intron-containing mRNAs are retained in the nucleus and degraded. Preventing unspliced mRNA from nuclear export is one role of the cellular quality control system to produce only functional mRNAs [36, 208]. A preliminary round of translation in the cytosol is believed to remove the EJC, but retention of the EJC by a premature stop codon will result in mRNA degradation.

Many viruses, including retroviruses that have a nuclear phase in their replication cycle, need to overcome or adapt to the regulation of nuclear export by the host cell. Retroviruses have to deliver their genomic RNA, an unspliced RNA form, to the cytoplasm where the packaging of retroviruses takes place. Retroviruses often utilize unspliced mRNAs to generate more viral proteins. Two main strategies have been developed by retroviruses for nuclear export of viral unspliced RNAs. Most simple retroviruses, such as Mason-Pfizer Monkey Virus (MPMV), have a *cis*-acting RNA structure called the constitutive transport element (CTE) that can be recognized by the Tap-p15 export proteins [36, 68, 224]. On the other hand, complex retroviruses, such as

HIV-1 and MMTV, encode *trans*-acting viral export proteins to facilitate nuclear export of unspliced viral mRNAs [85, 134, 142].

1.2.1 CONSTITUTIVE TRANSPORT ELEMENT (CTE) OF SIMPLE RETROVIRUSES.

The type D betaretrovirus, MPMV, contains a constitutive transport element (CTE) that allows the export of intron-containing viral mRNAs [50, 51]. The CTE is required for MPMV replication, recruiting cellular export proteins, such as Tap and RNA helicase A (RHA) [213, 214]. The human Tap protein is a 619 amino-acid protein containing two nuclear localization signals (NLSs), a nuclear export signal (NES) [102], and an RNA-binding domain that binds to the CTE. The p15 protein, also known as nuclear export family 1 (NXF1), is a cofactor of Tap. The Tap-p15 heterodimer binds to the nuclear pore and facilitates mRNA export [23, 55, 105]. Nuclear export mediated by the CTE is Crm1-independent since it is insensitive to leptomycin B, a Crm1 inhibitor [102]. In addition to nuclear export, Tap is known to enhance the translation of CTE-containing RNAs [100].

Other simple retroviruses, such as the alpharetrovirus avian sarcoma/leukemia virus (ASV/ALV) also contain CTEs. Although the ASV/ALV CTE lacks sequence homology with the MPMV CTE, both CTEs have a similar secondary RNA structure, which is an extended stem-loop structure [236]. Rous sarcoma virus (RSV), an ASV, contains direct repeats (DR), which flank the *src* oncogene near the 3'-end of the viral genome [159]. The DR mediates the nuclear export of unspliced RNAs, independent of the Crm1 pathway. However, unlike CTE-mediated RNA export, Tap does not bind to the DR directly. Instead, Tap affects DR-mediated nuclear export by binding to the DEAD box helicase Dbp5, which directly binds to the RSV DR [118, 164]. Murine

leukemia virus (MuLV), a gammaretrovirus, is known to facilitate the nuclear export of its intron-containing full-length RNA through the *Psi* packaging signal. MuLV does not contain a CTE or DR-like *cis*-acting structure. Therefore, MuLV has an alternative way for transport of its unspliced RNA, using the highly structured packaging signal instead. This suggests that the nuclear export and the packaging processes may be related to each other [205].

1.2.2 VIRAL EXPORT PROTEINS OF COMPLEX RETROVIRUSES.

To adapt to the highly regulated nuclear export of host cells, complex retroviruses encode viral RNA export proteins that bind unspliced viral mRNA for cytoplasmic export. Complex retroviruses also contain a *cis*-acting RNA structure within their genomes that is recognized by viral RNA export proteins.

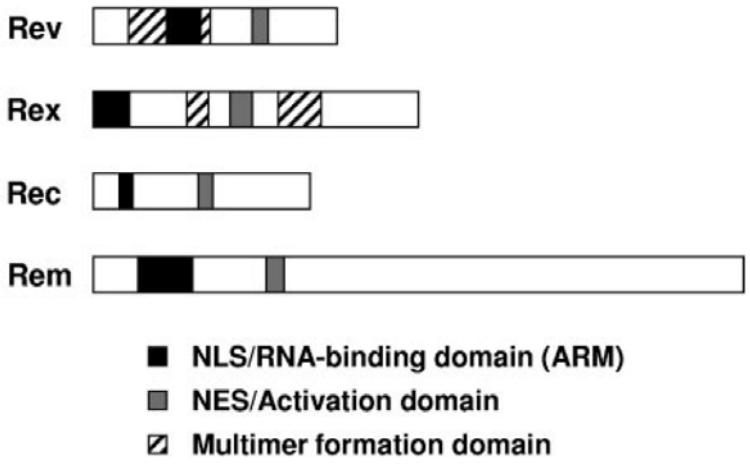

Figure 1.4: Domain structure of Rev-like proteins. (Taken from Mertz *et al*. [142].)

1.2.2.1 HIV-1 Rev.

HIV-1 encodes at least nine genes, including canonical genes encoding structural proteins, such as *gag*, *pol*, and *env*. In addition, multiple accessory and regulatory factors are encoded by mRNAs derived by alternative splicing. HIV-1 produces viral proteins from full-length unspliced RNA (Gag and Pol), singly spliced intron-containing RNAs (Env, Vif, Vpr, and Vpu), and fully spliced RNA (Rev, Nef, Tat). In the early stages of HIV-1 infection, only fully spliced mRNA can exit through nuclear pores because of nuclear export regulation by the host. Thus, only the regulatory and accessory proteins Rev, Tat and Nef are made early in the infectious cycle [36, 174].

Rev is a 116 amino-acid protein. Rev contains an NLS, an NES and a multimerization domain [231]. The NLS overlaps an arginine-rich RNA binding domain. Rev is known to be phosphorylated by casein kinase-2 (CK-2), a serine/threonine kinase [135]. The Rev NES domain binds to the cellular export factor Crm1. Crm1 is sufficient for export and translation of the late HIV-1 mRNAs, even following replacement of the RNA-binding site of Rev with a heterologous RNA-binding domain [243]. The Rev-binding site on the HIV-1 genome is known as the Rev response element (RRE). The minimal RRE of 250 nucleotides is located in the intron of the envelope gene. The predicted RRE structure is a complex, folded RNA structure containing multiple stem-loops [39, 71, 134, 209].

The human Crm1 protein, a cellular nuclear export factor, binds various cellular proteins as well as Rev to transport RNA to the cytoplasm. Crm1 functions as a nuclear export factor in conjunction with the small GTPase protein, Ran. In the nucleus, Crm1 binds its cargo in the presence of the GTP-bound Ran GTPase. Crm1 interacts with the nuclear pore complex, which is critical for Crm1-mediated nuclear export of RNA. After nuclear export, Ran hydrolyzes bound GTP to GDP, which causes a conformational

change and cargo release in the cytoplasm [36, 152]. Crm1 also binds to the RNA helicase DDX3, a cellular ATP-dependent DEAD box protein that shuttles between the nucleus and cytoplasm. Rev-RRE mediated nuclear export of unspliced HIV-1 mRNAs is suppressed following DDX3 knockdown, suggesting DDX3 is involved in HIV-1 RNA export [242].

Nuclear import of Rev back to the nucleus is mediated by importin-β. Importin-β binds to Rev via the Rev NLS and then directs it to the nucleus. Ran-GDP also binds to importin-β of this complex in the cytoplasm. When the Rev complex moves to the nucleus, Ran-GDP is converted to Ran-GTP, resulting in dissociation of Rev from importin-β. B23, aka nucleophosmin, interacts with Rev during nuclear import [54, 209]. B23 is a multifunctional phosphoprotein located predominantly in the nucleolus, but also shuttles between the nucleus and the cytoplasm [22, 54].

1.2.2.2 Human T-cell leukemia virus-1 (HTLV-1) Rex.

HTLV-1, a deltaretrovirus, causes adult T-cell leukemia and HTLV-1-associated myelopathy [10, 59, 163]. HTLV-1 encodes multiple accessory and regulatory proteins, including Rex in the 3' region of the genome [10, 57]. Rex is a 189 amino acid (27 kDa) phosphoprotein, containing the basic arginine-rich RNA-binding motif (ARM) that overlaps with the NLS, a leucine-rich NES, and multimerization domains [1, 76, 84]. Rex binds to the *cis*-acting viral response element, the RxRE, using the ARM domain. A 255-nucleotide RxRE is located in the U3/R region of the 3' LTR and contains a complex stem-loop structure. The RxRE is present in all viral mRNAs [2, 76, 219].

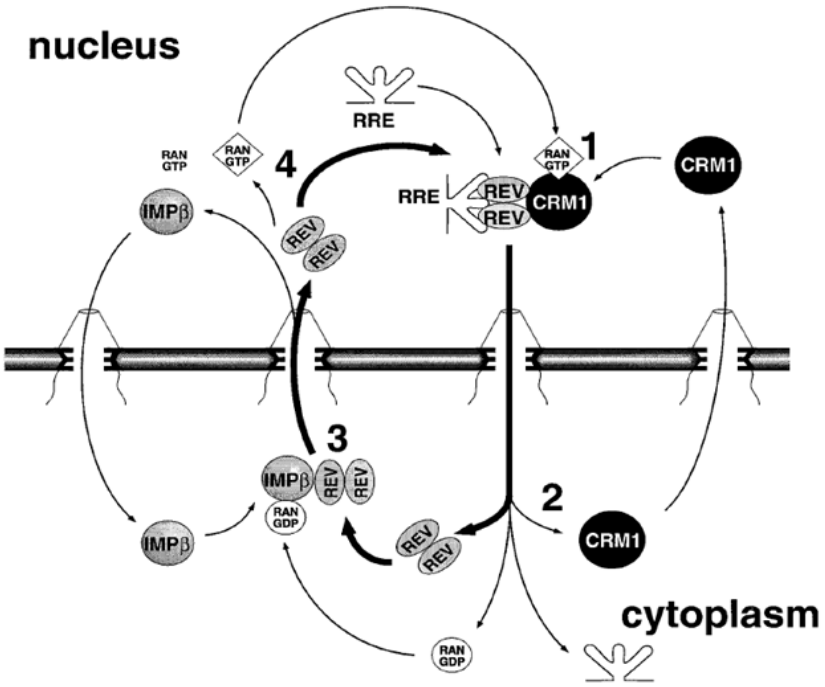

Figure 1.5: Viral RNA export by HIV Rev.

(1) Rev binds to viral intron-containing mRNAs and Crm1-Ran-GTP. (2) After nuclear export of the Rev-Crm1 complex, hydrolysis of GTP to GDP leads to dissociation of the Rev-Crm1 complex. (3) Dissociated Rev binds to importin-β-Ran-GDP and is imported into the nucleus. (4) Conversion of Ran-GDP to Ran-GTP causes dissociation of a Rev-importin-β complex. Modified from Hope, T. J. [85].

Like Rev, Rex interacts with Crm1 via the NES, which allows Rex to export unspliced viral mRNAs to the cytoplasm. Although Rex also contains two multimerization domains that are separated by an NES, multimerization of Rex is not required for binding to the RxRE. A Rex mutant that is deficient for multimerization still can bind to the RxRE and performs Rex-mediated nuclear export of unspliced RNA [76]. Nevertheless, the multimerization-deficient mutant does not induce *trans*-activation in assays using a Rex-responsive reporter vector [76, 77].

Although Rex and Rev do not share significant sequence homologies, Rex binds the HIV RRE, and Rex can substitute for Rev during expression of HIV Gag proteins [96, 77]. Rev does not bind to the RxRE, but a hybrid protein containing the ARM of Rex and the NES of Rev is active on the RxRE [10, 84]. Therefore, Rev and Rex may have identical modes of action and biological function [52]. Despite their similarities, Rex multimerization is not required for RNA export, whereas Rev has a high tendency to multimerize and a multimerization-deficient Rev mutant shows cytoplasmic, rather than nucleolar localization. Wild-type Rex is localized predominantly in the cytoplasm. These results suggest that Rex and Rev have different requirements for their function [77]. In addition, Rex inhibits splicing of intron-containing sequences of HTLV-1 and pre-mRNA stabilization, indicating that Rex is a multifunctional protein [65, 96].

1.2.2.3. MMTV Rem.

Rem is a 301 amino-acid protein that functions as a nuclear export protein similar to Rev and Rex [95, 142]. In contrast to Rev and Rex, Rem consists of a 98 amino-acid N-terminal signal peptide (SP) and an extended C-terminus of 203 amino acids. Rem is generated from a doubly spliced mRNA that overlaps the MMTV *env* gene. Since both

rem and *env* genes use the same reading frame to produce their mRNAs, both Rem and Env proteins contain the same SP for targeting to the ER. Rem and Env-derived SP is unusually long since the typical ER signal sequence is 20 to 30 amino acids [74]. The C-terminus of Rem contains the N-terminal part of the SU and the C-terminal part of the TM. Although the function of the C-terminus is not yet known, the SP contains many functional elements, such as a nuclear localization signal (NLS), a nucleolar localization signal (NoLS), an arginine-rich motif (ARM) and a nuclear export signal (NES), which are necessary for nuclear export function. Like Rev and Rex, Rem uses the cellular factor Crm1 for nuclear export of unspliced RNA [95, 142].

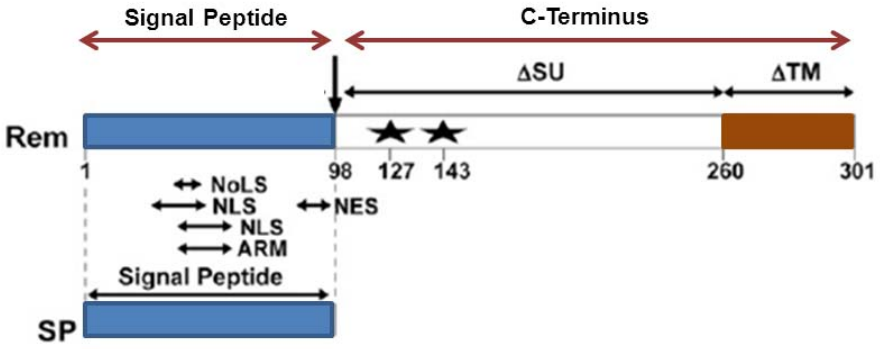

Figure 1.6: Diagram of Rem and signal peptide (SP).

The Rem C-terminus is a fusion between internally deleted versions of the envelope surface (SU) and transmembrane (TM) proteins. Glycosylation sites are indicated by stars. Adapted from Byun, *et al*. [29].

Mertz *et al*. have established that the Rem response element (RmRE) overlaps the junction of the *env* gene and the 3' LTR [142]. A pHM*Rluc* reporter vector was developed to measure Rem activity. The vector contains a CMV promoter upstream of the *Renilla* luciferase gene, followed by a portion of the *env* gene and the 3' MMTV LTR. This reporter plasmid was designed to measure Rem-specific activity by inserting the luciferase gene between the splice donor site and the splice acceptor site within the *env* gene. When the 3'-end of the *env* gene and the 3' LTR were removed from the pHM*Rluc* vector, Rem responsiveness was lost. Nevertheless, when a 496-nucleotide region overlapping the junction of the *env* gene and the 3' LTR was re-inserted, the vector became fully responsive to Rem. Therefore, these results indicate that the MMTV RmRE is located within the 496-nucleotide region [140, 142].

Rem is required for the nuclear export of viral unspliced mRNAs since mutations in Rem significantly decrease the amount of *gag-pol* mRNA in the cytoplasm as well as Gag protein production [95, 142]. Surprisingly, RNA fractionation experiments using the pHM*Rluc* reporter vector revealed that Rem did not affect the nuclear export of the *Renilla* gene transcripts. These data suggest that Rem may also have additional post-export activities, possibly an enhancement of protein expression through the regulation of translation [141]. Rev also has been shown to have post-export functions that may involve targeting of Gag to the plasma membrane [99].

Unlike Rev and Rex, Rem should target Rem translation to the ER followed by cleavage into SP and the C-terminus [48, 142]. Dultz *et al*. have reported that the generation of SP and the Rem C-terminus was dependent on the presence of an ER-derived membrane using *in vitro* transcription and translation of *rem* cDNA. The release of SP from the membrane was not affected by $(Z\text{-}LL)_2$-ketone, an inhibitor of signal

peptide peptidase (SPP). SPP is an ER intramembrane protease that cleaves the internal signal sequences of hepatitis C virus polyprotein [91]. SP contains all functional motifs for nuclear export function. SP alone can induce the same level of activity as the full length Rem, indicating that reporter function requires only the Rev-like portion of Rem [29, 142]. Both green fluorescent protein (GFP)-tagged full length Rem and SP showed nucleolar localization [142]. Therefore, SP seems to utilize a unique trafficking system in the cells since Rem is processed in the ER, yet Rem/SP functions in the nucleus. The function of the C-terminus is not yet fully understood, although the C-terminus appears to regulate SP activity in the pHM*Rluc* reporter assay. The C-terminus of Rem is known to be glycosylated at two sites [48]. Since Rem does not contain the ER retention signal, the C-terminus may be transported to the cell membrane or secreted into the extracellular environment.

1.2.2.4 Other Rev-like proteins.

Like the endogenous *Mtv*s found in mice, the human genome contains multiple copies of endogenous retroviral sequences. These retroviral sequences are collectively called human endogenous retrovirus Ks (HERV-Ks) and account for ~8% of human cellular DNA [107, 116, 161]. Endogenous proviruses, which represent the integrated form of retroviral DNA, were acquired by germ-line infection with exogenous retroviruses. HERV-K genomes are approximately 9.2 to 9.5 kb and are found in numbers up to 50 copies per haploid human genome. HERV-K sequences are homologous to MMTV proviruses [11, 161, 162]. The majority have multiple inactivating mutations, but they retain potentially functional viral open reading frames (ORFs) encoding Gag, Pro, Pol and Env as well as viral LTRs.

HERV-K generates a 105 amino-acid Rev-like protein, cORF or Rec, from the *env* gene by alternative splicing [132, 237]. The *rec* mRNA overlaps with the *env* gene in a different reading frame. Rec has Rev-like motifs including an arginine-rich NLS and a leucine-rich NES. Magin *et al*. have shown that Rec enhances stabilization and export of incompletely spliced viral mRNA, which is Crm1-dependent [132]. By indirect immunofluorescent microscopy, Rec was observed to be localized mainly in the cytoplasm and moderately in the nucleolus. Treatment of cells with Crm1 inhibitors led to the accumulation of Rec in the nucleoli, suggesting that the Rec NES is dominant over the NLS [237]. Rec recognizes a response element (RcRE) in the U3R region (nt 8720 to 9148) of the 3' LTR. The RcRE is predicted to have a stem-loop structure that is similar to the HTLV Rex-binding domain, RxRE [132]. Yang *et al*. have shown that HIV Rev also recognizes and activates the RcRE-containing reporter vector. These results suggest the possibility that HIV infection might induce HERV-K gene expression in humans [237].

Recently, Hofacre *et al*. have shown that Jaagsiekte sheep retrovirus (JSRV), a betaretrovirus, also encodes a Rev-like *trans*-acting factor for viral nuclear export of unspliced RNA, Rej. Rej is required for the Gag expression from the unspliced viral RNA and is encoded within ca.100 amino acids at the N-terminus of the *env* gene [83]. This region includes the putative signal sequence for Env, which is sufficient for Rej activity [31]. Nevertheless, the active form of Rej has not been determined [83].

The Env SP and gene products from the isolated doubly spliced *env* mRNAs show similar Rej activity on Gag expression. These products of doubly spliced JSRV mRNAs have some, but not all, of the motifs found in the Env SP. Rej is localized in the nucleoli exclusively and contains putative functional domains such as an NLS, NoLS, and basic

residues. Interestingly, unlike other Rev-like proteins, Rej does not facilitate nuclear export of unspliced viral RNA in many cell lines. Rej enhances translation of Gag-Pol [31, 83, 155]. A *cis*-acting element required for Rej activity, a Rej response element (RejRE), is located at the 3' end of the JSRV *env* gene [31, 155]. The RejRE has been shown to relocalize Rej to the cytoplasm and is required for both synthesis of Gag protein and accumulation of unspliced viral RNA in the cytoplasm. Since relocalization of Rej by the RejRE is observed in cells in which Rej does not affect export of unspliced RNA, the association of Rej and RejRE may be necessary for translation of unspliced viral mRNA. Nitta *et al*. suggested that JSRV may utilize a CTE and cellular proteins for export of unspliced viral RNA [155]. The cytoplasmic accumulation of JSRV unspliced RNA is known to be dependent on Crm1 [31, 155]. Because CTE-mediated export is dependent on Tap, the mechanism of Rej function on unspliced RNA remains elusive.

1.3 ENDOPLASMIC RETICULUM-ASSOCIATED PROTEIN DEGRADATION (ERAD).

In eukaryotic cells, about one-third of the cellular proteins are either secretory or membrane proteins [60, 116]. The endoplasmic reticulum (ER) is a cellular organelle located in the cytoplasm, but contains membranes contiguous with the nuclear envelope. Secretory and membrane proteins enter the ER co-translationally for proper folding and post-translational modifications, such as glycosylation [87, 222]. Properly folded proteins in the ER are transferred to the Golgi apparatus for further modification and eventually are relocated to the cell membrane or they are secreted into the extracellular space [72]. Misfolded, defective proteins are identified and subjected to degradation in the

proteasome located in the cytoplasm by the ER-associated degradation (ERAD) pathway [138, 151, 222].

1.3.1 PROTEIN TARGETING TO THE ER.

Secretory and membrane proteins contain a signal sequence to direct translation to the ER. The typical ER signal sequence is 20 to 30 amino acids long and located at the N-terminus of nascent proteins [74]. The size and amino acid composition vary among different ER signal sequences, but they all contain a hydrophobic core region composed of 9 to 12 large hydrophobic residues in a cluster, a flanking basic residue, and a slightly polar region [44, 74, 223]. Once the ER signal sequence of nascent peptides of the secretory and membrane proteins emerges from the ribosome, a signal recognition particle (SRP) binds to the ribosome nascent chain complex (RNC). SRP is a ribonucleoprotein complex that recognizes and binds a hydrophobic region of the ER signal sequence. This binding interaction slows down further protein synthesis. The newly bound RNC-SRP complex then binds to the membrane-bound SRP receptor complex (SR). After docking of the RNC-portion of the complex with the translocon, SRP-SR is dissociated from the RNC. Finally, the SRP and SR are separated from each other. The SRP cycle is regulated by guanosine triphosphatase (GTPase) activity in both the SRP and SR [44, 66].

1.3.2 PROTEIN FOLDING IN THE ER.

Proper folding of a protein is as crucial for protein function as correct translation [72]. Many modifying enzymes and protein chaperones reside in the ER to monitor and facilitate the folding of newly synthesized secretory and membrane proteins. Once newly

synthesized proteins emerge into the ER lumen through the translocon, facilitated by the Sec61αβγ complex from ER-bound ribosomes, the proteins encounter modifying enzymes, including oligosaccharyltrasferase, protein oxidoreductases and chaperones [8, 72, 222]. Oligosaccharyltransferase, a glycosylating enzyme, attaches glycans to nitrogens of asparagine side chains of target proteins. In general, glycosylation facilitates further protein folding and leaves the proteins more hydrophilic in nature [8, 72] . Protein disulfide isomerase (PDI) assists many secretory proteins in forming thioester bonds, intra- and interchain disulfide bonds between cysteines. Peptidyl-prolyl *cis-trans* isomerase (PPI) assists in isomerization of peptidyl-prolyl bonds. These enzymatic folding processes result in structural maturation of proteins [8, 72, 87]. Chaperones protect unfolded proteins from aggregation and facilitate proper protein folding. The ER lumen provides a more oxidizing environment than the cytosol, which further contributes to secretory protein stability [87, 93, 222]. A high concentration of calcium ions in the ER is required for folding of some proteins, such as the low density lipoprotein (LDL) receptor protein [166].

Although many folding enzymes and chaperones support the correct folding of proteins in the ER, the folding process is nonetheless highly error-prone and sensitive to environmental stress. Therefore, a significant portion of newly synthesized proteins remain misfolded. To allow transfer to the Golgi apparatus of only properly folded proteins, the ER maintains a protein quality control system (PQC) or ER quality control (ERQC) mechanism to monitor and assist in the complete folding of immature proteins. Retaining proteins that have failed to fold properly for a certain time induces stress in the ER. Therefore, ERQC is coupled to ERAD to remove aberrant proteins [8, 73]. The ER

contains ubiquitination enzymes, which tag proteins destined for degradation to be directed by ERAD to the cytosolic 26S proteasome [73, 81, 222].

1.3.3 MAJOR ER QUALITY CONTROL (ERQC).

1.3.3.1 Classical Chaperones.

Various chaperone proteins reside in the ER in high concentrations. Generally, chaperones prevent aggregation of native polypeptides and assist in protein folding [72]. Chaperones are key components of ERQC. Several families of chaperones are involved in protein folding in the ER. These families include: the 40 kDa heat shock proteins (BiP cofactors; ERdj1-5), the 70 kDa heat shock proteins (GRP78/Bip), the 90 kDa heat shock proteins (GRP94), the 100 kDa heat shock proteins (Torsin A), and GrpE-like proteins (BAP/Sil1 and GRP170). These proteins are not induced by elevated temperatures, like the Hsp families in the cytoplasm, but by ER overload stress, glucose deprivation or other environmental stresses [72, 119, 203].

BiP, also known as GRP78, is a master regulator located in the ER lumen. This protein prevents aggregation of unfolded or misfolded proteins by binding to the hydrophobic regions of target proteins with relatively low affinity (1-100 mM) [72]. BiP localizes near translocons and facilitates translocation of newly synthesized proteins. It is also important in ER calcium homeostasis and in the ERAD pathway [123, 137]. BiP functions via its ATPase activity and its affinity for immature proteins is regulated by binding either ADP or ATP. ADP-bound BiP binds to substrate proteins with high affinity, whereas ATP-bound BiP releases them. ERdj1-5 cofactors, members of the Hsp40 family, are known to deliver unfolded substrates to BiP and assist in ATP hydrolysis by BiP. Other BiP regulatory chaperones in the GrpE-like family act as

nucleotide exchange factors that facilitate the exchange of ADP for ATP, inducing low affinity binding by BiP, resulting in the release of protein substrates [72, 222]. Changes in the level of cellular BiP serve as a marker for ER stress since an increase in ER load either by cellular differentiation or by accumulation of aberrant proteins increases BiP levels.

GRP94 is the most abundant chaperone protein in the ER [72]. Unlike BiP, it binds substrate proteins selectively; therefore, not all substrate proteins are dependent on GRP94. This chaperone sequentially binds to some substrates, the "advanced folding intermediates", such as immunoglobulin heavy chains, integrin, and Toll-like receptors, after release from BiP [72, 139, 177]. GRP94 is crucial for the folding of insulin-like growth factor I and II. GRP94 also has ATPase activity, but it is not clear how ATP hydrolysis is involved in GRP94 binding to substrates [41, 94, 206]. This chaperone binds OS-9, which is a participant in the ERAD pathway [34].

1.3.3.2 Calnexin/calreticulin cycle for glycoprotein folding.

Calnexin and calreticulin are both ER-resident chaperones and lectins, which are carbohydrate binding proteins [72, 73, 87]. Calnexin is a type I membrane protein, whereas calreticulin is a soluble protein. Both proteins assist folding of glycosylated proteins [72]. Most nascent proteins entering into the ER lumen co-translationally are glycosylated on asparagines of the sequence, Asn-X-Thr/Ser (X=not Pro). Glycosylation is initiated by the oligosaccharide transferase, attaching $Glc_3Man_9GlcNAc_2$ (Glc: glucose, Man: mannose, GlcNAc: N-acetylglucosamine) oligosaccharides. Immediately following attachment, glucosidase I and II quickly remove the two outer glucoses in a sequential action, resulting in a monoglucosylated side-chain ($Glc_1Man_9GlcNAc_2$) recognized by

calnexin and/or calreticulin. Binding by calnexin and/or calreticulin facilitates folding of glycosylated proteins [73, 87]. ERp57, a glycoprotein-dedicated oxidoreductase, binds to substrate proteins associated with calnexin and calreticulin to assist in the folding process [74, 78]. When the third glucose is removed by glycosylase II, the proteins are dissociated from the complex. Properly folded proteins at this stage are transported to the Golgi apparatus. Proteins that remain misfolded are re-glycosylated by the folding sensor, UDP-glucose:glycoprotein glycosyl transferase (UGGT) and rebound to calnexin and/or calreticulin for re-folding [72, 222].

1.3.3.3 Protein disulfide isomerase (PDI) family disulfide bond formation.

The formation of disulfide bonds is crucial for the stability of tertiary structure and protein maturation [8, 72]. The ER maintains an oxidative environment that is favorable for formation of disulfide bonds by members of the PDI family. These chaperones catalyze the formation of disulfide bonds by an oxidation reaction with their CXXC motifs in a thioredoxin-like domain. The PDI family also isomerizes the disulfide bonds, leading to stabilization of the correctly folded substrate proteins [72]. Additionally, PDI inhibits misfolded proteins from aggregation while protecting misfolded proteins that do not contain disulfide bonds [30]. The CXXC motif is not involved in the chaperone-like activity of PDI [176]. Many PDI family proteins localize to the ER, and different members have varying numbers of thioredoxin-like domains. For example, although PDI has two motifs, ERdj5 has four motifs [72]. ERdj5 is known to have reductase activity and binds to BiP and other ERAD factors [38, 88].

1.3.4 UNFOLDED PROTEIN RESPONSE (UPR)

Although multiple chaperones and folding enzymes of ERQC participate in the folding of nascent proteins in the ER, the capacity to successfully enable folding or posttranslational modification can be overwhelmed when cells are undergoing normal development and differentiation [112]. Conditions, such as accumulation of mutant proteins that fold improperly in the ER or viral infection, can induce ER stress [64, 112, 199]. To relieve ER stress, cells initiate an unfolded protein response (UPR). The UPR increases the expression of chaperones and folding/modifying enzymes and cellular factors involved in the ERAD pathway by activation of a signaling cascade and specific transcription factors. This signaling cascade also inhibits translation so that fewer nascent proteins are synthesized and introduced into the ER [64, 112, 199].

The UPR is activated by three sensor proteins for ER stress: inositol-requiring enzyme 1 (IRE1), double-stranded RNA-activated protein kinases, e.g., ER kinase (PERK), and activating transcription factor 6 (ATF6). All are transmembrane proteins whose ER luminal domains function as sensors of ER stress. The ER luminal domains of all three sensor proteins contain BiP-interacting regions. Each sensor protein remains inactive when bound by BiP in the unstressed state. However, if BiP dissociates from these proteins due to its chaperone activity in preventing aggregation of unfolded proteins in the ER, then IRE1, PERK and ATF6 are activated.

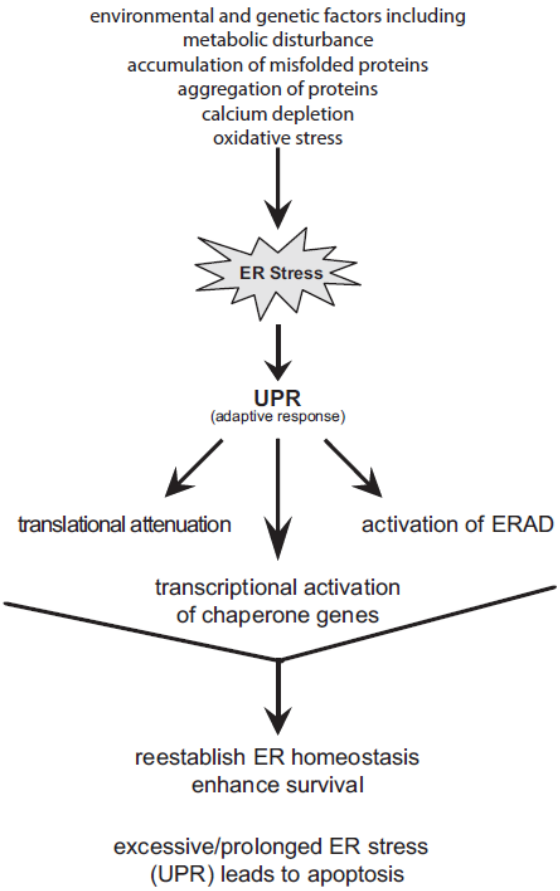

Figure 1.7: Unfolded protein response (UPR) induced by ER stress. (Taken from Groenendyk, J. *et al*. [64]).

Both IRE1 and PERK are type I transmembrane proteins. Both contain BiP-binding and oligomerization domains in the ER luminal region and kinase domains in the cytoplasmic region. The cytoplasmic domain of IRE1 also contains an RNase domain at the C-terminus that is homologous to RNase L [146, 199]. Under normal ER conditions, BiP binds to the luminal domain, which inhibits the oligomerization of IRE1 or PERK. Dissociation of BiP due to ER stress allows IRE1 to dimerize, leading to activation by *trans*-autophosphorylation. When IRE1 is phosphorylated, its RNase activity is activated,

facilitating cleaving 28S rRNA and the splicing of a 26-nt intron from the X-box binding protein-1 (XBP-1) mRNA in a splicesome-independent manner [64, 246]. Spliced XBP-1 mRNA, XBP-1s, encodes a basic leucine zipper (bZIP) transcription factor. XBP-1 is responsible for the induction of ER chaperones, such as BiP, ERdj4 and PDI, by binding to the unfolded protein response element (UPRE) in the promoters of ER chaperone genes. This transcription factor also induces ERAD pathway-related genes, such as EDEM, to reduce ER stress [120, 64, 199]. Additionally, XBP-1 plays an important role in plasma-cell differentiation [202].

Dimerization of PERK also leads to activation of its kinase activity. PERK phosphorylates the α-subunit of the eukaryotic translation initiation factor 2 (eIF2α) and the bZIP Cap'n'Collar transcription factor Nrf2 [37, 67]. Phosphorylation of eIF2α generally results in translational inhibition by interference with the 80S ribosome assembly [67, 192, 199]. In addition, phosphorylation of eIF2α increases the translation of activating transcription factor 4 (ATF4), a transcription factor that induces genes involved in apoptosis. Normally translation of ATF4 is attenuated because of its upstream open reading frames (uORFs) [199, 221]. Phosphorylation of Nrf2 results in activation, leading to the stimulation of oxidative genes [155, 199].

ATF6 is a type II transmembrane protein, and BiP binds to its luminal domain similar to binding of IRE1 and PERK. The N-terminal cytoplasmic region contains a bZIP domain that acts as a DNA-binding motif and transcription activation domain [69, 112]. After dissociation of BiP from ATF6, this factor is transported to the Golgi apparatus where the N-terminal cytoplasmic region of ATF6 is released by cleavage of both the serine protease site-1 protease (S1P) and the metalloprotease site-2 protease (S2P) [112, 238]. Cleaved ATF6 is transported to the nucleus for transcriptional

activation of target genes including BiP, GRP94, XBP1, and proteins involved in ERAD [64, 247].

Besides the ERQC and ERAD-related genes, the UPR also increases expression of apoptosis-inducing genes, such as TNF-receptor-associated factor-2 (TRAF2) and C/EBP-homologous protein (CHOP) [131, 199]. Thus, cells induce the apoptotic pathway if ER stress is not resolved [64, 199].

1.3.5 ER-ASSOCIATED PROTEIN DEGRADATION (ERAD) AND KEY ERAD COMPONENTS.

Since protein folding is error-prone, significant numbers of secretory and membrane proteins remain terminally misfolded [8, 73]. Various environmental stresses to cells also contribute to increased misfolded protein levels in the ER. Spontaneous genetic mutations in DNA or in the processes of transcription and translation are another factor leading to the production of aberrant proteins [8, 64, 199]. Therefore, the removal of misfolded proteins by the ERAD pathway is crucial to protect the ER from excess stress due to the accumulation of misfolded proteins.

The ERAD pathway is composed of a series of steps: recognition of terminally misfolded proteins, ubiquitination and retrotranslocation of target proteins to the cytoplasm, and ultimately protein degradation by the 26S proteasome [8, 81, 222]. Like other cellular regulatory pathways, the ERAD pathway is a complex system involving many enzymes and protein factors (see Figure 1.8).

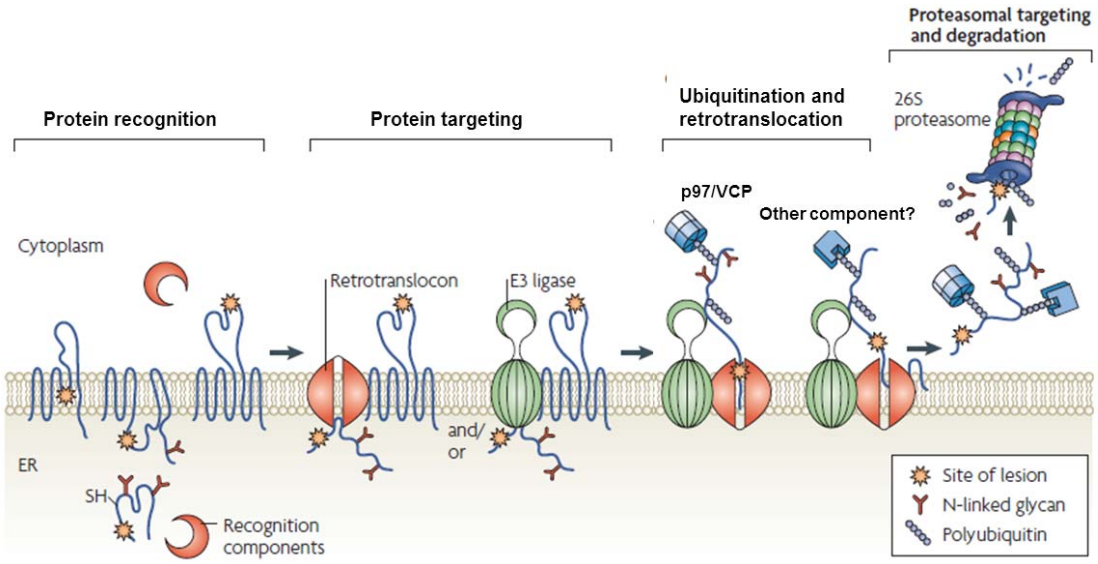

Figure 1.8: Progression of the ERAD pathway.

Misfolded proteins are recognized by ER chaperones and lectin proteins. ERAD substrates are targeted to the retrotranslocation machinery and/or E3 ligases. E3 ligases ubiquitinate ERAD substrates, which are delivered through the retrotranslocon to the cytoplasm. Cytoplasmic AAA ATPase p97/VCP provides energy derived from ATP hydrolysis for protein extraction through the ER membrane. Once ERAD substrates are localized in the cytoplasm, these misfolded proteins are recognized by the 19S subunit of the 26S proteasome and degraded in the proteasome. Modified from Vembar, S. S. and Brodsky, J. L. [222].

1.3.5.1 Recognition of aberrant proteins.

The proteins that fail to fold properly during the ERQC process are subject to the ERAD pathway. Chaperones that participate in ERQC are critical for the recognition step of ERAD [87, 222]. Molecular chaperones, such as BiP, bind to misfolded proteins to prevent aggregation. Cofactors, also called co-chaperones, such as the ER-localized Hsp40 family members and nucleotide-exchange factors, regulate the ATPase function of BiP and its affinity for binding to substrate proteins. BiP and GRP94 are known to interact with ERAD adaptor proteins, such as XTP3-B and OS-9 [34, 75, 89]. Possibly these ERAD adaptor proteins recognize misfolded proteins, including non-glycosylated proteins, by their attenuated release from BiP or other chaperones [75].

The ER-resident α1,2-mannosidase I (ERManI) and ER-degradation-enhancing α-mannosidase-like lectins (EDEM) family recognize and remove terminal α1,2-bonded mannoses from N-glycans of folding-defective glycoproteins, decreasing binding affinity for the calnexin-calreticulin cycle [8, 75, 87]. Further removal of mannoses from these substrates leads to the binding of ERAD-adaptor proteins, OS-9 and XTP3-B.

OS-9 and XTP3-B reside in the ER lumen [3, 89]. Both are lectin proteins that contain mannose 6-phosphate receptor homology (MRH) domains, homologous to the sugar recognition sites of the mannose 6-phosphate receptor [150]. OS-9 and XTP3-B interact with HMG-CoA reductase degradation 1 (HRD1), a suppressor of Lin12-like protein (SEL1L) and BiP [87, 89]. HRD1 is a ubiquitin E3 ligase. SEL1L is also a substrate receptor protein with transmembrane domains [73, 147, 148]. Although OS-9 and XTP-3 are lectin proteins, they interact with non-glycosylated substrates such as the glycosylation site mutant of the ERAD substrate, α1-antitrypsin variant null Hong Kong (NHK) protein [3, 15, 34, 89]. The homoCys-response ER-resident protein (HERP) also functions as an adaptor protein for non-glycosylated misfolded proteins [160, 222].

Therefore, these ER lectins provide the ERQC connection for substrate recognition and recruitment and direct them to the ERAD pathway [75]. OS-9 and XTP3-B are induced by UPR [3, 73].

1.3.5.2 Ubiquitin tagging of ERAD substrates.

Most folding-defective proteins are ubiquitinated by ubiquitin ligases for degradation via the 26S proteasome [81, 222]. Therefore, ubiquitinition is a central part of the ERAD system. Ubiquitination is the process by which ubiquitin, a 76 amino-acid peptide, is attached to target proteins by the sequential enzymatic reactions of E1 ubiquitin-activating enzymes, E2 ubiquitin-conjugating enzymes and E3 ubiquitin ligases. In yeast, Hrd1 and Doa10 facilitate degradation of substrate proteins in the ER. Both are RING-finger E3 ligases containing multiple transmembrane domains [222]. Hrd1 targets soluble ER luminal substrates and integral membrane proteins containing misfolded regions either in the ER luminal domain or in their transmembrane domains. Doa1 targets integral membrane proteins containing defective cytoplasmic domains [81].

Ubiquitin E3 ligases form a complex with the E2 enzymes, ubiquitin-conjugating enzyme 1 (Ubc1), Ubc6 and Ubc7, as well as substrate-recruiting proteins such as Yos9 [81]. Additional ligases and associated factors participate in the ERAD pathway in mammalian cells. HRD1/synoviolin and gp78/AMFR are homologues of Hrd1, whereas TEB4 is the orthologue of Doa10. Other mammalian ubiquitin ligases, e.g., the RING-finger protein with membrane anchor 1 (RMA1), the C-terminus of the HSC70-interacting protein (CHIP), and gp78 are required for the degradation of the cystic fibrosis transmembrane conductance regulator (CFTR) protein. Also cytosolic ubiquitin

ligases, such as Parkin, CHIP, and SCF^{FBX2}, are associated with the ERAD pathway [81, 222, 245].

1.3.5.3 Retrotranslocon.

When ERAD substrates are polyubiquitinated, they are delivered to the cytoplasm for degradation in the 26S proteasome [8, 73, 222]. The possibility of a specialized channel (retrotranslocon) dedicated to the transfer of ERAD substrates to the cytoplasm has been suggested. The existence of a specialized retrotranslocon and its composition are unclear [8, 222]. Three possible candidates or key components of a retrotranslocon have been suggested: the Sec61 translocon, Derlin family members, and E3 ligases.

The Sec61 translocon, a channel for entry to the ER, may also serve as a retrotranslocon. The Sec61 translocon is composed of three different subunits, Sec61α, Sec61β, and Sec61γ. The main subunit, Sec61α, is a transmembrane protein that forms a pore for passage of nascent peptides [8, 178]. Some data suggest that the Sec61 translocon is involved in the ERAD pathway. For example, human cytomegalovirus (HCMV) viral proteins US2 and US11 are known to bind to major histocompatibility complex (MHC) class I and facilitate its degradation by the ERAD pathway [8, 229]. In the process, binding of Sec61α to MHC class I protein was observed. Cholera toxin A-subunit, which is known to be retrotranslocated to the cytoplasm, also has been shown to bind to the Sec61 complex [198]. Furthermore, yeast Sec61 binds to various cellular ERAD substrate proteins [170, 222]. Mutations in the Sec61 complex slow down the degradation of ERAD substrates [170, 173]. Nevertheless, it is difficult to distinguish the binding of the ERAD substrates from delayed transport of nascent proteins and to determine whether misfolded proteins are completely separated from the translocon after

entering the ER [8]. Other conflicting evidence is that the Sec61 channel is only opened when newly synthesized proteins enter the ER after displacement of the plug [8, 122].

Derlin is a multi-spanning protein that has four transmembrane domains [8, 73]. Yeast Der1 and the mammalian homologues Derlin-1, -2 and -3, have been shown to interact with the ER ubiquitin ligases [8]. Both Derlin-1 and -2 have a ubiquitous expression, whereas Derlin-3 is expressed in a limited number of tissues [158]. Each mammalian Derlin protein shows distinctive substrate specificity. Derlin-1 is involved in the HCMV US11-mediated degradation of MHC class I, and the retrotranslocation of simian virus 40 (SV40) virion during entry. In contrast, ERAD of the NHK mutant protein and dislocation of murine polyomavirus from the ER are dependent on Derlin-2 [124, 125, 158]. Derlin proteins interact with p97/VCP, an AAA ATPase in the cytoplasm, and Derlin-2 also binds to EDEM, suggesting that Derlin proteins connect the ERAD factors in the ER lumen and those in the cytoplasm [158, 240]. Derlin proteins are inducible by IRE-XBP1 signaling in the UPR pathway [158].

E3 ubiquitin ligases are key components of the retrotranslocon that contain multiple transmembrane segments. Also these ERAD-associated ligases form complexes with Derlin family members through interaction with U1 SNP-associating protein-1 (Usa1) [8, 86, 222]. The Derlin family proteins and ubiquitin ligases are crucial in recruitment of ERAD substrates to the luminal side of the ER membrane in conjunction with ERAD adaptor proteins [8, 222].

Since each potential component has known substrate specificity, it has been difficult to define a universal retrotranslocon [222]. In addition, not all ERAD substrates have proven to be dependent on the potential retrotranslocon compartments [8, 222]. For

example, the degradation of CD4 by HIV Vpu protein via the ERAD pathway is not dependent on these potential channel proteins [8, 19].

1.3.5.4 Retrotranslocation to the cytoplasm.

Retrotranslocation of polyubiquitinated ERAD substrates to the 26S proteasome in the cytoplasm requires their extraction from the ER membrane by p97/VCP [8, 222]. p97/valosin-containing protein (VCP), the mammalian homologue of the yeast cell-division cycle-48 (Cdc48) complex, is a hexameric AAA ATPase. This ATPase must interact with a number of players during the extraction process. p97/VCP associates with two cofactors, ubiquitin fusion degradation 1 (UFD1) and nuclear protein localization 4 (NPL4) [143]. Also the ubiquitin chain-elongation factor Ufd2 and other proteins, including deubiquitinating enzymes (DUBs), are known to interact with p97/VCP [181, 189]. Derlin-1 binds to p97/VCP directly or by binding to the VCP-interacting membrane protein (VIMP) [240, 241]. The gp78 E3 ligase also interacts with p97/VCP directly [9]. The p97 monomer contains an N-domain and two ATPase domains (D1 and D2). The N-domain of p97 is required for binding to cofactors and to the ER membrane, whereas the ATPase domains support a driving force for p97/VCP to extract the ERAD substrates into the cytoplasm [240].

Polyubiquitinated ERAD substrates can interact with both p97 and the Ufd1-Npl4 complex [151, 222]. A significant amount of p97/VCP is known to be attached to the cytosolic side of the ER membrane, interacting with ubiquitin ligases via the ubiquitin regulatory X (UBX) domain containing proteins such as UBXD2/erasin [8, 126]. However, the mechanism for p97/VCP initial recognition of ERAD substrates is unknown [222]. p97/VCP is an abundant protein in the cytoplasm and is also involved in

other cellular processes such as cell cycle progression, transcription factor processing and homeotypic membrane fusion [8]. Nevertheless, not all ERAD substrates are dependent on p97/VCP [151]. Cholera toxin is retrotranslocated from the ER by a p97-independent mechanism [111]. Related to this observation, the 19S subunit of the proteasome has been shown to participate in the extraction of ERAD substrates from the ER membrane [151].

The extracted ERAD substrates in the cytoplasm are transferred to the 26S proteasome by adaptor proteins radiation-sensitive 23 (Rad23) and dominant suppressor of Kar1 (Dsk2) in yeast and their homolog proteins in mammalian cells [181, 222]. Rad23 and Dsk2 are ubiquitin-association (UBA)-motif and ubiquitin-like (UBL) domain-containing proteins that interact with polyubiquitinated ERAD substrates, possibly functioning to protect substrates from ubiquitin hydrolases [81]. N-glycanase, which removes oligosaccharides from ERAD substrate proteins, interacts with Rad23 to facilitate their entry into the proteasome [81, 212]. In addition, DUBs bind to substrates and remove polyubiquitin moieties. The de-ubiquitination step is essential for degradation of ERAD substrates in the proteasome, but such a process may permit escape from degradation [222]. The regulatory portion of the proteasome, the 19S subunit, unfolds substrate proteins using their ATPase domains, and then the 20S core degrades proteins into a peptide mixture [53].

Some ERAD substrates such as human α1-antitrypsin Z variant (ATZ) are degraded by either the proteasome or an alternative system known as the autophagic system [167, 222]. Autophagy provides a degradation pathway for cellular organs by forming membrane-bound vesicles, autophagosomes [110]. It has been suggested that

autophagy is an alternative ERAD pathway for protein aggregates and is utilized in situations where there are defective proteasomes [222].

1.3.5.5 Defects in protein folding and human diseases.

Protein misfolding due to mutations in protein sequences leads to loss of function. Many diseases, including cystic fibrosis and familial hypercholesterolemia, result from the loss of critical cellular proteins due to misfolding. Also the accumulation of folding-defective proteins due to mutations can result in a toxic effect or cell death by apoptosis after UPR-mediated signaling [73]. Alzheimer's disease, Parkinson's disease, and liver cirrhosis where there is an accumulation of α1-antitrypsin are well-known examples [73, 130, 184]. Since every step in the ERQC and ERAD pathways is crucial for preventing ER stress and removing terminally misfolded proteins, any inefficiency in these pathways can cause diseases by retention/deposition of misfolded proteins. For example, defective p97/VCP proteins that interfere with retrotranslocation of specific substrates result in inclusion body myopathy and frontotemporal dementia [73, 225].

1.3.5.6 Retrotranslocation of bacterial and viral proteins.

The retrotranslocation step in the ERAD pathway allows transfer of misfolded proteins in the ER to the cytoplasm. Recent studies have shown that many bacterial toxins exploit retrotranslocation for protein delivery to the cytoplasm. Bacterial AB-toxins are composed of two components, an enzymatically active A subunit and a cell binding B subunit [70]. One group of AB-toxins, including diphtheria toxin (DT), uses endosomes or lysosomes to reach the cytoplasm. Several toxins of the other AB-toxin group, including cholera toxin (CT), Shiga toxin and ricin, use ERAD for transfer to the

cytoplasm [70]. CT is composed of one A subunit, cleaved to A1 and A2 chains, and five B subunits. The CT holotoxin is delivered to the ER by endocytosis and retrograde transport via the secretory pathway [121, 183]. In the ER, the A1 chain is unfolded and dissociated from the rest of the CT by PDI prior to retrotranslocation [14, 220]. Once released in the cytoplasm, the A1 chain is quickly refolded and escapes degradation by the 26S proteasome. Although details of this mechanism are not fully understood, low numbers of lysines in the A1 chain that are sites for polyubiquitination as well as fast refolding of the A1 chain may contribute to retrotranslocation and proteasomal escape [79, 183, 227].

Viruses also exploit the ERAD pathway to complete viral replication. The open reading frame (ORF) 2 protein of Hepatitis E virus, its major capsid protein, has been shown to be retrotranslocated to the cytoplasm in a p97-dependent manner. ORF2 escapes from proteasomal degradation, possibly due to a lack of ubiquitination or fast refolding similar to mechanisms proposed for the CT A1 chain [210]. Also Lilley *et al*. have shown that entry of murine polyomavirus (Py) to the cytoplasm from the ER is dependent on Derlin-2 [124]. The US2 and US11 proteins of HCMV bind to MHC class I to facilitate degradation by the ERAD pathway and immune evasion [8, 229]. Like many other cellular pathways exploited by viruses, viruses utilize the retrotranslocation step of the ERAD pathway for their efficient replication in host cells.

1.4 CELLULAR STRESS RESPONSE.

1.4.1 IMMUNE RESPONSES TO DOUBLE-STRANDED RNA (DSRNA).

Host cells develop antiviral immune responses to eliminate or combat viral infection. Double-stranded RNA is a crucial factor that triggers host responses since

dsRNA is usually either a viral replication intermediate or genomic RNA for certain virus groups (dsRNA viruses). Cells also produce small single-stranded RNA molecules, microRNAs (miRNAs), from larger partially dsRNA precursors. These miRNAs have an important role in development as well as recognition of foreign dsRNA from viral infections. Production of miRNAs is connected to cellular responses against infection, such as RNA interference (RNAi), translational inhibition by dsRNA-activated protein kinase (PKR) and oligoadenylate synthase (OAS), and Toll-like receptor 3 (TLR3)-related responses.

1.4.1.1 Gene silencing.

Dicer is a type III RNase that resides in the cytoplasm. Dicer plays a critical role in RNA silencing after recognition of dsRNA and activation. Once activated, Dicer cleaves the dsRNA into 21 to 23 bp fragments, yielding small interfering RNAs (siRNAs) [16, 104]. siRNAs contain 2 nt 3' overhangs at each end. Dicer-siRNAs and HIV-1 trans-activating response RNA-binding protein (TRBP) transfer the siRNAs to an RNA-induced silencing complex (RISC). Argonaute 2 (Ago2), an endonuclease and the major component in the RISC, binds to the antisense strand and cleaves the target mRNA between the 10^{th} and 11^{th} nt of the paired base from the 5' end of the antisense strand [127, 168]. When antisense siRNA is completely complementary to the target mRNA, Ago2 cleaves the target mRNA, leading to its degradation. When complementarity is imperfect, target mRNA translation is inhibited [18, 168]. In each case, the host cell specifically removes the dsRNA or inhibits viral infection. The RNAi pathway is also involved in cellular development, differentiation of immune cells, and the regulation of immune responses [128].

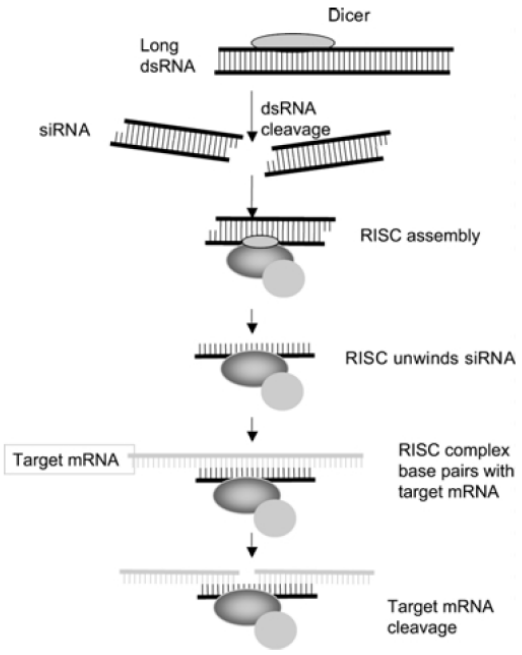

Figure 1.9: RNA interference (RNAi) pathway. (Taken from Karpala *et al.* [104])

1.4.1.2 dsRNA-activated protein kinase (PKR).

The dsRNA-activated protein kinase or protein kinase R (PKR) is a ubiquitously expressed protein. PKR expression is low under normal conditions, whereas it is strongly induced by stress-associated responses [171]. PKR is interferon (IFN)-inducible [35, 194]. It functions by binding to dsRNA in the cytoplasm via its dsRNA binding motifs (dsRBM) at the N-terminus. Binding to dsRNA leads to PKR activation by relieving the steric inhibition of the kinase domain [171]. Although the classical activator of PKR is dsRNA, PKR can be affected by endogenous mRNAs containing a pseudoknot structure, such as IFN-γ mRNA, polyanionic molecules, and caspases [171]. Cell type and cell health status are also thought to affect PKR activity [248].

Once activated, PKR phosphorylates substrate proteins, such as eukaryotic initiation factor 2 (eIF2). PKR is a serine/threonine kinase for most substrates, but it has been reported to autophosphorylate tyrosine residues in PKR itself [171, 194]. PKR is one of four kinases that phosphorylate the alpha subunit of eIF2. Phosphorylation of eIF2α inhibits eIF2B, which is the guanine nucleotide exchange factor for eIF2. GTP-bound eIF2 associates with ribosomes and participates in the initiation of translation, whereas GDP-eIF2 is dissociated from the translational machinery. Therefore, phosphorylation of eIF2α inhibits translation [171, 179, 226]. In addition, PKR phosphorylates the B56α regulatory subunit of phosphatase 2A (PP2A), a major serine/threonine phosphatase that regulates many cellular processes. Phosphorylation of B56α leads to inhibition of its activity, thereby activating PP2A [171]. PKR regulates the activity of the eIF4E and BCL2 via PP2A activity [101, 191, 235].

1.4.1.3 Oligoadenylate synthetase (OAS) and RNase L.

The 2',5'-oligoadenylate synthetase (OAS) is induced by type 1 IFNs, IFN-α and –β, and dsRNA. OAS inhibits the translation machinery of host cells [104, 194]. OAS is activated by dsRNA and converts ATP molecules to 2'-5' linked oligoadenylates, which are commonly known as 2-5A oligomers. These 2-5A oligomers bind to a latent endoribonuclease, RNase L, resulting in the dimerization and activation of RNase L [32, 104, 194]. Activated RNase L then initiates the destruction of various RNAs, including viral RNAs to clear the viral infection, and the host ribosomal RNA. Destroying ribosomal RNA results in the inhibition of translation [42, 172, 232]. RNase L activation also can lead to apoptosis of host cells [104]. Recently, Bridge *et al*. have shown that

short hairpin RNA (shRNA)-expressing vectors can induce the OAS gene, suggesting that common shRNA constructs can induce an interferon response [25].

1.4.1.4 Toll-like receptor 3 (TLR3).

Toll-like receptors (TLRs) recognize molecular patterns associated with bacterial and viral pathogens. These innate immune-recognition receptors induce anti-bacterial and anti-viral immune responses [4, 104]. More than 10 TLRs have been identified in humans and mice [201, 204]. TLR3 is a dsRNA pattern-recognition receptor, expressed on the surface of many cell types, including fibroblasts, macrophages, and some dendritic cells. TLR3 is the only receptor that recognizes external dsRNA. When TLR3 binds to dsRNA, a downstream signaling pathway is activated through the interleukin-1 receptor-associated kinase (IRAK1) and the tumor necrosis factor receptor-associated factor6 (TRAF6). Signaling ultimately induces IFN-β, interleukin-6 (IL-6), IL-12 and tumor necrosis factor- α (TNF-α), which help to shape the overall immune response [4, 46]. The TLR3 response likely is important for uninfected cells as a warning of viral infection since dsRNA may be released from lysed infected cells [194].

1.4.1.5 dsRNA-stimulated genes.

Double-stranded RNA is known to regulate transcription of many genes, including the IFN genes. Most dsRNA-stimulated genes are IFN-stimulating genes (ISGs), which are also induced by type I IFNs [104, 194]. Using cDNA microarray analysis, Geiss *et al*. have shown that dsRNA induces 175 genes and down-regulates 95 genes. dsRNA induces a variety of genes including ISGs, genes involved in TNF-signaling and apoptosis, and growth factors. Some genes involved in metabolism, cell

cycle regulation, and cell adhesion are repressed by dsRNA [58]. The fact that some dsRNA-stimulated cytokine genes, such as IFN, TNF, or IL-1, are also induced by viruses indicates that signaling pathways induced by dsRNA, IFN, and viruses partially overlap. At least four families of transcription factors are known to be activated by dsRNA: NF-κB, IRF-3, c-Jun and ATF2 [43, 201]. In addition, PKR can induce the MAPK pathway by phosphorylating MAPK activator MKK6. The RNA helicase RIG-I, which resides in the cytoplasm, activates a dsRNA-signaling pathway by recognizing dsRNA through its C-terminal helicase domain [244].

1.4.2 STRESS GRANULES AND PROCESSING BODIES.

Fully processed cellular mRNA transcripts in the nucleus are exported to the cytoplasm to generate proteins. Some mRNAs are immediately bound to ribosomes for translation. After translation, these mRNAs are deadenylated, dissociated from ribosomes and then either degraded or stored. Other mRNAs that are programmed for delayed translation are stored until they are needed. Translationally silenced mRNAs from either scenario are packaged into ribonucleoprotein (RNP) granules. Known RNP granules, which lack a boundary membrane, include stress granules, processing bodies, germ-cell granules and neuronal granules [6].

Stress granules (SGs) were first observed as heat stress granules in tomato cells exposed to heat shock [157]. These granules contained most of the cellular mRNAs, with the exception of mRNAs encoding heat shock proteins. SGs can be formed in the cytoplasm of cells exposed to various stresses, such as heat, UV irradiation, and oxidative conditions. SGs are thought to play an important role in regulating mRNA metabolism when cells are exposed to stress by inhibiting translation of many housekeeping mRNAs

and enhancing the translation of molecular chaperones and damage repair proteins [5, 6]. SGs are heterogeneous in size and shape [108] and contain stalled 48S pre-initiation complexes including small ribosomal subunits and the early translation initiation factors, such as eIF2, eIF3, eIF4E, and eIF4G. Many RNA-binding proteins involved in translation, RNA stability, RNA decapping, and RNA interference are also localized to SGs [5, 109]. SGs represent a transient storage compartment for untranslated mRNAs, and many SGs-associated RNA-binding proteins shuttle in and out of SGs [6].

SGs are not observed under favorable cell growth conditions, but they are assembled rapidly under environmental stress [6]. The phosphorylation of eIF2α by stress-activated kinases, such as PKR and PERK, is a critical factor for SG assembly. Also overexpression of RasGAP SH3 domain-binding protein (G3BP) or T-cell restricted intercellular antigen-1 (TIA-1) is known to promote SG assembly [108, 218]. Various mitochondria-associated factors are able to regulate SG assembly or disassembly [6, 108]. SGs have also been detected in tissues from stressed animals [6].

Processing bodies (PBs) contain the components for translation, RNA interference, and the mRNA decay machinery [12]. The translation initiation factor eIF4E and the translation inhibiting protein, p54/RCK, are also found in PBs, indicating that these structures are sites for mRNA decay and translation repression [6]. PBs are uniform spheroid-shaped particles and increase in size and number in response to stress. PBs are highly mobile [108, 216, 230].

PBs and SGs share many protein components and interact with one another in stressed mammalian cells [6]. Some mRNAs in SGs are delivered to PBs, probably for RNA decay when they meet. These data suggest that SGs are intermediates between

polysomes and PBs for regulating untranslated mRNAs under stressful conditions [6, 108].

1.5 RATIONALE FOR THIS STUDY.

MMTV is a betaretrovirus that primarily induces mammary carcinomas in mice. Like HIV-1, MMTV is a complex retrovirus that encodes a viral RNA regulatory protein (Rem) for the nuclear export of MMTV unspliced/genomic RNA to the cytoplasm. Cytoplasmic localization of MMTV genomic RNA is required for translation of Gag and Pol precursor proteins and for packaging into virion particles. Rem is a 33 kDa glycosylated protein containing an unusually long ER signal peptide that contains all the functional motifs for RNA binding and nuclear export. Rem is crucial for MMTV replication.

Complex retroviruses contain a virally encoded export protein that binds to a *cis*-acting element within viral RNA. Previous studies suggested that the *cis*-acting element for Rem activity, the Rem responsive element (RmRE), overlaps the junction of the *env* gene and the 3' MMTV LTR. To understand details of Rem activity, further anaylsis to determine the boundary of the minimal RmRE and RmRE structure is necessary.

Unlike many other viral export proteins of complex retroviruses, Rem contains an unusually long ER signal peptide (SP). Previous studies have shown that SP is functionally active after full-length Rem is cleaved and SP is released from the ER membrane. These observations suggested that SP is redirected to the cytoplasm after being generated from a full-length Rem precursor that is translated in association with the ER membrane. However, the mechanism of Rem/SP trafficking from the ER for RNA binding in the nucleolus remains to be defined.

Rem is an important regulatory protein for MMTV replication. In this study, the boundary of the minimal RmRE at the junction of the *env* gene and the 3' MMTV LTR and favorable secondary structure of RmRE were defined. In addition, the mechanism of Rem processing in the ER and "retrotranslocation" of SP was investigated. This study provides a better understanding of Rem function in MMTV replication. Further, our understanding of MMTV exploitation of the ERAD system should provide important insights for normal cellular function and how escape from ERAD may lead to disease.

2. MATERIALS AND METHODS

2.1 CELL LINES.

XC rat fibroblast cells transformed by Rous sarcoma virus were grown in Dulbecco's modified Eagle's medium (DMEM) (Invitrogen, Carlsbad, CA) supplemented with 5% heat-inactivated (30 min at 56°C) fetal bovine serum (FBS) (Invitrogen), 100 Units/ml penicillin, 100 μg/ml streptomycin (Invitrogen), 2 mM L-glutamine and 50 μg/ml gentamycin sulfate (Elkins-Sinn, Inc., Cherry Hill, NJ). Jurkat human T lymphoma cells were maintained in suspension using Roswell Park Memorial Institute (RPMI) 1640 medium (Invitrogen) containing 5% FBS, 100 Units/ml penicillin, 100 μg/ml streptomycin, 2 mM L-glutamine and 50 μg/ml gentamycin sulfate. HC11 normal mouse mammary epithelial cells were grown in RPMI 1640 medium supplemented with 10% FBS, 0.5 μg/ml insulin (Sigma, St. Louis, MO), 0.5 μg/ml epidermal growth factor (Invitrogen), 2 mM L-glutamine and 50 μg/ml gentamycin sulfate. Human embryonic kidney cells (293) were maintained in DMEM containing 10% FBS, 100 Units/ml penicillin, 100 μg/ml streptomycin, 2 mM L-glutamine and 50 μg/ml gentamycin sulfate. All cell lines were maintained at 37°C in a humidified atmosphere containing 7.5 % CO_2.

2.2 PLASMIDS.

Rem reporter assays included the Rem-responsive pHM*Rluc* (*Renilla* luciferase) vector and a second reporter plasmid, pGL3-control [142]. The pGL3-control vector lacks the RmRE and expresses firefly luciferase from the SV40 promoter (Promega). The pHMΔeLTR+XR*luc* constructs with deleted versions of the RmRE were made by

insertion of the mutant RmRE (X) into an engineered *Sca*I site downstream of the splice acceptor site and upstream of the simian virus 40 (SV40) poly (A) signal in pHMΔeLTR*luc* [142].

The plasmids encoding GFPRem and GFP-SP were cloned by insertion of the *rem* or the SP cDNA sequences in the EGFPC1 vector (Promega) downstream in frame with green fluorescent protein (GFP) coding sequences. The GFP-RemP71L construct was created by site-directed mutagenesis (SDM) of the GFPRem plasmid, substituting the proline at position 71 with leucine, the consensus residue [140]. SDM was performed according to the instructions of the QuikChange® II Site-directed mutagenesis kit (Stratagene, La Jolla, CA). Briefly, the plasmid vector was mixed with complementary primers containing the substitution mutation at position 71. After PCR using *Pfu*Turbo (Stratagene), the reaction was digested with *Dpn*I, thus cleaving the methylated parental wild-type DNA. The undigested mutant plasmids then were recovered by transformation of *Escherichia coli* DH5α.

Glycosylation mutants of *rem* cDNA were generated through SDM of the RemP71L construct, changing the asparagines to glutamines at positions 127 or 143 (N127Q, N143Q). The double glycosylation mutant was obtained by site-directed mutagenesis of the N127Q construct using N143Q SDM primers. Similarly, the ER signal peptidase cleavage site mutants of GFP-RemP71L and pQ61 were generated by SDM substitution of the position 96 valine and/or position 98 glycine to arginine, respectively. The pQ61 plasmid (kindly provided by Dr. Susan Ross) contains the C3H-MMTV envelope gene downstream of the CMV promoter in the pcDNA3.1 vector.

The pLK0.1-puro control vector and the pLK0.1-based p97/VCP-specific shRNA expression vectors were obtained from Sigma. LKΔHP was generated by removing a

hairpin using SDM. LKΔU6 and LKΔPsi were generated by SDM insertion of additional *EcoR*I sites upstream of the U6 promoter and *Psi* packaging signal locations, respectively. These SDM products were then digested with *EcoR*I, and the desired LK0.1 fragments from which the lentiviral elements were removed were gel-purified and ligated using T4 DNA ligase (Invitrogen). A number of expression vectors were generously provided by colleagues (listed in Table 2.2).

Restriction enzymes were obtained from New England Biolabs (NEB) (Beverly, MA) and Invitrogen. All primers were synthesized by Integrated DNA Technologies (IDT) (Coralville, IA). After plasmid purification, the deletion and insertion sequences were confirmed using sequence primers in the GFP region. Automated fluorescence sequencing was performed by the DNA sequencing facility at UT Austin's Institute for Cellular and Molecular Biology (ICMB).

Table 2.1: Summary of constructs designed for this study

Plasmid	**Backbone**	**Description**
pHM*Rluc*		*Renilla* luciferase reporter vector
pHMΔeLTR*luc*	pHM*Rlucm*	Modified *Renilla* luciferase reporter vector
pHMΔeLTR+XR*luc*	pHM*Rluc*	Modified *Renilla* luciferase reporter vector
pRRE-*Rluc*	pHM*Rluc*	Rev responsive *Renilla* luciferase reporter vector
pRxREI-*Rluc*	pHM*Rluc*	Rex1 responsive *Renilla* luciferase reporter vector
pGL3-control		Firefly luciferase reporter vector
GFPRem	pEGFPC1	Rem expression vector, N-terminally GFP-tagged
GFP-SP	pEGFPC1	SP expression vector, N-terminally GFP-tagged
GFPΔ150	pEGFPC1	Rem C-terminus deletion mutation, N-terminally GFP-tagged
Rev-GFP	pEGFPN3	Rev expression vector, C-terminally GFP-tagged
Rex1-GFP	pEGFPN3	Rex1 expression vector, C-terminally GFP-tagged
Rem	pEGFPN3	Rem expression vector
RemN127Q	pEGFPN3	Single glycosylation site mutation of Rem
RemN143Q	pEGFPN3	Single glycosylation site mutation of Rem
RemN127QN143Q	pEGFPN3	Double glycosylation site mutation of Rem
GFPRemG98R	pEGFPC1	Single cleavage site mutation of Rem, N-terminally GFP-tagged
GFPRemV96RG98R	pEGFPC1	Double glycosylation site mutation of Rem, N-terminally GFP-tagged
pQ61G98R	pcDNA3.1	Single cleavage site mutation in Env
pQ61V96RG98R	pcDNA3.1	Double cleavage site mutation in Env
pQ61 SD1	pcDNA3.1	Second splice donor site mutation in Env
pLK0.1-puro		shRNA expression vector (Sigma)
pLKΔHP	pLK0.1-puro	Truncated shRNA expression vector
pLKΔU6	pLK0.1-puro	Truncated shRNA expression vector
pLKΔPsi	pLK0.1-puro	Truncated shRNA expression vector

Table 2.2: Vector plasmids provided by colleagues for this study

Vector	Expression	Donor	Location
pQ61	MMTV Env	Dr. Susan Ross	University of Pennsylvania, Philadelphia, PA
ER-mCherry	Red fluorescent protein containing a calreticulin signal peptide at the N-terminus and a KDEL ER retention signal at the C-terminus	Dr. Nobuko Hosokawa	Kyoto University, Kyoto, Japan
NHKQQQ-GFP	An α1-antitrypsin mutant, null Hong Kong (NHK), glycosylation-defective	Dr. Nobuko Hosokawa	Kyoto University, Kyoto, Japan
p97QQ	Dominant-negative p97/VCP	Dr. Yihong Ye	National Institutes of Health, Bethesda, MD
Derlin-1-YFP	Dominant-negative Derlin-1	Dr. Billy Tsai	University of Michigan Medical School, Ann Arbor, MI
Derlin-2-YFP	Dominant-negative Derlin-2	Dr. Billy Tsai	University of Michigan Medical School, Ann Arbor, MI
pCEP4-H1		Dr. Jon Huibregtse	University of Texas at Austin
pCEP4-H1 E6AP-3	shRNA against E6AP	Dr. Jon Huibregtse	University of Texas at Austin
pCEP4-H1 HPV18E6	shRNA against HPV18E6	Dr. Jon Huibregtse	University of Texas at Austin

2.3 ANTIBODIES

The GFP- and actin-specific antibodies were obtained from Clontech (Mountain View, CA) and Calbiochem (La Jolla, CA), respectively. SP-specific antibody was prepared by immunization of rabbits following standard protocols of Cocalico Biologicals (Reamstown, PA). The p97/VCP- and phospho-eIF2α-specific antibodies

were purchased from Cell Signaling (Beverly, MA). B23-specific antibody was obtained from Sigma (St. Louis, MO). RasGAP-SH3-binding protein (G3BP)-specific antibody and the Alexafluor 594-conjugated anti-rabbit secondary antibody (Invitrogen) were kindly provided by Dr. Richard Lloyd (Baylor College of Medicine, Houston, TX) and Dr. Phil Tucker (The University of Texas at Austin), respectively.

2.4 LARGE SCALE PREPARATION OF PLASMID DNA.

Alkaline lysis and cesium chloride (CsCl) gradient centrifugation was used for large-scale preparations of plasmid DNA. *Escherichia coli* bacterial cells from a single colony containing the plasmid of interest were used to inoculate 25 ml of Luria-Bertani (LB) broth (1% tryptone w/v, 0.5% yeast extract w/v, 0.5% NaCl w/v, pH 7.4) containing appropriate antibiotics at a final concentration of 50 μg/ml and incubated overnight with shaking at 37°C. Twenty-five ml of the overnight culture was inoculated into 500 ml of LB containing antibiotic in a 2L Erlenmeyer flask and grown at 37°C with shaking until an A600 reading of 0.9-1.2 was attained. The plasmids were amplified by addition of 2.5 ml of freshly prepared chloramphenicol (Sigma, 34 mg/ml in ethanol) to a final concentration of 170 μg/ml. The bacteria were grown with shaking at 37°C for another 18 h. The bacterial cultures were pelleted by centrifugation (Avanti J-E centrifuge, Beckman) at 7,000 rpm in a JA10 rotor (Beckman) for 10 min at 4°C, and the supernatant was discarded. The pellet was resuspended in 10 ml of Solution I (50 mM glucose, 25 mM Tris-HCl, pH 8.0, and 10 mM EDTA) and transferred to a 50 ml conical tube. Lysozyme [stock concentration of 10 mg/ml (Sigma)] was added to a final concentration of 1 mg/ml, and the suspension was incubated at RT (25°C) for 10 min. Twenty ml of freshly prepared Solution II [0.2 N NaOH and 1% sodium dodecyl sulfate (SDS)] was

added to lyse the bacterial cells, and the suspension was mixed gently by inverting the tube several times. Thorough mixing was followed by a 10 min incubation at room temperature (RT). The alkaline reaction was neutralized by adding 15 ml of cold Solution III (3 M potassium acetate, pH 4.8, in glacial acetic acid) and mixed thoroughly by shaking the tube several times. The mixture was incubated on ice for 10 min, followed by centrifugation in an Allegra X-15R centrifuge (Beckman Coulter) at 3,800 rpm for 30 min at 4°C to remove the denatured chromosomal DNA. The resulting supernatant was filtered through cheesecloth into a new 50 ml conical tube. The pellets containing the chromosomal DNA were discarded. To precipitate the DNA, 0.6 volume of isopropanol was added to the supernatant, mixed well, and incubated at RT for 15 min. The DNA was precipitated by centrifugation at 3,800 rpm for 30 min at RT in an Allegra X-15R centrifuge. The DNA pellets were washed with 70% ethanol and air dried for 10 min. Pellets were resuspended in 3.5 ml of TE (10:10) (10 mM Tris-HCl, pH 7.4, and 10 mM EDTA).

The DNA was further purified using CsCl gradient ultracentrifugation to remove RNA and proteins. CsCl (4.7 g) was added to the DNA solution and dissolved. Ethidium bromide (EtBr) (0.78 ml of a 5 mg/ml solution) was added, and the insoluble debris (RNA and protein) was removed by centrifugation at 3,500 rpm for 15 min at 4°C in an Allegra X-15R centrifuge. The supernatant was transferred to a Beckman Optiseal tube, and the suspension was separated by centrifugation in a Beckman L7-65 ultracentrifuge at 50,000 rpm for 18 h at 20°C using an NVT 65.2 rotor. The plasmid band was collected with a 5 ml syringe and an 18-gauge needle and transferred to a 15 ml conical tube. The EtBr was extracted several times using 2 volumes of N-butanol saturated with G-50 buffer (20 mM Tris-HCl, pH 7.4, 0.1 M NaCl, and 2 mM EDTA), vortexed and separated

at 3,500 rpm for 2 to 5 min until no visible pink color remained. For DNA precipitation, TE (10:10) was added to a final volume of 5 ml. Two volumes of ice-cold ethanol were added, and the solution was incubated on ice for 30 min. The DNA was precipitated by centrifugation at 3,800 rpm for 30 min at 4°C in an Allegra X-15R centrifuge. The DNA pellet was washed in 70% ethanol, air dried, and resuspended in 2 ml of TE (10:10).

The DNA was digested with 100 μg/ml of pancreatic RNase A (Sigma) and 200 U of RNase T1 (Sigma) to remove RNA, prior to incubation at 37°C for 30 min. The DNA was then treated with 0.5% SDS and 100 μg/ml of proteinase K and incubated at 37°C for 30 min. After phenol:chloroform extraction, the DNA in the aqueous phase was dialyzed against 2 L of TE (10:1) (10 mM Tris-HCl, pH 7.4, and 1 mM EDTA) overnight at 4°C using a 10,000 MW cutoff Slide-A-Lyser dialysis cassette (Pierce, Rockford, IL). The buffer was changed three times. The dialyzed DNA was collected, and 5 M NaCl was added to bring the solution to a final concentration of 0.2 M. Plasmid DNA was then precipitated with two volumes of ice-cold ethanol, and washed with 70% ethanol before resuspending in 500 μl of TE (10:0.1). The concentration of the DNA was determined using a NanoDrop 1000 spectrophotometer (Thermo Fisher Scientific Inc. Waltham, MA). The absorbance at both 260 nm and 280 nm was determined to assess both the quantity and purity of the DNA.

2.5 TRANSFECTION ASSAYS.

Tissue culture cell lines were transfected using different methods that yield the highest transfection efficiency.

2.5.1 DMRIE-C TRANSFECTION.

XC cells were harvested the day before the transfection and counted using a Bright-line hemacytometer (Reichert, Buffalo, NY). Cells ($5x10^5$) were plated in each well of a 6-well tissue culture (TC) plate in 2 ml of tissue culture medium. Different concentrations of plasmid DNA were mixed in 0.5 ml of transfection medium (tissue culture medium without serum and antibiotics) in a 1.7 ml microcentrifuge tube. In a separate tube, 10 µl of DMRIE-C transfection reagent (Invitrogen) was mixed with 0.5 ml of transfection medium. The DNA/medium mixture was added to the DMRIE-C/medium in a 1:1 ratio and incubated at RT for 45 min. The plated XC cells were washed with transfection media, and 1 ml of the transfection mixture was added to the well. Plates were then returned to the 7.5% CO_2 environment and incubated for 6 to 8 h at 37°C. The transfection was terminated by adding 1 ml of complete medium containing twice the normal concentration of FBS without removing the DNA-containing medium. Cells were incubated at 37°C in a CO_2 incubator for a total of 48 h.

2.5.2 ELECTROPORATION.

Jurkat T cells and HC11 mammary epithelial cells were transfected by electroporation using a BTX Electro Cell Manipulator (BTX, San Diego, CA). On the day prior to transfection, Jurkat cells were replated at $1.2x10^7$ cells in 20 ml of complete growth media. On the day of transfection, $1x10^7$ cells were mixed with 20 to 40 µg of total DNA in 400 µl of serum-free RPMI. The Jurkat cell/DNA mixture was added to a 4 mm gap cuvette (BTX) and electroporated using the following parameters: 260V, 1050 µF, and R10 (720 Ω). After a 10-min incubation at RT, transfected Jurkat cells were replated in 60 mm dishes in 4 to 5 ml of complete medium.

HC11 cells were treated with trypsin and diluted 1:3 from a confluent 100 mm plate on the day before transfection. On the day of transfection, $1x10^7$ cells were mixed with 15 to 20 μg of total DNA in 200 μl of serum-free RPMI. Using a 2 mm gap cuvette, the HC11 cell/DNA mixture was subjected to electroporation using the following optimized conditions: 140V, 1750 μF, and R4 (72 Ω). After a 10-min incubation at RT, transfected HC11 cells were replated in 60 mm TC plates in 4 to 5 ml of complete medium. After a 48 h incubation, cells were harvested for further assays.

2.5.3 CALCIUM PHOSPHATE PRECIPITATION.

The 293 cells were transiently transfected by the calcium phosphate method. One day prior to transfection, cells ($5x10^5$) were plated in 6-well TC plates in 2 ml of complete medium. For the transfection, DNA (6 μg total) was mixed with 10 μl of $CaCl_2$ (final concentration of 0.25 M) in a 1.7 ml microcentrifuge tube. The volume was adjusted to 100 μl with H_2O and added dropwise to a second tube containing 100 μl of 2X-HBS, pH 7.1 or 7.2 (280 mM NaCl, 10 mM KCl, 1.5 mM $Na_2HPO_4 \cdot 2H_2O$, 12 mM dextrose, 50 mM HEPES) while vortexing. The mixture was incubated at RT for 15 min and added to the cells dropwise. At 6 to 8 h post-transfection, the media was changed to remove the calcium phosphate precipitate. Cells were harvested after 48 h.

2.5.4 LIPOFECTAMINE 2000 TRANSFECTION.

In some cases, 293 cells were also transiently transfected using Lipofectamine 2000 Reagent (Invitrogen). The day before transfection, $5x10^5$ cells were seeded per well of a 6-well plate in 2 ml of complete medium without antibiotics. For each transfection, a total of 6 μg of DNA was added to 250 μl DMEM without additives. In a separate tube, 5

µl of Lipofectamine 2000 Reagent was diluted in 250 µl DMEM containing 4% FBS without antibiotics. The DNA/medium mixture then was added to the Lipofectamine 2000/medium at a 1:1 ratio and incubated at RT for 20 min. The DNA-Lipofectamine 2000 Reagent complexes were added to cells dropwise. Cells were harvested after a 48 h incubation.

2.6 REPORTER GENE ASSAYS.

The dual-Luciferase Reporter Assay System (Promega, Madison, WI) was used to detect luciferase reporter gene activity. Transfected cells were harvested, washed with 1X PBS, and resuspended in 1X Passive Lysis Buffer (Promega). Subsequently, three cycles of freezing at -80ºC for 20 min and thawing in a 37ºC water bath were performed. The lysates were centrifuged at 8,000 rpm in a Beckman Coulter Microfuge 18 Centrifuge for 10 min at 4ºC, and the supernatant was transferred to another tube. The Bio-Rad Protein assay system was used to quantitate protein concentration. A total of 40 µg or 20 µl of lysate was used to obtain readings for both firefly and *Renilla* luciferase using a Turner TD-20e luminometer (Turner Designs, Inc., Sunnyvale, CA) that was set to 0 delay and 10 sec integration. Luciferase Assay Reagent II (LAR II) (Promega) (50 µl) was added to the sample, and the firefly luciferase activity was determined. The *Renilla* luciferase activity was determined after the addition of 50 µl Stop and Glo Reagent (Promega). The firefly luciferase was expressed in relative light units (RLUs), and the relative values were normalized to 100 µg of protein.

2.7 WESTERN BLOTTING.

Whole cell extracts were prepared by adding either one volume of 2X-SDS loading buffer [250 mM Tris-HCl, pH 6.8, 20% glycerol, 2% sodium dodecyl sulfate (SDS), 5% β-mercaptoethanol, 0.2% bromophenol blue] to cells in one volume of phosphate-buffered saline (PBS) or one volume of 6X-SDS loading buffer (0.35 M Tris-HCl, pH 6.8, 10% SDS, 36% glycerol, 0.6 M DTT, 0.012% bromophenol blue) to cells in five volumes of PBS. Samples were boiled for 5 min for protein denaturation.

Total protein (15 to 100 μg) from the extracts was resolved in 10 or 12% polyacrylamide gels containing 1% SDS and transferred to Optitron 0.45 μm nitrocellulose membranes in Western transfer buffer [39 mM glycine, 48 mM Tris base, 1% SDS, 20% (v/v) methanol] overnight at 150 mA at 4ºC. The membrane was incubated with 5% nonfat dry milk in Tris-Buffered Saline Tween-20 (TBS-T) buffer (20 mM Tris-HCl, pH 7.4, 137 mM NaCl, 0.1% Tween 20) for 1 h. The membrane was then incubated with different antibodies diluted in TBS-T buffer containing 5% nonfat dry milk for 1 to 2 h followed by three washes with TBS-T buffer for 10 min each. The membrane then was incubated with horseradish peroxidase-tagged secondary antibodies diluted in TBS-T buffer containing 5% nonfat dry milk for 1 to 2 h and washed three times with TBS-T buffer for 10 min each. Binding of the secondary antibody was detected using the Western Lightning Enhanced Chemiluminescent Reagent (Perkin Elmer, Wellesley, MA) as recommended by the manufacturer.

2.8 SUBCELLULAR FRACTIONATION

The commercially available NE-PER™ Nuclear and Cytoplasmic Extraction Reagent (Pierce) and the ProteonExtract® Subcellular Proteome Extraction Kit (Calbiochem) were used as recommended by the manufacturers.

2.9 PREPARATION OF TOTAL RNA FROM CELL LINES.

All solutions used for RNA preparation were treated with 0.1% diethyl pyrocarbonate (DEPC) (Sigma) overnight to eliminate RNase activity and then autoclaved to remove the residual DEPC.

Total RNA was extracted from tissue culture cells grown to confluence in 100 mm plates using the guanidine isothiocyanate method. Culture medium was removed, and one ml of home-made TRI-Reagent (2M Guanidine isothiocyanate, 12.5 mM sodium citrate, pH 7.0, 0.25% Sarkosyl, 0.36% β-mercaptoethanol, 200 mM sodium acetate, pH 4.0, and 50% water-saturated phenol, pH 7.5) was added to cells. The supernatant was transferred to a clean microcentrifuge tube, and 0.1 ml of 1-Bromo-3-Chloropropane (BCP) (Molecular Research Center, Inc., Cincinnati, OH) was added. The solution was mixed using a Vortex mixer for 15 sec followed by centrifugation at 12,000 X g for 15 min at 4°C. The top layer was transferred to a clean fresh tube. Isopropanol (0.5 ml) was added to precipitate RNA prior to incubation for 20 min at RT. RNA precipitates were concentrated by centrifugation at maximum speed in a microcentrifuge for 30 min at 4°C. After washing with 75% ethanol, the pellet was resuspended in 100 to 200 µl of DEPC-treated water. The DNA contaminants were removed by high-salt precipitation using 3 volumes of 4 M sodium acetate (pH 6.0). After incubation for 15 min at RT, the RNA

was pelleted at maximum speed in a microcentrifuge for 30 min at 4°C and then washed with DEPC-treated 70% ethanol. The RNA was then resuspended in 50 to 100 µl of DEPC-treated water. RNA concentration and purity was determined from the A260 and A280 nanodrop spectrophotometer readings.

2.10 REVERSE-TRANSCRIPTASE POLYMERASE CHAIN REACTION (RT-PCR).

Purified RNA (20 µg) from tissue culture cells was treated with 3U of amplification-grade DNase I (Invitrogen) and 0.5 U of RNaseOUT RNase inhibitor (Invitrogen) for 1 h at 37ºC. The DNase I reaction was stopped by the addition of 5 µl of 25 mM EDTA. Samples then were incubated at 72ºC for 15 min. To make cDNAs in a reverse transcription reaction, oligo primer poly(dT_{17}) and deoxynucleotide triphosphates (dNTPs) were added to the DNase-treated RNA at final concentrations of 2.5 pmol/µl and 1 mM, respectively. The mixure was then boiled for 5 min, followed by immediate incubation on ice for 5 min. The RNA was reverse transcribed with 400 U of Moloney murine leukemia virus (M-MLV) reverse transcriptase (Invitrogen), 5 U of RNaseOUT, and 10 mM dithiothreitol in a 50 µl reaction mixture for 1 h at 37ºC. A reaction lacking reverse transcriptase was added to monitor DNA contamination. The cDNA (1 to 5 µl) was used in the reverse transcription-polymerase chain reaction (RT-PCR) with 25 pmol of specified primers and 10 µl of JumpStart REDTaq PCR Reaction Mix (Sigma) in a 20 µl reaction. Primers are listed in Table 2.2. The following PCR conditions were used: initial denaturation at 94°C for 5 min, 30 cycles of denaturation at 94°C for 1 min, annealing at 50°C for 45 sec, and polymerization at 72°C for 45 sec with a final extension step at 72°C for 10 min. The levels of glyceraldehyde-3-phosphate dehydrogenase

(*gapdh*) were used as an internal control for RNA integrity and cDNA synthesis. For the amplification of *gapdh,* Klentaq polymerase (Ab peptides Inc., St. Louis, MO) was used. Each PCR product was analyzed by electrophoresis on a 1% agarose gel at 65V and stained with ethidium bromide prior to visualization using an AlphaImager (Alpha Innotech).

Table 2.3: Primers used in semi-quantitative RT-PCR.

Primer name	**Sequences (5'-3')**
Human *Derlin-1*+	TCT ACG CGA CTT GAA ACA GGA
Human *Derlin-1*-	CCA ACC AGA TTT CCA ATA AGC
Mouse *Derlin-1*+	TCT ACT CGG CTT GAA GCA GGA
Mouse *Derlin-1*-	CCG ACA AGG TTT CCA ATG AGC
Derlin-2+	TGT CGA ATG CTA GAA GAA GGC
Derlin-2-	ATT TGG ATC CTC ATC TGG TGT
Gapdh+	CAT GTT TGT GAT GGG TGT GAA CCA
Gapdh-	GTT GCT GTA GCC GTA TTC ATT GTC

2.11 INDIRECT IMMUNOFLUORESCENCE.

Transfected cells were plated on glass coverslips in 6-well tissue culture plates approximately 48 h prior to detection with antibodies. Cells were fixed in 4% paraformaldehyde for 15 min. Cells were then permeabilized with 0.05% Triton X-100 (Sigma) in PBS for 30 min at RT and washed three times with PBS for 5 min each. Cells

were then incubated with antibody dilution solution (2% FBS, 0.1% Tween-20, 150 mM NaCl, 10 mM Tris-HCl, pH 7.4) for 1 h at 37°C. After blocking, cells were incubated with stress-granule marker, RasGAP-SH3-binding protein (G3BP)-specific antibody (1:100 dilution) for 1 h at 37°C and washed three times for 5 min each in PBS. Cells then were incubated with goat anti-rabbit Alexafluor 594 antibody (Invitrogen) (1:500 dilution) at 37°C for 1 h in the dark. All subsequent steps were performed in the dark. After three washes in PBS, cells were stained with 150 nM 4'6-diamidino-2-phenylindole (DAPI) (Invitrogen), followed by three additional washes in PBS. The coverslips were mounted on glass slides in VECTASHIELD (Vector Labs, Burlingame, CA), sealed with VALAP (equal weight of Lanolin, Vaseline, and paraffin) and examined under an Olympus IX70 fluorescence microscope.

2.12 STATISTICAL ANALYSIS.

All results were expressed as the mean +/- standard deviation of at least three different transfections. Statistical significance was determined using the two-tailed Students' *t* test. A P value of less than 0.05 was considered to be significant.

3. RESULTS

3.1 MAPPING OF THE REM RESPONSE ELEMENT (RmRE).

Previous studies by Mertz *et al*. identified Rem as an RNA export protein that allows the nuclear export of unspliced MMTV genomic RNA, similar to the Rev protein of HIV [142]. Rev recognizes the Rev response element (RRE) located in the intron of the HIV envelope gene. Rev facilitates export of intron-containing viral mRNA, including unspliced genomic RNA and singly spliced *env* mRNA [85, 134]. Rex1, another Rev-like protein, is encoded by HTLV and recognizes its own response element (RxRE1) [10, 57]. This suggests that Rem, like the other Rev-like proteins, recognizes a Rem response element (RmRE) in the MMTV genome. pHM*Rluc*, an MMTV-based reporter plasmid, was developed to measure Rem responsiveness. This plasmid contains a cytomegalovirus (CMV) promoter and the 3'-end of the MMTV genome, which includes part of the envelope (*env*) gene and the 3' LTR. Additionally, a *Renilla* luciferase gene is located between the splice donor and acceptor sites within the *env* gene (Figure 3.1). Since the *Renilla* luciferase gene is localized between the splice donor and acceptor sites, only unspliced RNA in the cytoplasm will yield luciferase activity [142]. When pHM*Rluc* was transfected with and without the Rem expression vector, a Rem-specific activation response was observed only in the presence of Rem. Rem activity also requires the nuclear localization sequence [142]. These data suggest that a potential RmRE is located within the 3'-end of the MMTV genome.

3.1.1 A 476-NT RMRE IS LOCALIZED AT THE JUNCTION OF THE MMTV ENVELOPE GENE AND THE 3' LTR.

Mertz *et al*. have shown that insertion of the 496-nt BglII to ScaI fragment containing the junction of the MMTV envelope gene and the 3' LTR in pHMΔeLTR*luc* had the same level of Rem activity as the wild-type pHM*Rluc* vector. Since this 496-bp fragment displayed the same Rem response as the wild-type RmRE, several deletion mutations were introduced into the BglII/ScaI fragment (1-496) to determine the minimal RmRE. A series of deletion mutations were introduced into the reporter vector, pHMΔeLTR*luc*, lacking the MMTV 3' LTR, but terminating in a simian virus 40 polyadenylation signal. These mutations resulted in several pHMΔeLTR+XR*luc* vectors (Figure 3.1). Each deletion mutant was transfected with and without N-terminally GFP-tagged Rem into XC rat fibroblast cells to measure Rem responsiveness. Deletion of 10 or 20 nt from the 5'-end did not affect Rem responsiveness, whereas deletion of 30 nt greatly reduced the Rem response. All deletions of more than 40 nt from the 5'-end completely abolished the Rem response (Figure 3.2A). On the other hand, deletions at the 3'-end gradually decreased the Rem response, with the 150-nt deletion mutant still showing a partial Rem response of about 2-fold (Figure 3.2B). Therefore, the minimal wild-type RmRE has been defined as a 476-nt sequence located at the junction of the MMTV envelope gene and the 3' LTR (Table 3.1).

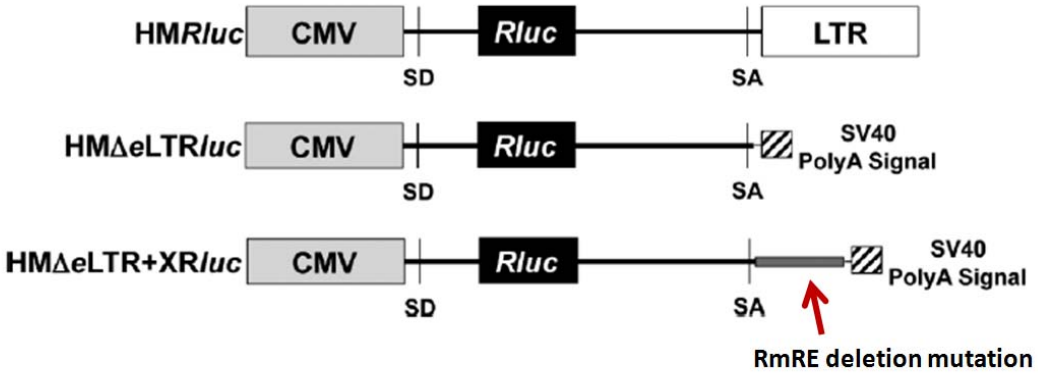

Figure 3.1: Reporter constructs used for the determination of the minimal RmRE.

Gray, Black, white, and hatched boxes represent the cytomegalovirus promoter, the *Renilla* luciferase gene, the MMTV 3' LTR and simian virus 40 (SV40) polyadenylation sequences, respectively. SD, splice donor; SA, splice acceptor.

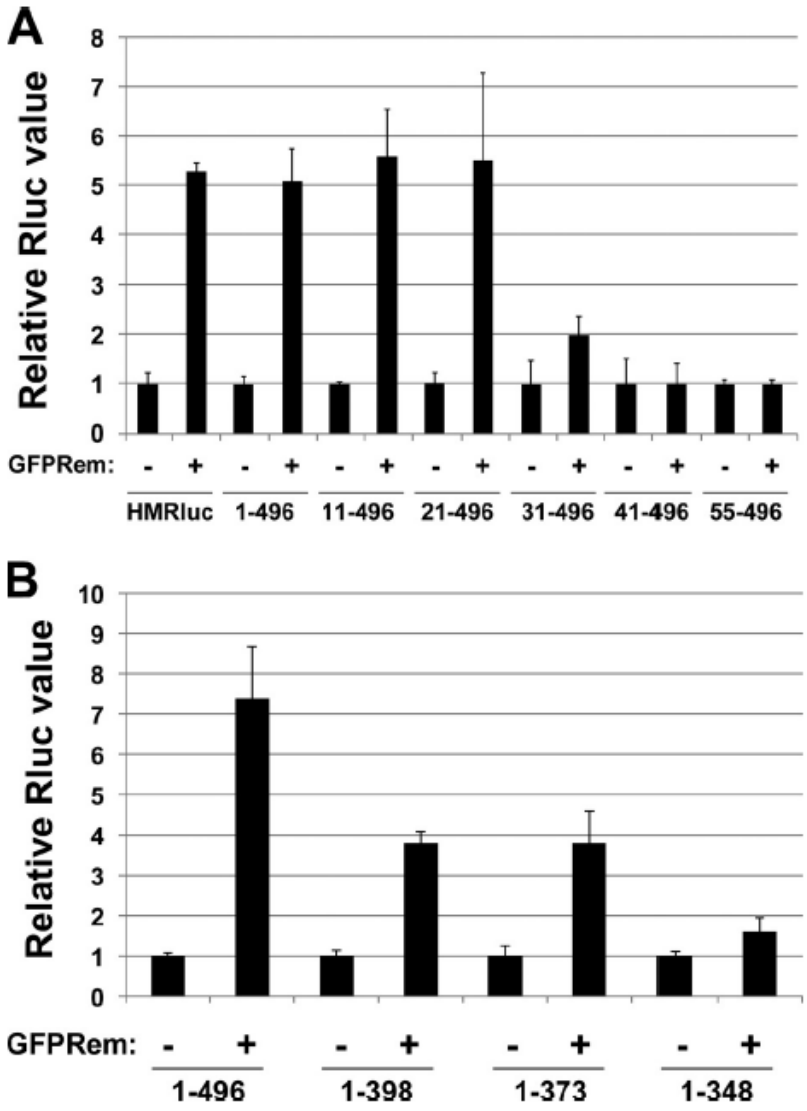

Figure 3.2: Serial deletions in the Env-LTR junction to define the minimal response element.

XC cells were transfected with 5'-deletion mutants (A) and 3'-deletion mutants (B) with and without the N-terminally GFP-tagged Rem expression vector, GFPRem. Each transfection without the Rem expression vector was set to 1. The average and standard deviations of triplicate transfections are shown. Additional details are available in materials and methods.

Reporter gene activity of RmRE deletion and substitution mutants

RmRE construct	Relative Rem response[a]
	%
Wild-type (1–496)	100 ± 14[b]
11–496	110 ± 21
21–496	108 ± 38
31–496	39 ± 7.1
41–496	0
55–496	0
1–398	50 ± 4.0
1–373	51 ± 11
1–348	21 ± 4.7
Δ50–369	8.9 ± 0.2

[a] Average luciferase activities of triplicate mutant transfections in XC cells are given relative to the wild-type (WT) RmRE construct (±S.D.).
[b] The Rem-dependent increase for the wild-type plasmid was 5–7-fold, which was designated as 100%.

Table 3.1: Summary of reporter activity of RmRE deletions.

When a previously isolated Rem sequence in our lab was compared to the sequences of several wild-type MMTV isolates, differences in 4 amino acids were observed. Mutations at three of the sites to restore the wild-type sequence resulted in no significant change in Rem activity. In contrast, the change at position 71 (proline to leucine) showed increased Rem activity and Rem cleavage (Figures 3.3A and 3.3B). With GFP-tagged Rem containing a proline at position 71, cleaved signal peptide (SP) is difficult to detect. However, GFP-RemP71L with a leucine at position 71 yields a strong band for GFP-SP using Western blotting (Figure 3.3A). To determine whether this more active form of Rem, RemP71L, requires the same minimal RmRE as the originally tested form of Rem, deletion mutants of the RmRE in the absence or presence of GFP-Rem (P71L) were tested in transient transfection of XC cells.

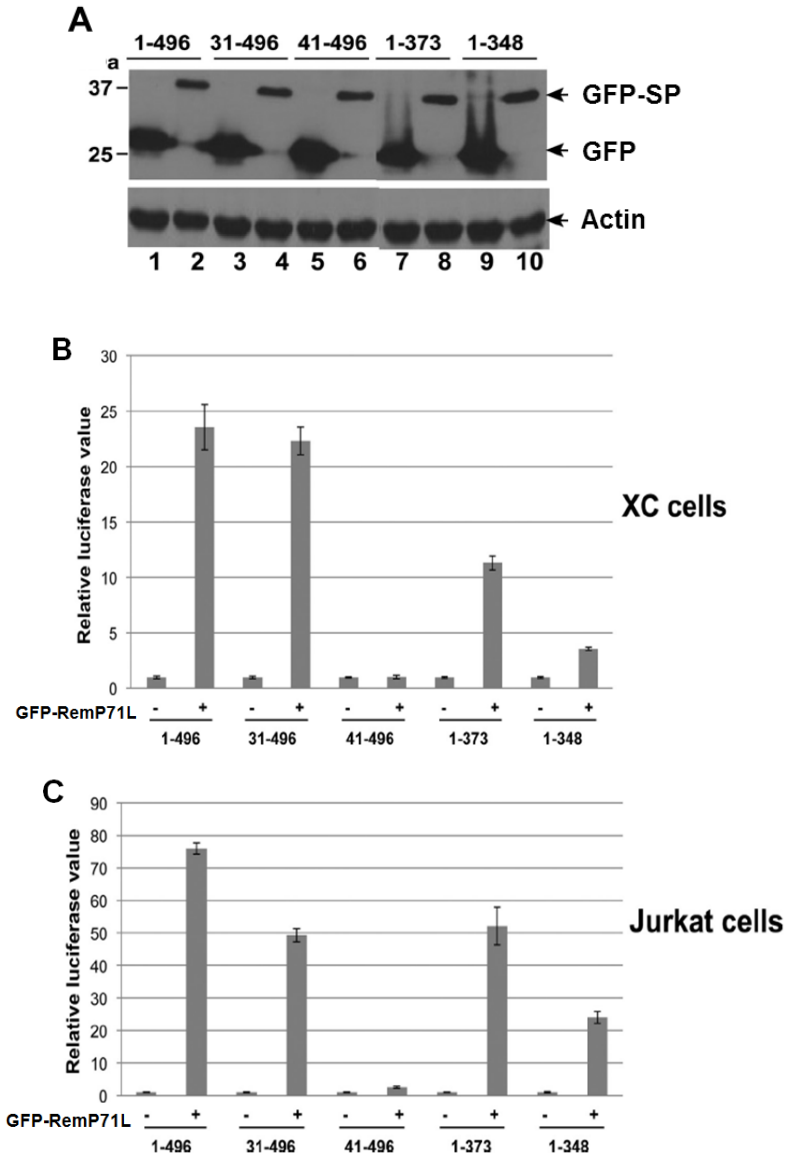

Figure 3.3: Response of the 5'- and 3'-RmRE deletion mutants of Rem with leucine at position 71 in XC cells and Jurkat human T cells.

(A) Western blotting of Jurkat cell extracts transfected with GFP-RemP71L using GFP-specific antibody (top panel). The blot was stripped and incubated with actin-specific antibody (bottom panel). (B) 5'- and 3'-RmRE deletion mutants were transfected into XC cells using GFP-RemP71L. (C) Jurkat cells were transfected with 5'- and 3'-RmRE deletion mutants with and without GFP-RemP71L. Results of luciferase assays are expressed as in Figure 3.2.

GFP-RemP71L showed greater induction of reporter activity (~22 fold) than the proline-containing (P71) Rem (Figures 3.3 and 3.2). Although the level of activation was different, the same minimal RmRE was required for both RemP71 and P71L. Deletions of more than 40 nt from the 5'-end resulted in complete loss of Rem responsiveness, whereas even deletion of 30 nt from the 5'-end showed response levels similar to the wild-type RmRE. Deletions from the 3'-end maintained partial activity, in agreement with the previous results (Figure 3.3B). Therefore, the same RmRE is required for the activity of Rem with either proline or leucine at position 71.

Expression of Rem in various cell types may require different cellular factors, which would affect the boundary of the RmRE. To check for that possibility, a Jurkat human T-cell lymphoma cell line was transfected with GFP-tagged RemP71L and the same 5'- and 3'-deletion mutants. Deletion of 40 nt from the 5'-end of the Bgl II/ Sca I fragment again eliminated the Rem response and the same prior pattern was repeated with the 3'-deletion mutants (Figure 3.3C). Since the same minimum RmRE was required in both XC cells and Jurkat T cells, the boundary for Rem responsiveness is likely not affected by cell type.

3.1.2 THE RMRE HAS A COMPLEX SECONDARY STRUCTURE.

Nuclease mapping experiments were performed to identify the possible secondary structures of the MMTV RmRE (Drs. Amanda Chadee and Rick Russell). The RmRE was digested with RNase T1, A and V1. RNase T1 causes cleavage at single-stranded G residues, whereas RNase A cleaves at single-stranded C or U residues. RNase V1 cleaves double stranded RNA positions without a nucleotide preference.

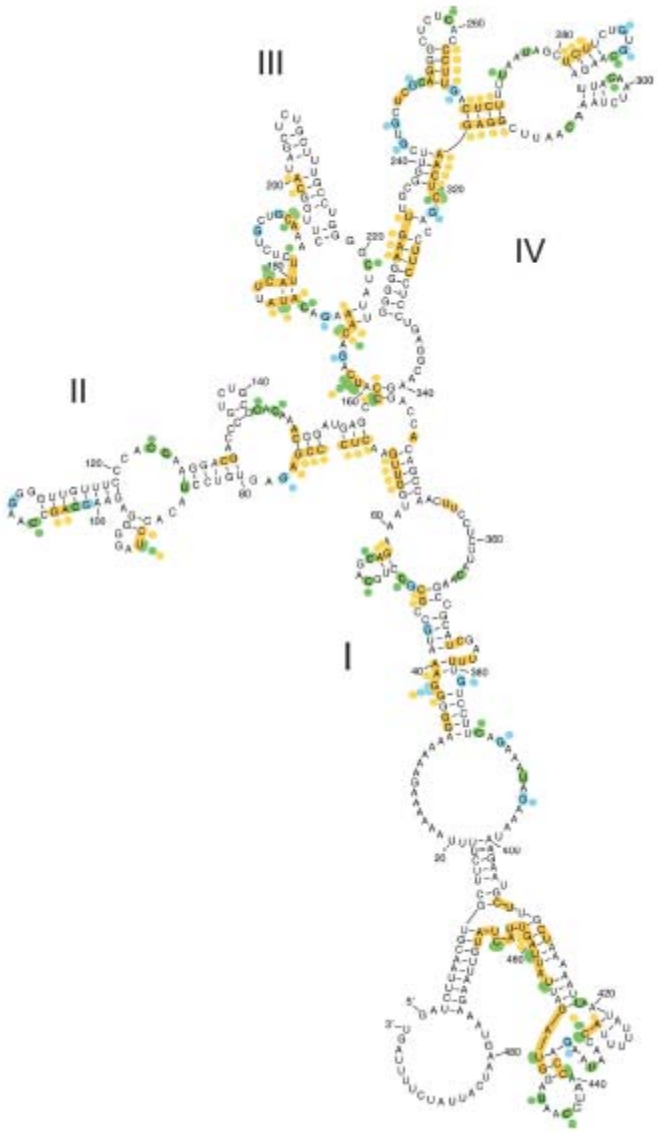

Figure 3.4: Secondary structure prediction of the MMTV RmRE based on the functional assays and RNase mapping data.

Yellow, green, and blue colors represent cleavage sites of RNase V1, A, and T1 respectively. The shaded regions that are not indicated with circles represent nucleotides that reacted with the indicated RNase, but did not give a level of cleavage sufficient to warrant inclusion as a constraint in the prediction.

The RNase mapping data, which suggested the base pairing status within the RmRE structure, was used to put constraints on a web-based version of Mfold, an RNA secondary structure prediction program. These results suggested that the RmRE contains multiple stem-loops and many single-stranded regions as shown in Figure 3.4. This extensive and complex structure is typical of the response elements of complex retroviruses, such as the HIV RRE [39, 71, 209]. However, this structure is different from the one suggested by Müllner *et al*., which is similar to a constitutive transport element found in the betaretrovirus, Mason-Pfizer monkey virus [149].

3.1.3 THE FUNCTION OF THE RMRE AT THE JUNCTION OF THE MMTV ENVELOPE GENE AND THE 3' LTR.

One of the HIV regulatory proteins, Rev, is known as a nuclear export protein and its function is dependent on binding to an RRE on unspliced and partially spliced HIV mRNAs [134]. The MMTV-encoded Rem protein has a nuclear export function for the export of unspliced *gag-pol* mRNA, which is critical for MMTV replication [142]. In addition to its functional similarity, the MMTV RmRE overlapping the 3' LTR has significant structural similarity to the RRE. Nevertheless, the 3' RmRE appears in both unspliced and spliced MMTV mRNAs (Figure 3.5). Unlike the RRE, the RmRE is not specific to intron-containing mRNAs and is present in all MMTV mRNAs.

Recent studies in our lab also have shown that Rem, Rev and Rex1 do not affect export or stability of unspliced RmRE-containing reporter transcripts [141]. No differences in nuclear and cytoplasmic mRNA levels were observed in the presence or absence of Rem, Rev and Rex1 in RNA fractionation experiments as detected by RT-PCR for the pHM*Rluc* reporter vector. Differential nuclear and cytoplasmic mRNA

distribution was documented in the control experiment using Rev with the homologous HIV-based reporter vector (pDM128) containing the RRE. Rev expression increased cytoplasmic levels of the unspliced transcript from pDM128. Although our pHM*Rluc* reporter vector was designed with a *Renilla* gene between the splice donor and splice acceptor to detect nuclear export, our results did not support this conclusion. These results suggest that the RmRE overlapping the 3' LTR might be important for another Rem function, for example, translation [141]. Since Rem also affects nuclear export of unspliced MMTV RNA [142], the data suggest that a separate RmRE may be localized to the 5'-end of the viral genome.

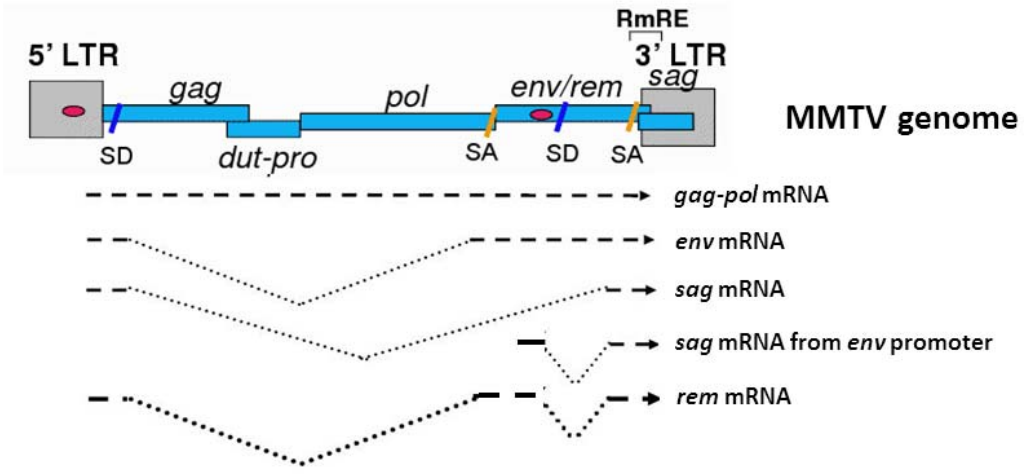

Figure 3.5: RmRE at the 3' LTR is present in all MMTV mRNA.

Light gray boxes represent the 5' and 3' LTRs. Blue boxes correspond to the MMTV encoding genes. Red oval shapes represent MMTV promoters. Dotted lines represent MMTV mRNAs. V-shaped dotted lines show introns: SD, splice donor; SA, splice acceptor.

3.2 MMTV REM IS PROCESSED BY SIGNAL PEPTIDASE IN THE ENDOPLASMIC RETICULUM (ER) AND RETROTRANSLOCATED FOR NUCLEAR FUNCTION.

Rem contains an N-terminal SP of 98 amino acids. This SP is unusually long and contains many functional elements including a nuclear localization signal (NLS), an arginine-rich motif (ARM), a nuclear export signal (NES), and a hydrophobic domain [29, 142]. SP can be produced from both Rem and Env proteins and is localized primarily in nucleoli [142]. These data suggest that, unlike other ER signal peptides, which are typically about 23 amino acids in length and rapidly degraded in the ER, MMTV SP must avoid degradation in the ER membrane prior to nuclear entry.

3.2.1 SIGNAL PEPTIDE (SP) IS A DOMINANT PRODUCT OF REM IN MMTV-INFECTED CELLS.

Previous studies by Mertz *et al*. have shown that when cells are transfected with a GFP-SP fusion construct, SP functions similarly to full-length Rem in an pHM*Rluc* reporter assay, verifying that SP contains all the functional motifs for reporter activity [142]. Dultz *et al*. have shown that SP is generated in the presence of microsomal membranes [48]. These results suggest that most full-length Rem is cleaved to produce SP. To determine which form of Rem is expressed, whole cell lysates from MMTV-infected cells were analyzed with Western blotting and antibodies prepared against the NLS/RNA-binding motif within SP. Only the 12 kDa SP was detected using whole cell lysates from GR-B2 cells, a mouse mammary tumor cell line that expresses GR-strain MMTV (Figure 3.6). Analysis of whole cell extracts from HC11 cells infected with C3H-MMTV or stably transfected with an infectious MMTV provirus also showed that SP, not full-length Rem, was detectable under these conditions. No band was detected from

uninfected HC11 cells, a normal mouse mammary cell line (Figure 3.6). Therefore, SP is a dominant form of Rem detected in MMTV-infected cells.

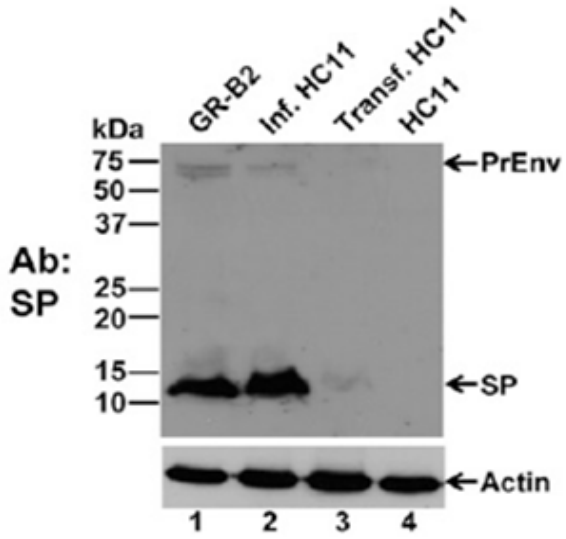

Figure 3.6: SP is a dominant product of the *rem* gene in MMTV-infected and transfected mammary cells.

Whole cell extracts from GR-B2 mammary tumor cells, HC11 cells infected with MMTV, HC11 cells stably transfected with the infectious provirus HYB-MTV, and uninfected HC11 cells were analyzed with SP-specific antibody by Western blotting. Actin levels are shown as a loading control.

3.2.2 ACTIVE SP IS GENERATED FROM EITHER *REM* OR *ENV* MRNA.

Rem is encoded from a doubly spliced MMTV mRNA and is translated in the same reading frame as the *env* gene (Figure 3.7A). SP is produced from both Rem and Env proteins [29]. Jaagsiekte sheep retrovirus (JSRV), another betaretrovirus, also expresses a signal peptide, known as JSE-SP, which has a function similar to MMTV SP [31, 83]. To compare the function of SP from Rem and SP from Env, increasing amounts (10 ng, 1 μg and 10 μg) of constructs expressing *rem* or *env* cDNA were transiently transfected into HC11 cells. All Rem experiments were conducted with the Rem construct encoding leucine at position 71 (RemP71L). Henceforth, RemP71L will be referred to as Rem. Mutations were also introduced into this parent construct. Transfection of either *rem* or *env* expression vectors with the pHM*Rluc* reporter plasmid resulted in dose-dependent increases in luciferase values (Figure 3.7B). In Western blots of the same cell extracts, SP was detected after either *rem* or *env* cDNA transfection. Thus, functional SP is produced from both Rem and Env (Figure 3.7C). The limited sensitivity of Western blotting made detection of SP possible only at the higher DNA concentrations.

Since doubly spliced *rem* mRNA can be produced from singly spliced *env* mRNA, the activity measured and attributed to *env* cDNA may result from Rem produced from *env* cDNA. To test this possibility, a mutation at the second splice donor site was introduced (Figure 3.7A).

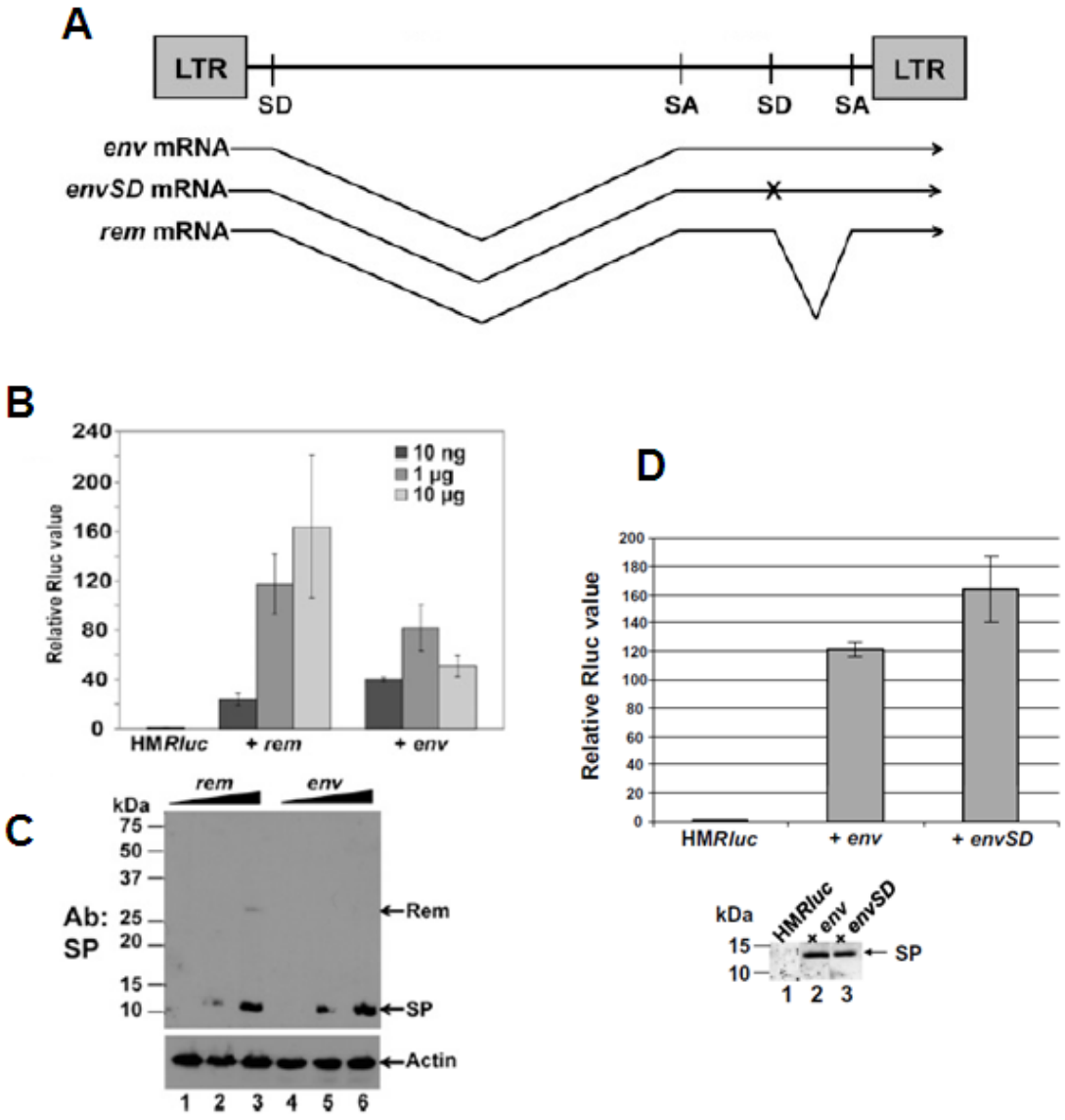

Figure 3.7: SP is generated from both *rem* and *env* mRNAs.

(A) Structure of *env* and *rem* mRNAs. SA, splice acceptor; SD, splice donor; x, mutation of the *env* splice donor site. (B) Dose-dependent activation of the *rem* and *env* mRNAs with the pHM*Rluc* reporter vector in HC11 cells. (C) Western blotting of the same whole cell extracts of HC11 cells transfected with either *rem* or *env* mRNA. (D) Rem activity after mutation of the second SD site of *env* mRNA. Luciferase assay (upper) and Western blotting of the same extracts (lower). Luciferase assay results are reported as described in Figure 3.2.

Transient transfections of this SD mutant into a human T lymphoma cell line (Jurkat) showed no differences in either luciferase reporter activity or SP levels by Western blotting (Figure 3.7D) compared to the wild-type Env expression construct. These results confirm that functional SP is generated from both *rem* and *env* mRNAs.

3.2.3 MUTATION OF GLYCOSYLATION SITES IN THE REM C-TERMINUS DOES NOT AFFECT SP FUNCTION.

Rem contains two N-glycosylation sites at positions 127 and 143 in a region shared with the SU protein, a part of the C-terminus [48]. Dultz *et al*. have shown that the treatment of cells with endoglycosidase H leads to a reduction in size of the Rem C-terminal gene product (RemCT), detectable by Western blotting. This result suggests that the RemCT is glycosylated [48]. To investigate whether glycosylation affects Rem processing or function, point mutations of one or both glycosylation sites (N127Q, N143Q and N127Q/N143Q) were introduced. Cells (293 human embryonic kidney) were transiently co-transfected with the pHM*Rluc* reporter plasmid and expression constructs for either wild-type Rem or the glycosylation mutants. Western blots of transfected cell extracts showed that a small portion of full-length Rem protein is glycosylated. Using either of the single site mutants (N127Q or N143Q), the size of glycosylated Rem was decreased. Mutation of both sites (N127Q/N143Q) eliminated glycosylated Rem. None of the mutations affected the size of SP. Further, Rem cleavage to SP was not affected by mutations of the glycosylation sites since wild type Rem and each of the mutants generated SP (Figure 3.8A). Extracts from the transient transfection of all glycosylation site mutants revealed no difference in luciferase activity compared to wild-type Rem (Figure 3.8B). Therefore, glycosylation sites do not affect Rem processing or function.

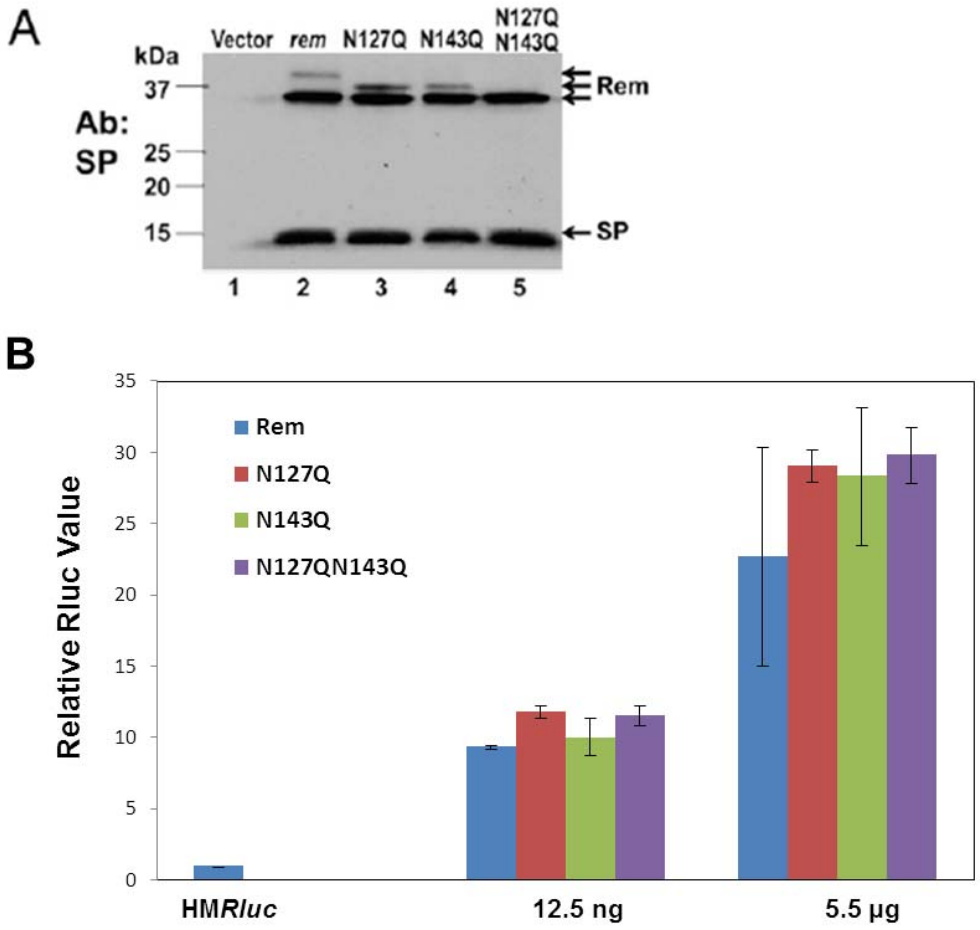

Figure 3.8: Glycosylation of the Rem C-terminus.

(A) Western blotting of whole cell extracts from 293 cell transfections of wild-type Rem and Rem glycosylation site mutants (single or double). SP-specific antibody was used. (B) Luciferase reporter activity of wild type Rem and single or double glycosylation site mutants in 293 cells. Results are reported as described in Figure 3.2.

3.2.4 MUTATION OF THE REM SIGNAL PEPTIDASE CLEAVAGE SITE INHIBITS REM PROCESSING AND FUNCTION.

Studies by Dultz *et al*. have shown that SP is generated from Rem in the presence of rough microsomes during in vitro transcription/translation. They also showed signal peptide peptidase (SPP)-independent release of SP from microsomal membranes [48], implying that ER signal peptidase is involved. To test whether ER signal peptidase is crucial for SP processing, mutations in the predicted cleavage site were introduced. In general, ER signal peptidase cleavage sites have preferred amino acids at both positions -1 and -3. Therefore, two signal peptidase cleavage mutations, G98R (mutation at position -1) and V96RG98R (mutations at both positions -1 and -3) were introduced into Rem (Figure 3.9A). The same mutations were also introduced into Env. Expression constructs for wild-type Rem, Env and their cleavage site mutants were transiently transfected into HC11 cells. Western blotting of cell extracts from the transfections, using an SP-specific antibody, revealed that none of the signal peptidase cleavage site mutants expressed from *rem* or *env* cDNAs produced SP (Figure 3.9B). A large Env precursor band was observed in cells transfected with *env* cDNA expressing the cleavage site mutations. In contrast, the Rem precursor was difficult to detect. Actin levels from all samples were equivalent. In addition, functional assays with the pHM*Rluc* reporter vector and signal peptidase cleavage site mutants showed that all of the mutated forms of *rem* and *env* completely lost Rem activity, presumably due to their inability to produce SP. Therefore, these results indicate that SP cleavage by ER signal peptidase is important for both Rem and Env processing and function.

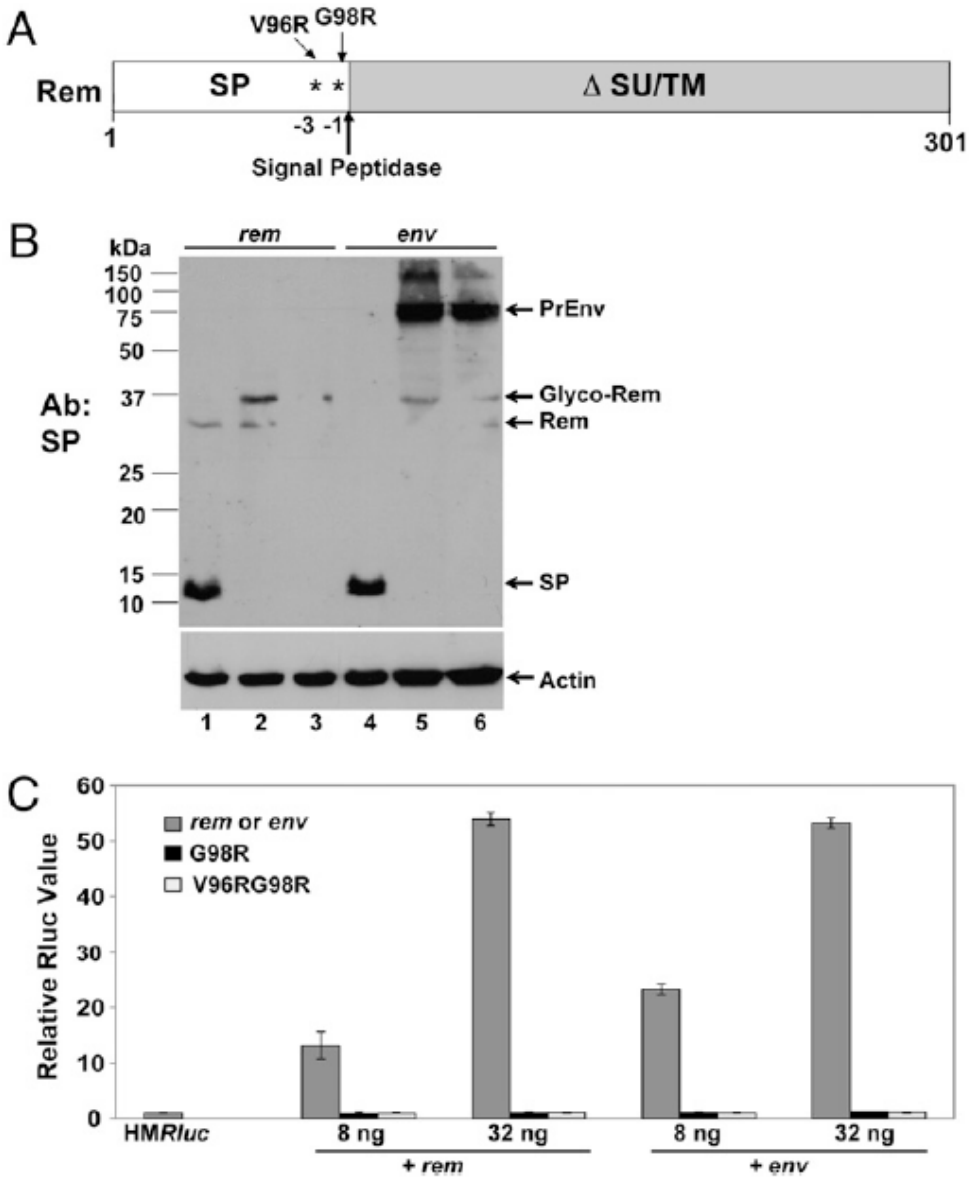

Figure 3.9: Inhibition of SP cleavage by ER signal peptidase prevents Rem function.

(A) Diagram of Rem with cleavage site mutations. (B) Western blotting of HC11 cell extracts after transient transfection. Lane 1: wild-type *rem*, lane 2: *rem* G98R, lane 3: *rem* V96RG98R, lane 4: wild-type *env*, lane 5: *env* G98R, lane 6: *env* V96RG98R. The upper panel shows the Western blots with SP-specific antibody, and the lower panel shows the same extracts with actin-specific antibody. (C) Reporter assay of the same transfection with wild-type and mutants of *rem* or *env*.

Similar to HIV Rev, N-terminally GFP-tagged wild type Rem localizes in the nucleoli [142]. To compare the localization of the wild-type and cleavage site mutants, constructs expressing GFP-tagged wild-type Rem or Rem with the cleavage site mutations, G98R and V96RG98R, were co-transfected with an ER-mCherry construct. The ER-mCherry construct contains a calreticulin ER signal peptide followed by a red fluorescent protein (RFP). At the end of the RFP, an ER retention signal, KDEL, was introduced. Therefore, ER-mCherry acts as an ER marker, causing a red fluorescent signal that is localized in the ER. After a 48 hr incubation, transfected cells were fixed and treated with DAPI for nuclear staining. Since both cleavage site mutants displayed lower protein expression levels, a higher concentration of both mutants (6 μg vs. 0.25 μg of wild-type Rem) was used for transfection.

Under a fluorescence microscope, wild-type Rem showed nucleolar localization as in previous studies, whereas both G98R and V96RG98R cleavage mutants did not localize to the nucleus (Figure 3.10A). Figure 3.10B indicates the percentage of cells marked with each color, red (ER-mCherry) and green (GFP-tagged wild-type Rem or the mutants), relative to the total cell number indicated by the blue DAPI-stained cells. The results show that both G98R and V96RG98R mutant proteins overall had very weak GFP signals, possibly because the mutant proteins were unstable or incorrectly folded. The same pattern was observed in 2 other cell lines, XC and HC11 (data not shown). Transfection of 0.25 μg of wild-type *rem* and 6 μg of either cleavage site mutant constructs had similar protein expression levels in Western blots (Figure 3.10C). Observation with a confocal microscope confirmed that both mutants were not localized in the nucleoli (Figure 3.11). The exact localization of the mutant proteins was not obvious. These results confirmed that cleavage site mutants, which are not able to be

cleaved by ER signal peptidase, are unstable and do not localize to nucleoi. Therefore, SP cleavage by ER signal peptidase is essential for both Rem processing and stability.

Subcellular fractionation of HC11 and 293 cells transiently transfected with wild-type Rem and cleavage site mutant expression vectors was performed to determine the localization of mutant proteins using the NE-PER™ Nuclear and Cytoplasmic Extraction Reagents (Pierce) and the ProteoExtract® Subcellular Proteome Extraction Kit (Calbiochem). Both wild-type and mutant Rem proteins were detected in all fractions when Western blotting was performed (data not shown). Antibodies specific to GAPDH (cytoplasmic fraction), calnexin (membrane fraction), and Cux1 (nuclear fraction) were used to verify fractionation steps. Whereas calnexin and Cux1 were detected in the expected fractions, GAPDH was detected in all fractions, which may indicate contamination by the cytoplasmic fraction. Since fractionation experiments were performed in cells transfected with excessive concentrations of Rem expression vectors to enhance detection, this may have compromised the results.

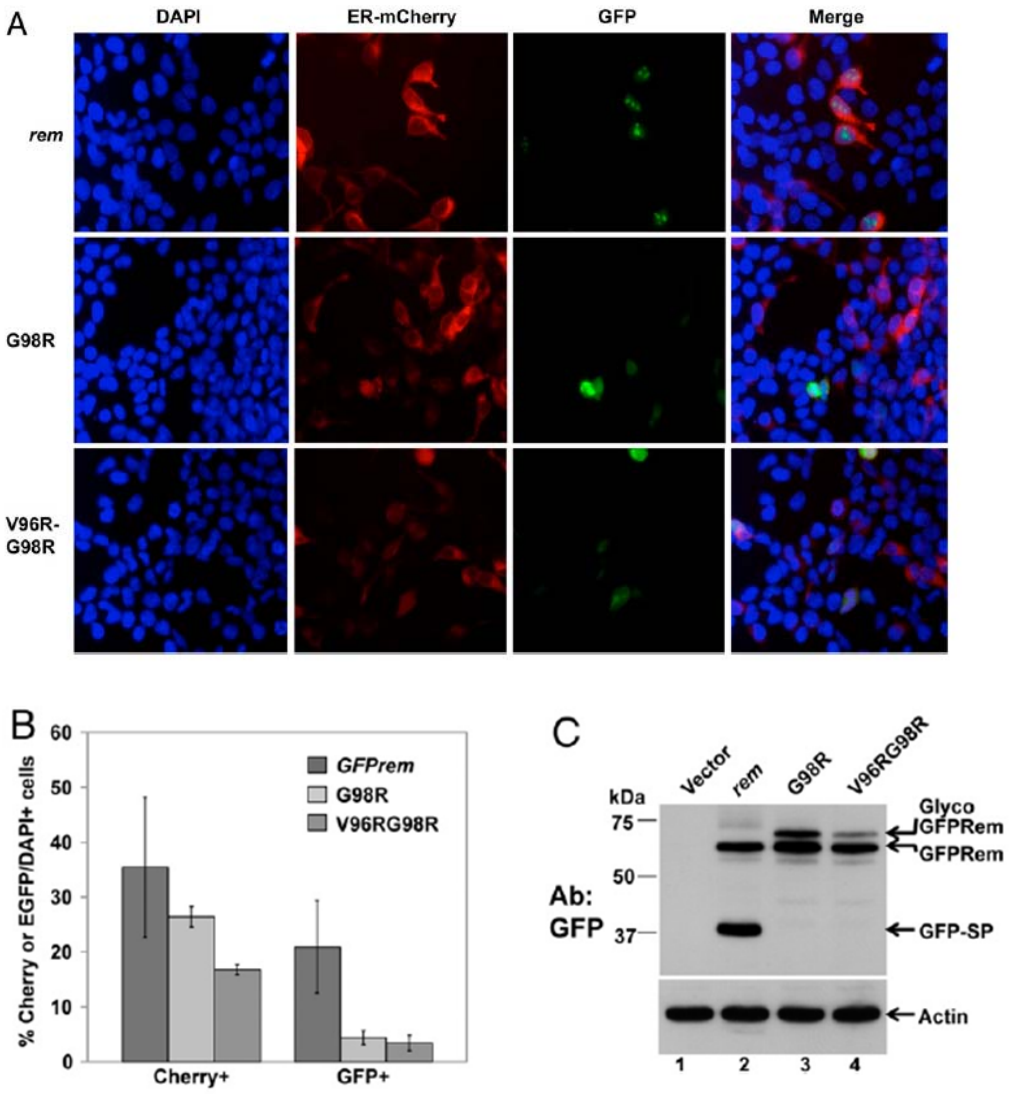

Figure 3.10: GFP-tagged Rem of cleavage site mutants show minimal fluorescent signal.

(A) Fluorescent microscopy of GFP-tagged Rem wild-type and cleavage site mutants. Both mutants were transiently transfected into 293 cells with 0.25 µg of wild-type *rem* or 6 µg of the mutant constructs together with 0.2 µg of ER-mCherry. Cells were treated with DAPI for nuclear staining. (B) Quantitation of fluorescence of wild-type Rem and both mutants, determined by calculating the percent of mCherry+ or GFP+ cells compared to the number of DAPI+ cells. Cell numbers were counted in each of three fields. (C) Western blotting of GFP-tagged wild-type Rem and cleavage-site mutants after incubation with GFP-specific antibody (top panel) or actin-specific antibody (lower panel).

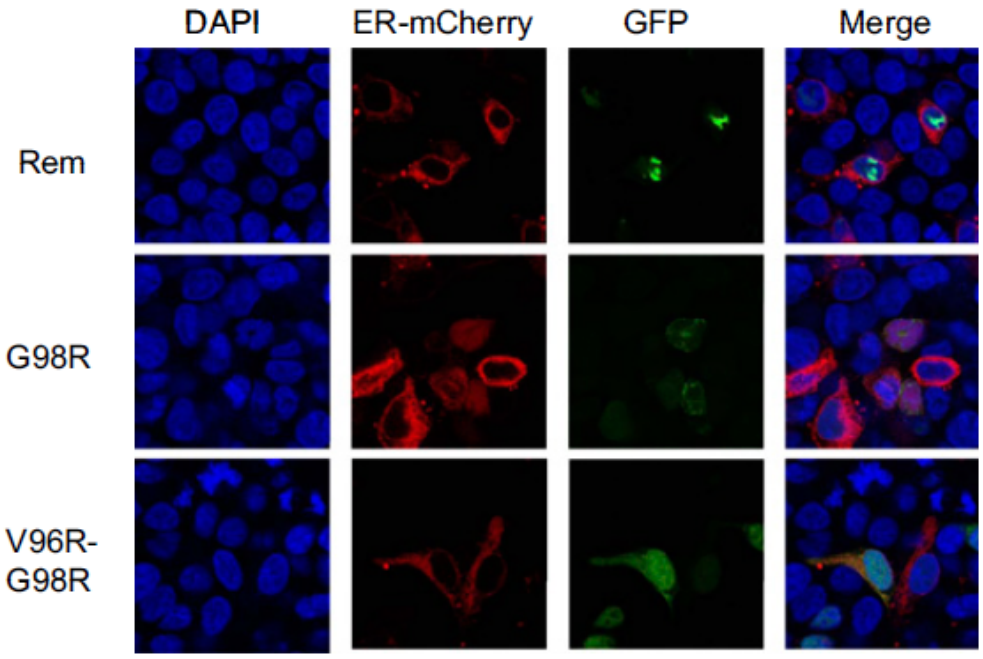

Figure 3.11: Mislocalization of Rem cleavage-site mutants.

Confocal microscopy of 293 cells transiently transfected with GFP-tagged wild-type *rem* (0.25 µg) and cleavage-site mutant constructs (1 µg of G98R and 6 µg of V96RG98R) together with 0.2 µg of the ER-mCherry construct. After 48h, cells were treated with DAPI for nuclear staining. Green and red fluorescence of both mutants was artificially enhanced to allow visualization.

3.2.5 PROTEASOME INHIBITORS AFFECT REM PROCESSING AND ACTIVITY.

During translation, Rem is directed to the ER for cleavage. When membrane and extracellular cellular proteins are directed to the ER during translation, various sensor/chaperone proteins that reside in the ER provide protein quality control monitoring the folding of each newly synthesized protein. Unfolded or defective proteins are retrotranslocated to the cytoplasm by this ER-associated degradation (ERAD) system to prevent ER stress. Defective and misassembled proteins are degraded by the 26S

proteasome in the cytoplasm [8, 81, 222]. Some bacterial toxins, such as the cholera toxin, and viral proteins, such as human cytomegalovirus (HCMV) US2 and US11, are known to manipulate ERAD, allowing retrotranslocation of toxins or cellular proteins to the cytoplasm for their benefit [8, 229].

To test whether the proteasome affects Rem processing, two proteasome inhibitors, lactacystin and MG132, were added to cells transiently transfected with *rem* expression constructs. Each inhibitor (10 μM) was added 12 hr prior to harvesting the cells. Since both inhibitors were prepared by dissolving them in DMSO, the same volume of DMSO was added to sets of control cells. Following the treatment with lactacystin, an accumulation of SP as well as full-length GFPRem was observed. Full-length GFPRem stabilization was more dramatic (Figure 3.12A, lanes 1 and 2). Transfection of a known substrate for retrotranslocation, the α1-antitrypsin mutant, null Hong Kong (NHK) QQQ-GFP, also showed accumulation in the presence of lactacystin (Figure 3.12A, lanes 3 and 4). The second proteasome inhibitor, MG132, also showed a similar effect on Rem processing (Figure 3.12B). Again, treatment with MG132 increased the levels of SP and, more dramatically, full-length GFPRem. Therefore, these results suggested that SP preferentially avoids proteasomal degradation after Rem cleavage in the ER.

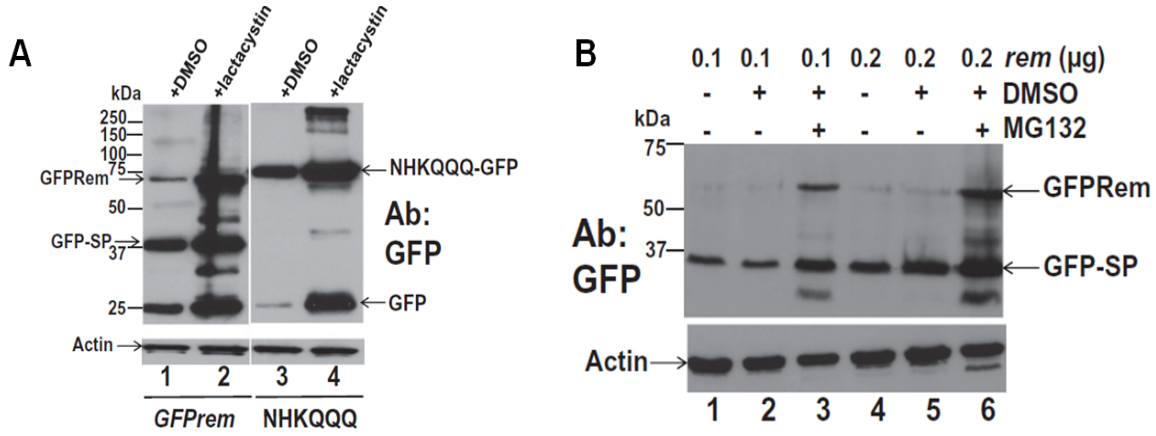

Figure 3.12: Proteasome inhibitors, lactacystin and MG132, increased protein levels of both GFP-SP and full-length GFPRem.

(A) Western blotting of HC11 cell extracts transfected with constructs expressing GFPRem or a C-terminally GFP-tagged α1-antitrypsin mutant (NHKQQQ-GFP). Cells were treated with DMSO or lactacystin (10 µM) in DMSO. (B) Western blots of HC11 cells transiently transfected with constructs expressing GFPRem. The amounts of DNA transfected are indicated. Cells were treated with DMSO or MG132 (10 µM) in DMSO. Both blots were screened for GFP-tagged proteins using a GFP-specific antibody. Actin-specific antibody confirmed uniform protein loading.

To determine whether the protease inhibitor, MG132, affects SP function, HC11 cells transiently transfected with either *env* or *rem* constructs were treated with MG132. As shown in Figure 3.13, MG132 led to an increase of SP function. This result might be due to increased SP levels resulting from treatment with MG132, as shown in Figure 3.12B.

Since the Rem precursor is preferentially susceptible to proteasomal degradation relative to SP, it is possible that the proteasome is involved in the SP retrotranslocation process.

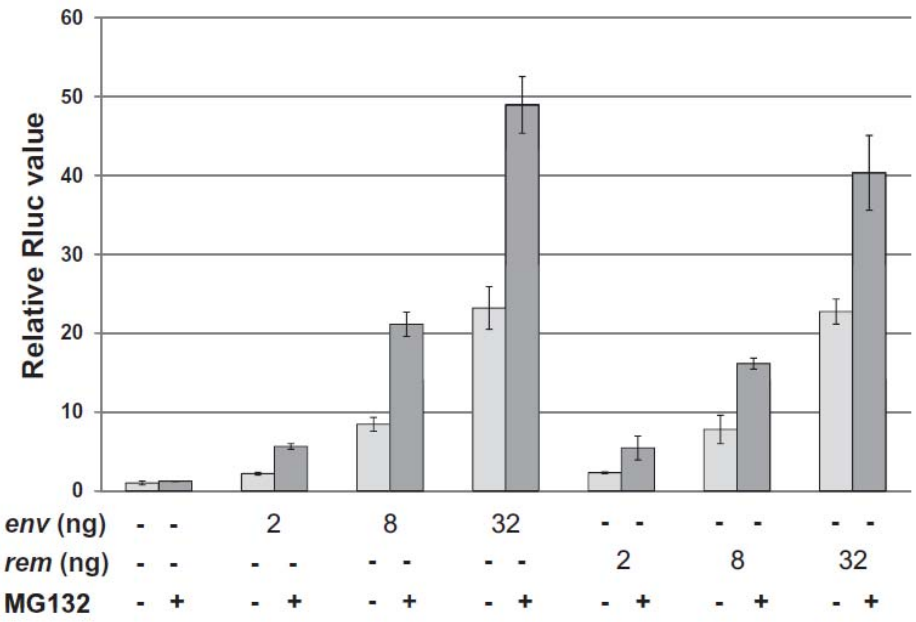

Figure 3.13: Proteasome inhibitor MG132 induces Rem activity.

HC11 cells were transfected with three different concentrations of either *env* cDNA or *rem* cDNA expression vectors. Cells were treated with DMSO or MG132 (10 μM) in DMSO for 12 h before extract preparation. Results are reported as in Figure 3.2, except that reporter vector controls were treated with DMSO.

3.2.6 DOMINANT-NEGATIVE P97/VCP PROTEINS AFFECT REM FUNCTION.

Most ERAD substrates are polyubiquitinated and retrotranslocated by the AAA ATPase p97/VCP and the 19S proteasome subunit [8, 151]. To determine whether p97/VCP is involved in the retrotranslocation of SP, a dominant-negative (DN) form of p97/VCP, p97QQ, was co-transfected with an expression construct for GFPRem and the luciferase reporter plasmid into 293 cells. The p97QQ protein has mutations in both ATPase domains [241]. As shown in Figure 3.14A and B, co-transfection of 5 μg of p97QQ inhibited Rem function, but it did not affect Rem processing since SP was

observed after Western blotting of the cell extract. The increased protein level of DN p97 due to the transfection was confirmed by Western blot. These results suggest that SP might be blocked during retrotranslocation by p97QQ after cleavage by signal peptidase, leading to a decrease in Rem activity. The same amount of p97QQ construct was shown to be functional when co-transfected with plasmids expressing NHKQQQ, a known substrate of retrotranslocation (Figure 3.15).

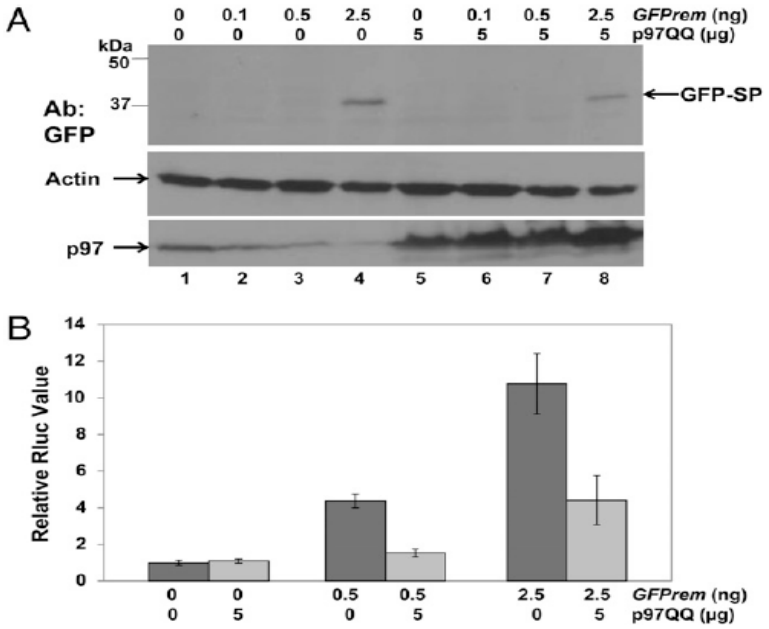

Figure 3.14: Dominant-negative p97/VCP, p97QQ, inhibits Rem activity, but not cleavage.

(A) Western blotting of 293 cell extracts transiently transfected with different amounts of constructs expressing GFPRem, with and without p97QQ (5 μg). GFP-specific antibody (top panel) and p97-specific antibody (lower panel) were used to detect GFP-SP and p97QQ, respectively. Actin-specific antibody was used to confirm equal protein loading. (B) Activity assay results for the transfection of constructs expressing GFPRem in the absence or in the presence of p97QQ. Results are reported as in Figure 3.2.

The protein levels of NHKQQQ were increased in the presence of DN p97, indicating that DN p97 inhibited the retrotranslocation of NHKQQQ and ERAD.

To determine whether DN p97 affected SP alone as well as full-length Rem, the same amount (2.5 ng) of constructs expressing GFPRem or GFP-SP were co-transfected with plasmid expressing DN p97. DN p97 did not affect the levels of either GFPRem or GFP-SP, but it inhibited the function of both (Figure 3.16). Therefore, p97 is required for the retrotranslocation of SP.

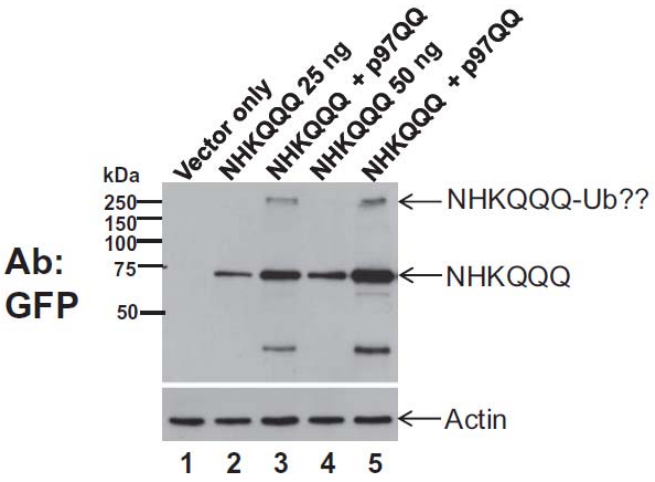

Figure 3.15: Dominant-negative p97/VCP, p97QQ, increased protein levels of the ERAD target NHKQQQ.

Western blotting of 293 cells transfected with plasmid expressing GFP-tagged α1-antitrypsin mutant NHKQQQ in the absence (lane 2 and 4) or in the presence (lanes 3 and 5) of p97QQ. NHKQQQ-expression vector (25 ng or 50 ng) and 5 μg of p97QQ expression vector were used. Whole-cell lysates (15 μg) were loaded and GFP-specific antibody was used to detect GFP-tagged proteins (upper). Blotting with actin-specific antibody confirmed equal protein loading. In the presence of p97QQ, possible polyubiquitinated NHKQQQ was detected.

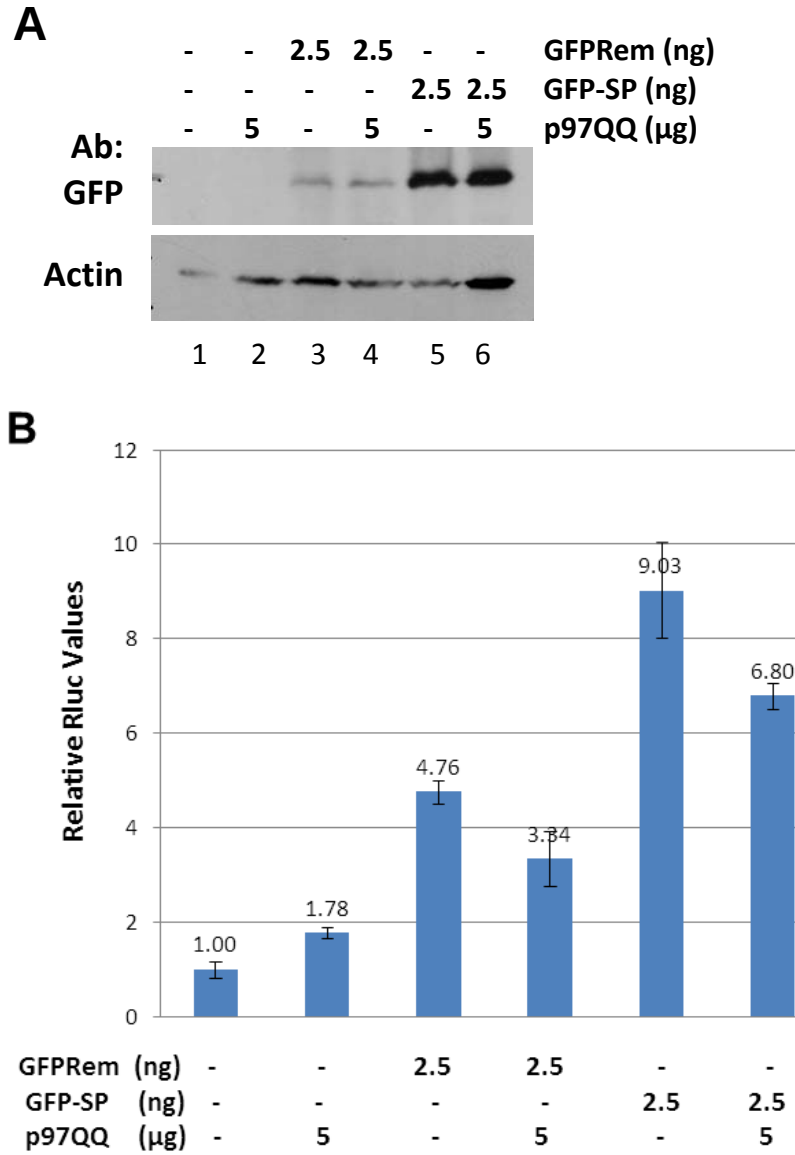

Figure 3.16: A DN p97/VCP inhibits the activity of both full-length Rem (GFPRem) and SP (GFP-SP).

(A) Western blotting of 293 cells transfected with 2.5 ng of vectors expressing GFPRem or GFP-SP in the absence and the presence of expression vectors for p97QQ (5 µg). GFP-specific antibody was used to detect GFP-tagged proteins (upper panel). Blotting with actin-specific antibody confirmed equal loading. (B) Luciferase activity was assayed to measure SP activity in the same transfected 293 cells. Results are reported as described in Figure 3.2.

3.2.7 DOMINANT-NEGATIVE DERLIN1 PROTEIN DECREASES REM ACTIVITY.

The Derlin protein family is known to be important for ERAD although the precise functions of these Derlin proteins in the ERAD system are not fully defined [8, 73]. Three members of the Derlin protein family, Derlin-1, -2, and -3, are found in mammalian cells. Both Derlin-1 and -2 are ubiquitously expressed, whereas Derlin-3 is expressed in a narrower range of tissues [158]. Cholera toxin is known to use Derlin-1 for retrotranslocation to the cytoplasm, whereas the exit of murine polyomavirus from the ER is dependent on Derlin-2 [13, 124]. In addition, the retrotranslocation of class I major histocompatibility complex (MHC) molecules by HCMV protein US2 and US11 involves Derlin-1 [125]. To determine whether Rem also requires the Derlin proteins for its retrotranslocation to the cytoplasm, dominant-negative forms of Derlin-1 and Derlin-2 (C-terminally GFP-tagged Derlin proteins) were used in reporter assays for SP function.

Initially, RT-PCR was performed to verify the expression of both Derlin-1 and -2 in HC11 and 293 cells. Derlin-1 and Derlin-2 mRNAs were detected in both cell lines as shown in Figure 3.17. To study the individual effects of Derlin-1 and Derlin-2 on Rem function, DN Derlin-1 or DN Derlin-2 was co-transfected with GFPRem in each cell line. The introduction of the DN Derlin-1 resulted in a greater repression of Rem activity than DN Derlin-2 in both HC11 and 293 cells (Figure 3.18). This result suggests that Derlin-1 is specifically involved in SP retrotranslocation. When a higher amount of Rem was introduced, the inhibitory effect by DN Derlin-1 was lost (data not shown).

To understand how Derlin-1 affects Rem activity, constructs expressing GFP-SP and DN Derlin-1 were co-transfected into 293 cells to compare with the activity of full-length GFPRem and DN Derlin-1. As shown in Figure 3.19A, the activity of GFPRem was decreased by DN Derlin-1, whereas GFP-SP was not significantly affected by DN Derlin-1. These results suggested that Derlin-1 recognizes the Rem C-terminus.

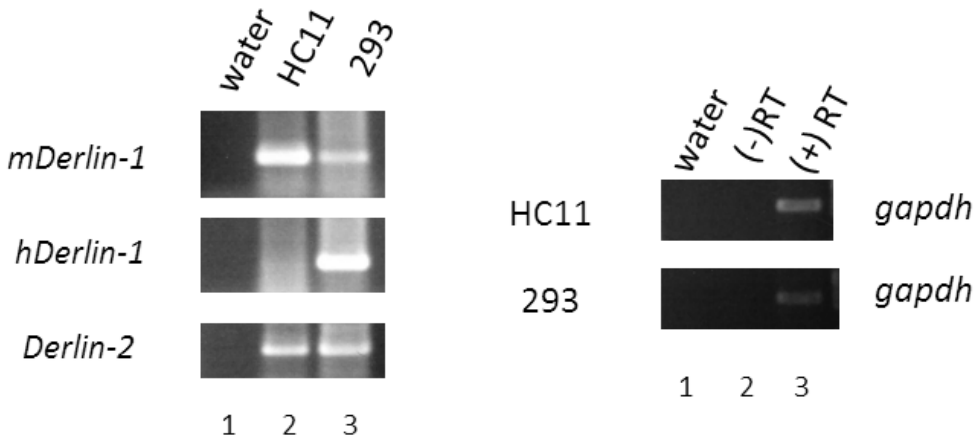

Figure 3.17: Both HC11 and 293 cells express Derlin-1 and Derlin-2 mRNAs.

Total RNA was isolated from HC11 mouse mammary cells and 293 human kidney epithelial tumor cells. For RT-PCR of *Derlin-1*, two different mouse specific (*mDerlin-1*) and human specific primers (*hDerlin-1*) were used. One set of primers for *Derlin-2* could detect both mouse and human *Derlin-2* mRNAs. RT-PCR with *gapdh* primers was performed as a control for RNA integrity.

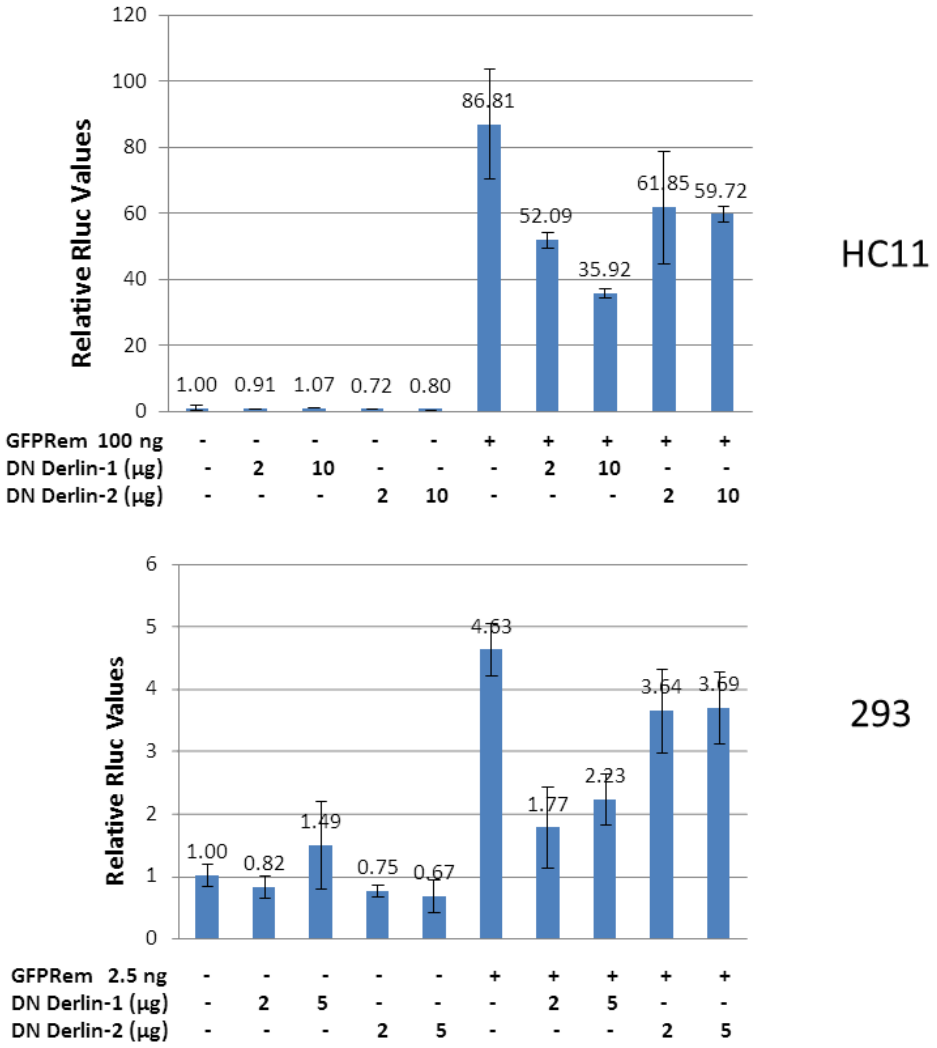

Figure 3.18: Dominant-negative Derlin-1 inhibits Rem activity.

GFPRem was co-transfected with two different concentrations of constructs expressing DN Derlin-1 and DN Derlin-2 in HC11 and 293 cells. In HC11 cells, 100 ng of GFPRem expression plasmid was co-transfected with 2 or 10 µg of DN Derlin-1 and DN Derlin-2. In 293 cells, 2.5 ng of GFPRem expression plasmid was co-transfected with 2 and 5 µg of DN Derlin-1 and DN Derlin-2. The luciferase value of the reporter vector co-transfected with an empty vector was set to 1 as described in Figure 3.2.

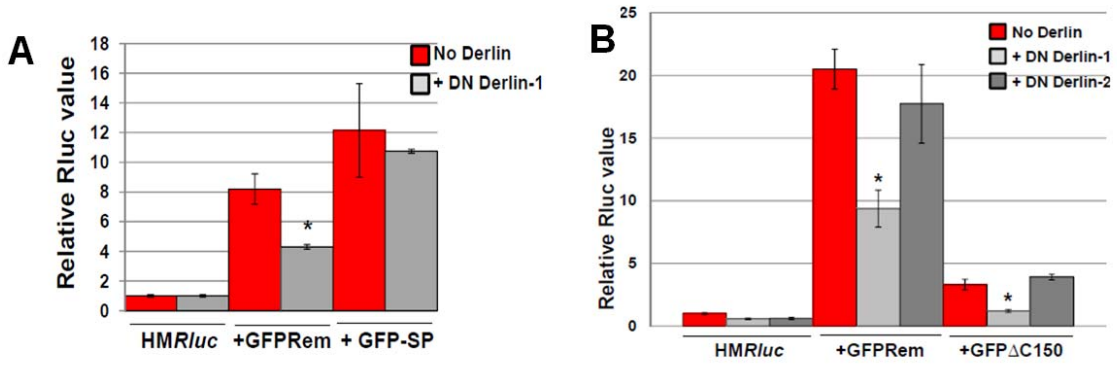

Figure 3.19: Dominant-negative Derlin-1 affects the activity of full-length Rem, but not SP alone.

(A) 293 cells were transiently transfected with 12.5 ng of GFPRem or GFP-SP expression constructs in the absence or in the presence of DN Derlin-1 (5 μg). Luciferase values of the pHM*Rluc* reporter vector with or without DN Derlin-1 were set to 1. (B) Plasmid expressing GFPRem or GFPΔC150 (12.5 ng) were co-transfected with either DN Derlin1 or DN Derlin2 expression constructs (each 5 μg) in 293T cells. The luciferase value of pHM*Rluc* vector co-transfected with an empty vector was set to 1. Values are reported as described in Figure 3.2.

GFPRemΔC150 (GFPΔC150), a construct containing Rem with a deletion of the C-terminal 150 amino acids, was also tested after expressing DN Derlin-1. Interestingly, DN Derlin-1 affected the activity of the C-terminal deletion mutant of Rem (GFPΔC150) as shown in Figure 3.19B. Therefore, the Derlin-1 response requires part of the Rem C-terminus, about 50 amino acids immediately following the SP. Since DN Derlin-1 did not affect GFP-SP, Derlin-1 might not be involved in the retrotranslocation step itself. Rather, recognition of Rem by the cellular ERAD system may require Derlin-1 before SP cleavage occurs, possibly by recognition of Rem as a misfolded protein.

3.3 COMMERCIAL shRNA VECTOR, pLK0.1-puro, INDUCES REM ACTIVITY.

To study the effect of p97/VCP on Rem retrotranslocation, commercially available shRNAs against p97 were utilized. Sigma shRNA vectors, a set of pLK0.1-based shRNAs (Figure 3.20A), were tested for their effectiveness in knocking down the level of p97/VCP. After screening the set of shRNAs, the most effective one, #4250, was co-transfected into 293 cells with GFPRem expression plasmid to confirm the effect of a dominant-negative p97/VCP vector, p97QQ, on Rem retrotranslocation. A shRNA control vector, LK0.1, and a non-effective vector, #4252, which contains p97-specific target sequences but does not knock down p97 protein levels, were also transfected as controls. Unexpectedly, all of the shRNAs tested, LK0.1 control, #4250 and non-effective #4252 induced Rem activity (Figure 3.20B). Because the shRNAs increased the Rem-induced expression levels from the pHM*Rluc* reporter, this phenomenon will be referred to as "super-induction". To understand how this super-induction was achieved, further experiments were executed with LK0.1 control vector since all of the shRNAs shared the LK0.1 vector backbone.

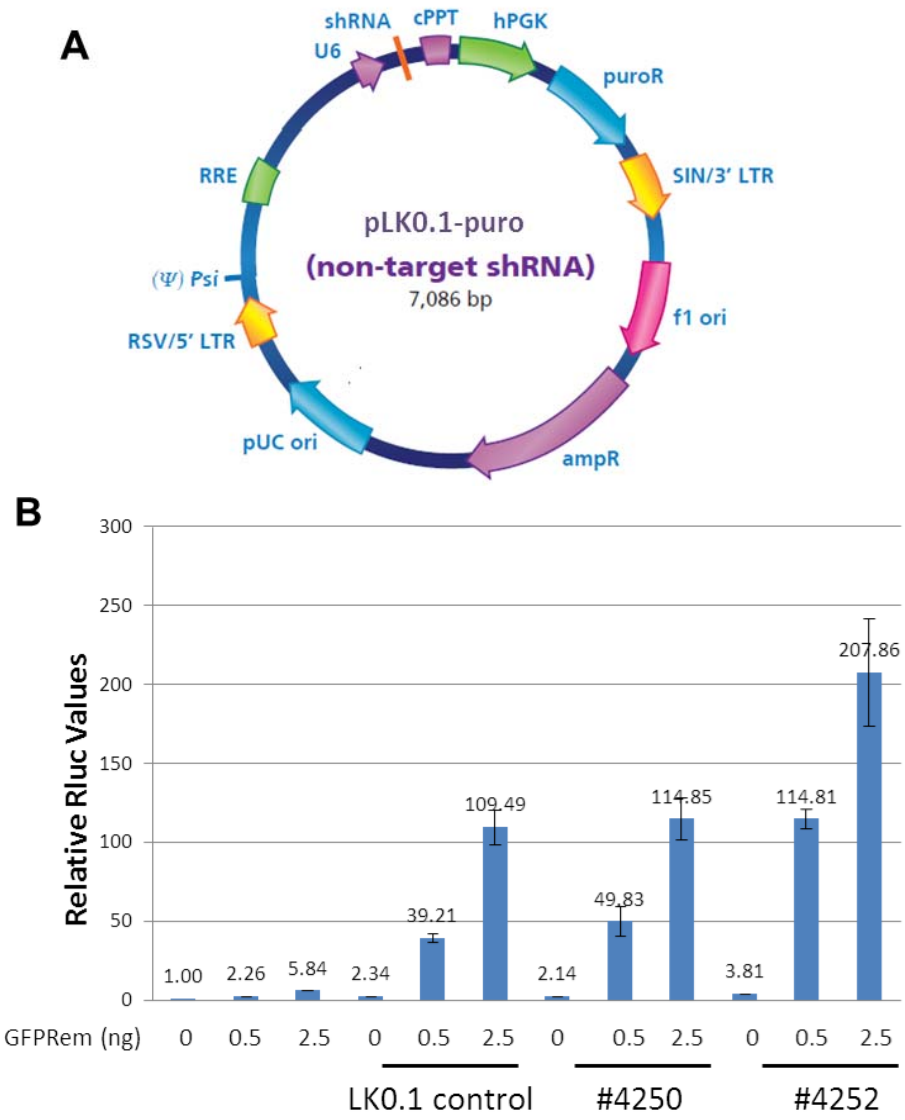

Figure 3.20: Commercial shRNA expression vector, pLK0.1-puro, gives Rem super-induction.

(A) Vector map of pLK0.1-puro. (B) Rem activity assay with 0.5 ng or 2.5 ng of GFPRem expression plasmid co-transfected with 5 µg of either LK0.1 control vector, #4250 p97/VCP-specific shRNA-containing vector, or #4252 non-effective p97/VCP shRNA-containing vector. A luciferase value of reporter vector co-transfected with an empty vector was set to 1 as described in Figure 3.2.

3.3.1 LK0.1 SUPER-INDUCES REM ACTIVITY AS WELL AS EXPRESSION LEVELS.

To confirm whether super-induction is Rem-specific, pHM*Rluc*, the Rem responsive reporter vector, was compared to pHMΔeLTR*luc*, which is not responsive to Rem because it lacks part of the RmRE. These reporter vectors were co-transfected with either Rem-expression vector alone, LK0.1 alone, or both Rem and LK0.1 expression vectors together into 293 and HC11 cells. With the pHM*Rluc* reporter vector, LK0.1 resulted in additional Rem activity in both cell lines. As expected, pHMΔeLTR*luc* reporter activity was not induced when Rem was introduced. Also pHMΔeLTR*luc* did not show super-induction of Rem activity when LK0.1 was added with Rem (Figure 3.21). Without Rem, LK0.1 induced a small (~2 fold) increase in reporter activity. However, super-induction was obviously dependent on the presence of the 3'LTR, which overlaps RmRE sequences. An additional transfection experiment using a deletion mutant of the RmRE with a smaller (40 nt) deletion (41-496 in Figure 3.2) gave the same result (data not shown). Therefore, super-induction of Rem activity by LK0.1 requires the RmRE. Since the same pattern was observed in both 293 and HC11 cells, super-induction by LK0.1 is not a cell-type specific phenomenon.

To determine whether the effect of LK0.1 was dose-dependent, two different amounts of LK0.1 control vector, 1 μg and 5 μg, were co-transfected with 2.5 ng or 12.5 ng of GFPRem expression plasmid in 293 cells. As shown in Figure 3.22A, the effect of LK0.1 was dose-dependent. Rem alone (2.5 ng) induced about a 3-fold increase in activity, whereas co-transfection of Rem expression plasmid with 1 μg of LK0.1 resulted in a 5-fold increase in activity. With the addition of 5 μg of LK0.1, an 18-fold increase in Rem activity was observed. Western blotting of cell extracts revealed that LK0.1 also increased protein expression levels (Figure 3.22B). The protein levels of GFP-SP were increased with co-transfection of LK0.1 by 1.6- to 10-fold and the increase in protein

levels was also LK0.1 dose-dependent. Therefore, super-induction of Rem activity may be due to increased protein levels.

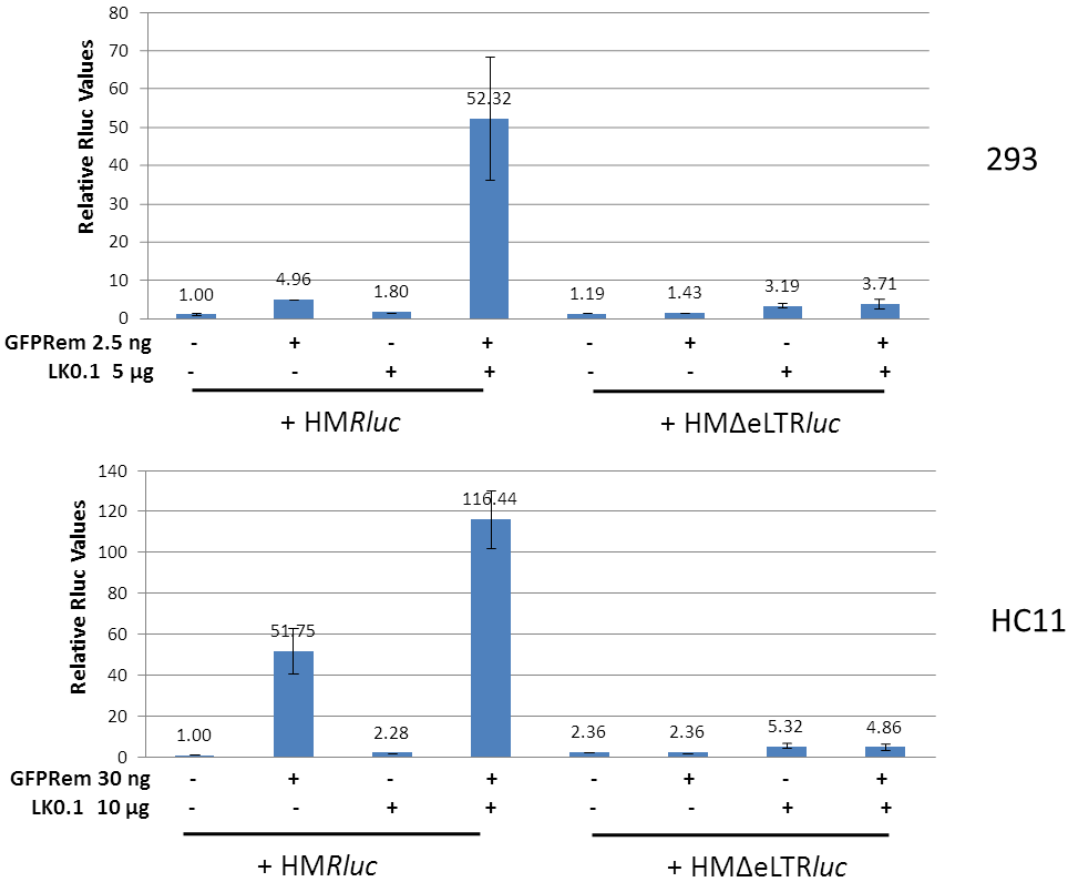

Figure 3.21: Rem super-induction by LK0.1 requires the RmRE in the reporter vector.

pHM*Rluc*, a reporter vector responsive to Rem, or pHMΔeLTR*luc*, which is not responsive to Rem due to deletion of the 3'LTR from pHM*Rluc*, was co-transfected with GFPRem expression plasmid in the absence or in the presence of LK0.1 in both 293 and HC11 cells. Rem and LK0.1 expression plasmids were used for 293 cells (2.5 ng and 5 µg, respectively) or HC11 cells (30ng and 10 µg, respectively). Luciferase value of pHM*Rluc* vector transfected with the same amount of empty vector from which the GFP gene was removed (ΔGFPN3) was set to 1 as described in Figure 3.2.

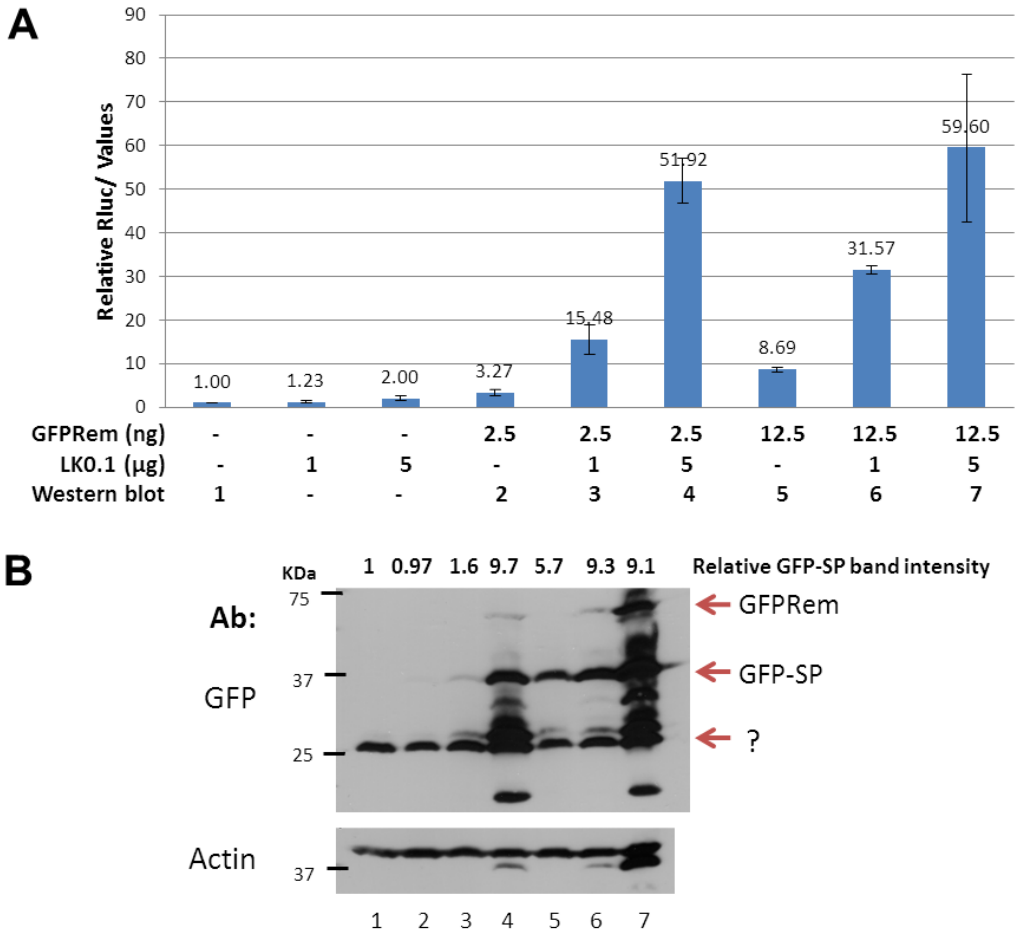

Figure 3.22: LK0.1 super-induces Rem activity as well as expression levels.

(A) Lucifease activity of the transient transfection of 2.5 ng or 12.5 ng of GFPRem expression vector with and without 1 µg or 5 µg of shRNA expression plasmid in 293 cells. Values are expressed as described in Figure 3.2. Western blot numbers indicate the lane numbers of the samples in the Western blot immediately below. (B) Western blotting with whole-cell extracts of the same transfection. GFP-tagged proteins were detected by GFP-specific antibody (upper). Actin blotting shows equal protein loading (lower). The question mark indicates an unknown protein detected by the GFP-specific antibody from Clontech. Relative GFP-SP band intensity is indicated. The intensity of the GFP-SP band is normalized to the intensity of the actin band of each lane and the normalized value of lane 1 is set to 1.

The activity of 12.5 ng of Rem expression vector was lower than the activity of 2.5 ng of Rem expression plasmid co-transfected with 1 µg of LK0.1, although the GFP-SP expression level of the former (Figure 3.22B, lane 5) was higher than that of the latter (lane 3). The increased SP protein levels did not correlate with increased activity. In our transfection system, a pGL3-control vector, which contains a firefly luciferase gene following the SV40 promoter, is used to normalize for transfection efficiency. Transfection of LK0.1 alone activated the control firefly vector (not Rem responsive) by about 2-fold (Figure 3.23). Although LK0.1 also induced the control vector, the induction was lower than that observed in the presence of Rem.

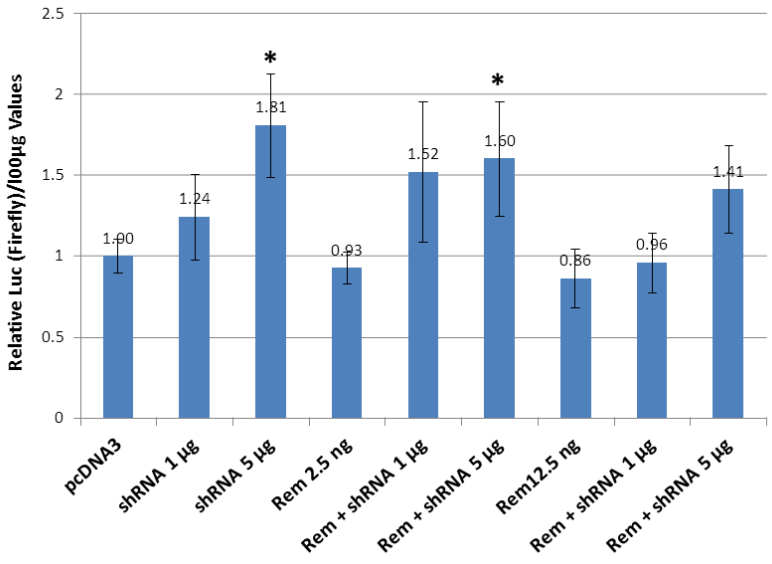

Figure 3.23: LK0.1 induces firefly luciferase values.

Firefly luciferase values of the transfection of pGL3-control vector from the same 293 transfection shown in Figure 3.22. The * indicates significantly induced firefly luciferase values ($P<0.05$) of LK0.1 shRNA relative to that of reporter vector with an empty vector, pcDNA3.

3.3.2 LK0.1 SUPER-INDUCES BOTH REV AND REX1 ACTIVITY, AS WELL AS THEIR EXPRESSION LEVELS.

Since Rem is one of several Rev-like proteins, it is possible that LK0.1 affects the activity of other Rev-like proteins. To confirm whether LK0.1 causes super-induction of Rev activity, pRRE-*Rluc*, the reporter vector containing the HIV Rev-responsive element (RRE) was co-transfected with Rev and LK0.1 expression contructs. This pRRE-*Rluc* is also an MMTV-based reporter vector that substitutes the RRE for the RmRE [141]. Transfection of a 293 cell line with 25 ng of Rev expression vector resulted in a pRRE-*Rluc* activation of about 3-fold, and co-transfection with LK0.1 induced five-fold more Rev activity (Figure 3.24B). Western blotting with the cell extracts from the same transfection showed that LK0.1 also induced Rev expression levels (Figure 3.24A). Rem expression plasmid and its pHM*Rluc* reporter vector, also independently transfected in the same experiment, confirmed the expected response (Figure 3.24A and B, lanes 7 and 8). Similar experiments were performed in 293 cells with Rex1 expression vector and the RxRE1-Rluc reporter vector containing its homologous response element. LK0.1 also induced Rex1 activity when less than 100 ng of Rex1 was transfected (data not shown). Therefore, similar to effects on Rem, LK0.1 caused super-induction of Rev and Rex1 activity.

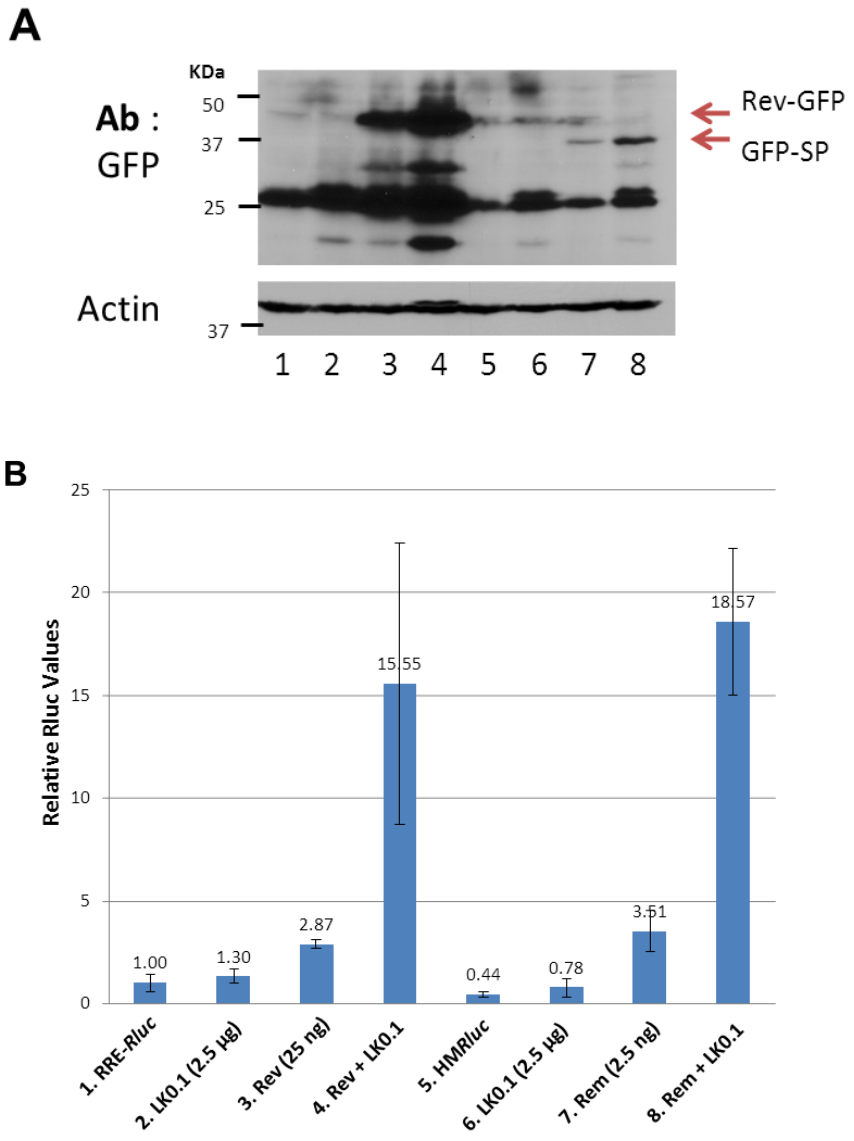

Figure 3.24: LK0.1 increases both the expression level and activity of Rev.

(A) Western blotting of 293 cells transfected with Rev-GFP or GFPRem in the absence and in the presence of LK0.1. GFP-specific antibody was used to detect GFP-tagged proteins and actin-specific antibody was used to show equal protein loading. (B) Luciferase activity of Rev and its responsive vector (pRRE-*Rluc*) or Rem with its pHM*Rluc* reporter. Rev-GFP (25 ng) or Rem (2.5 ng) expression vectors were transfected with 2.5 µg of LK0.1. The luciferase value of the pRRE-R*luc* reporter with an empty vector was assigned a relative value of 1. Corresponding lane numbers for the Western blot (A) are indicated.

3.3.3 REMOVAL OF THE HAIRPIN STRUCTURE FROM LK0.1 REDUCES SUPER-INDUCTION OF REV-LIKE PROTEINS.

LK0.1 is the control shRNA vector containing a hairpin structure. This hairpin consists of non-human/non-mouse shRNA sequence. In general, when an shRNA vector is transfected into cells, Drosha, a type III RNase localized in the nucleus, processes the hairpin to produce pre-miRNA. This pre-miRNA is exported to the cytoplasm and processed by Dicer and the RISC complex to make siRNA [168]. Depending on the degree of complementarity to a target sequence, the siRNA annealing leads to degradation of the targeted mRNA or inhibits its translation [18, 168]. To ascertain whether the hairpin structure in LK0.1 is important in Rem super-induction, the hairpin was deleted using PCR-based site-directed mutagenesis. The hairpin-deleted LK0.1 (LKΔHP) was transiently transfected into 293 cells to compare its effect on Rem with that of LK0.1. Interestingly, as shown in Figure 3.25A, LKΔHP had a reduced super-induction of Rem compared to LK0.1. However, co-transfection of Rem and LKΔHP expression vectors did show a slightly higher induction than transfection of Rem expression plasmid alone. Therefore, although the hairpin structure in LK0.1 is involved in Rem super-induction, the LK0.1 vector without a hairpin only slightly induced Rem activity. The same pattern was observed when GFP-SP was co-transfected with either LK0.1 or LKΔHP instead of full-length Rem expression plasmid (Figure 3.25A).

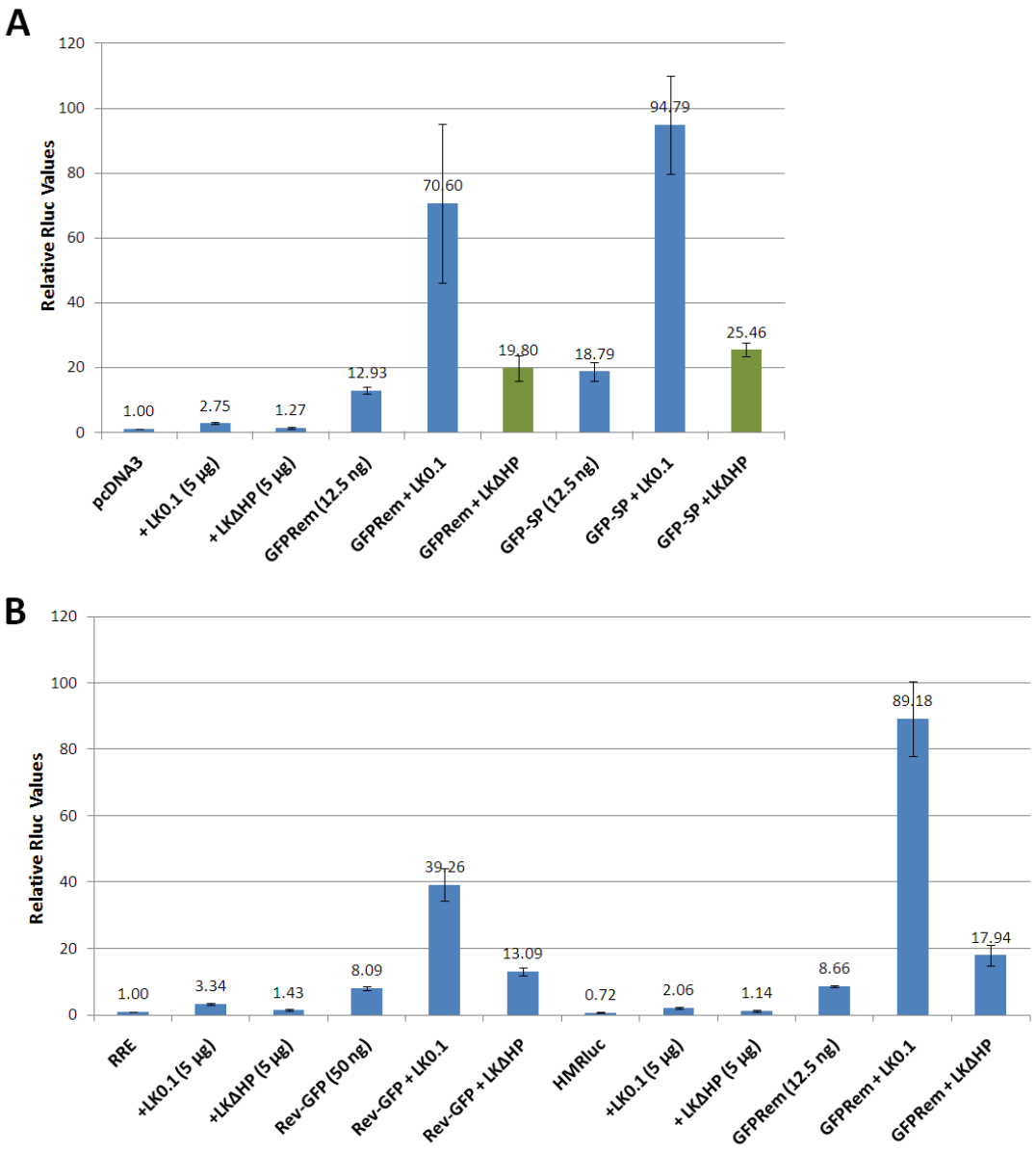

Figure 3.25: Removal of the hairpin structure from LK0.1 reduces its effect on super-induction of Rev-like proteins.

(A) Rem transfection activity of 293 cells with 12.5 ng of GFPRem or GFP-SP expression vectors and 5 µg of either LK0.1 or LKΔHP. Green bars show Rem activity when co-transfected with LKΔHP. The average luciferase value of the reporter vector with an empty expression vector (pcDNA3) was set to 1. (B) Luciferase activity of Rev with an RRE-containing reporter or Rem with pHM*Rluc*. Rev-GFP (50 ng) or GFPRem (12.5 ng) expression vector was transfected with 5 µg of LK0.1 or LKΔHP. Luciferase value of pRRE-R*luc* with an empty vector was set to 1.

Since LK0.1 also increased the activity of Rev and Rex1, Rev was co-transfected in 293 cells with either LK0.1 or LKΔHP to determine the effect of the hairpin deletion on Rev activity. In this experiment (Figure 3.25B), LK0.1 caused a slight (3-fold) increase in the basal activity of both reporter vectors, pRRE-*Rluc* and pHM*Rluc*, but LKΔHP did not increase the levels to the same degree. This moderate increase in activity was similar to that observed with Rem. Therefore, the deletion of the hairpin in LK0.1 resulted in a significant decrease in the super-induction of both Rem and Rev, but LKΔHP showed some residual induction.

3.3.4 SUPER-INDUCTION OF REM ACTIVITY IS NOT DEPENDENT ON THE CONTEXT OF THE REM EXPRESSION VECTOR.

Cellular miRNAs are located mostly in either gene coding regions or 3' untranslated regions (UTRs) [18, 168]. Thus the 3' UTR region in the *rem* expression vector may be responsible for Rem super-induction by LK0.1. Since *rem* cDNA was inserted into the pEGFPC1 (Clontech) expression vector, a vector-specific sequence may affect Rem activity. The pEGFPC1 vector contains an SV40 early mRNA polyadenylation (polyA) signal that follows the *rem* cDNA. To test the possibility that the EGFPC1 vector is responsible for the induction, an *env* expression vector, pQ61, was co-transfected with LK0.1 or LKΔHP in 293 cells. The backbone vector for pQ61 is pcDNA3 (Invitrogen), which contains a bovine growth hormone (BGH) polyA signal following the *env* cDNA. Transfection results revealed that the activity of pQ61 was also greatly induced by LK0.1. A slight increase was observed using LKΔHP (Figure 3.26A). Since no significant difference was detected between the induction of *rem* and *env*

expression vectors, the SV40 poly A signal and the 3' UTR of the Rem expression vector do not affect super-induction of SP activity.

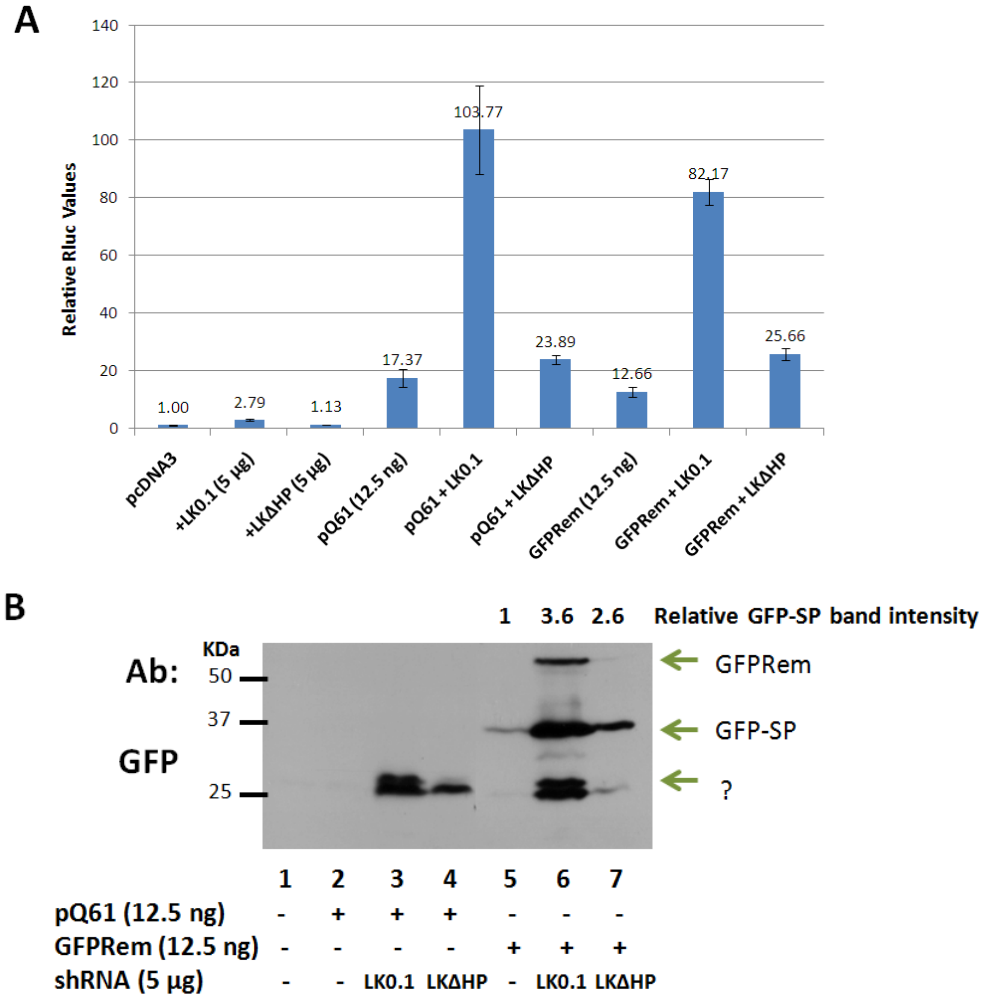

Figure 3.26: Rem super-induction by LK0.1 is independent of the 3' UTR element of the Rem-encoding vectors.

(A) Luciferase activity of 293 cells transfected with 12.5 ng of pQ61 or GFPRem expression plasmids in the presence of either 5 µg of LK0.1 or LKΔHP. Luciferase value of reporter vectors with an empty vector (pcDNA3) was set to 1. (B) Western blotting of cell extracts from the same transfection with GFP-specific antibody. Relative GFP-SP band intensity is indicated. The intensity of the GFP-SP band is normalized to the intensity of the actin band of each lane (not shown) and the normalized value of lane 5 is set to 1.

Western blotting of the cell extracts from the transfected 293 cells showed increased Rem expression levels when co-transfected with LK0.1 (Figure 3.26B, lanes 5 and 6) as seen previously. LKΔHP also increased Rem expression, but to a lesser degree than LK0.1 (lanes 6 and 7), in agreement with the slight induction of Rem activity caused by LKΔHP. Interestingly, unexpected protein bands of about 27 kDa were consistently detected in Western blotting with cell extracts from most transfections with LK0.1 (Figure 3.26B and Figure 3.22B). Although these bands are similar in size to GFP, these proteins also appear when no GFP-expressing constructs have been introduced. pQ61 does not contain a GFP-coding sequence, yet the 27 kDa single or double band is detected with an antibody against GFP (Figure 3.26B, lanes 1-4). Other GFP-specific antibodies (Santa Cruz) did not detect these proteins. These results suggest that the 27 kDa doublet represents cellular proteins induced by stress.

3.3.5 LK0.1 AND LKΔHP INCREASE THE FLUORESCENT SIGNAL OF GFP-TAGGED REV-LIKE PROTEINS AS WELL AS TRANSFECTED CDNAS ENCODING FLUORESCENT PROTEINS.

The LK0.1 plasmid greatly induced both Rem activity and Rem expression levels. LKΔHP also increased the activity and expression of Rem, although to a lesser degree. To determine whether Rem localization is affected by the increase in Rem expression levels due to LK0.1 and LKΔHP, 293 cells were first transiently transfected with GFPRem expression plasmid alone. Using a fluorescence microscope, these cells were compared to cells co-transfected with GFPRem expression vector and either LK0.1 or LKΔHP. The GFP signal from the transfection of 12.5 ng of GFPRem alone was detectable but weak, both in the presence and absence of fluorescent DAPI nuclear staining as shown in Figure 3.27. However, when cells were co-transfected with 12.5 ng

of GFPRem expression vector and 5 μg of LK0.1, a dramatic increase in the GFP signal intensity was observed. As expected, most of the GFP signal appeared to be nucleolar. Co-transfection with GFPRem and LKΔHP expression plasmids also led to an increase in GFP signal intensity, but that increase was notably less dramatic than that seen with LK0.1. Nonetheless, the increase in the GFP signal by LKΔHP was easily detectable.

To eliminate the possibility that the reporter plasmids, pHM*Rluc* and pGL3-control, might be responsible for the LK0.1-driven increase in Rem expression level, a transfection of the same DNAs without the reporter vectors was initiated. The GFP signals observed for each condition (vectors expressing GFPRem only, GFPRem with LK0.1 and GFPRem with LKΔHP) were similar to those signals noted when the cells were transfected with the reporter vectors (Figure 3.27, compare upper and lower panels). The same amount of Rev-GFP expression plasmid was co-transfected with LK0.1 and LKΔHP to confirm that Rev-GFP is affected in the same manner as GFPRem. As shown in Figure 3.28, cells co-transfected with Rev-GFP and LK0.1 displayed a greatly intensified GFP signal, and most of the GFP fluorescence overlapped with the DAPI nuclear staining. Cells tranfected with Rev-GFP and LKΔHP showed a significant increase in GFP signal over that of Rev-GFP alone, but the intensity was much less than that of Rev-GFP and LK0.1. This pattern was independent of the response element, since both the heterologous pHM*Rluc* and the homologous pRRE-*Rluc* yielded the same result (Figure 3.28). The increases in GFP signal might be correlated to the increase in the expression levels of both Rem and Rev, since the pattern is similar. However, the degree of increase in the GFP signal caused by LKΔHP appears greater than the relative increase in functional activity measured in the luciferase assay.

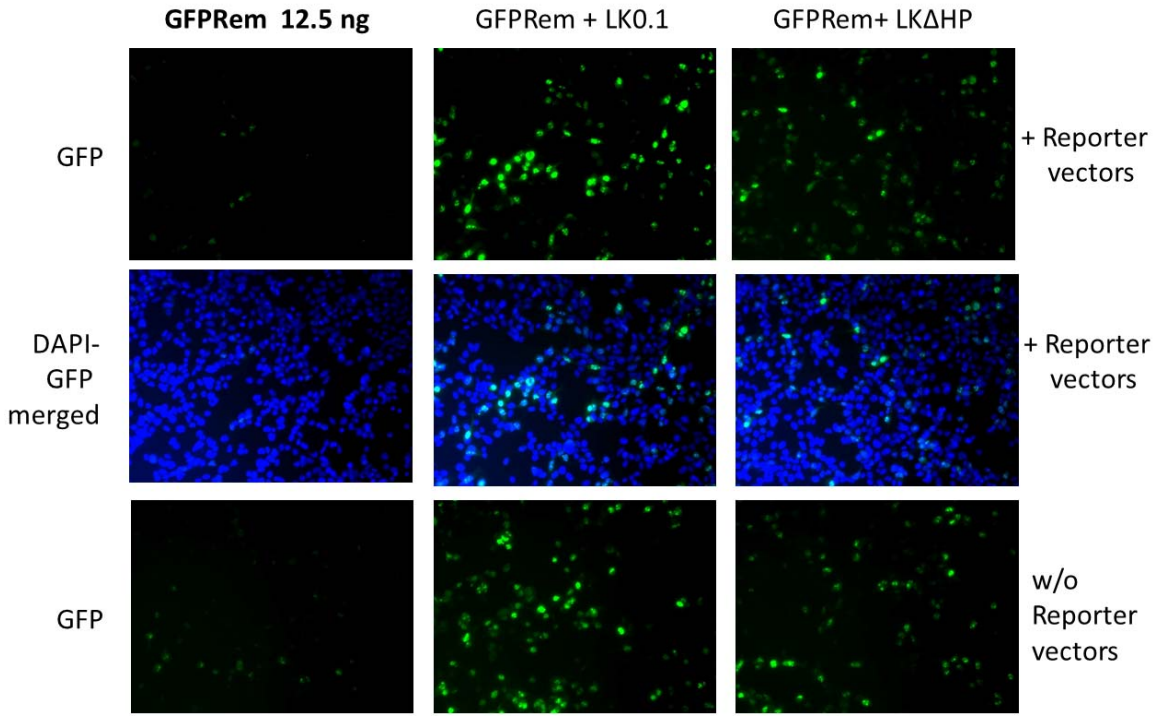

Figure 3.27: LK0.1 and LKΔHP increase the GFP signal intensity of GFPRem.

Transfection of 293 cells was performed with 12.5 ng of GFPRem expression plasmid in the absence and presence of 5 µg of LK0.1 or LKΔHP. After 48h, cells were treated with DAPI for nuclear staining and observed under a fluorescence microscope. GFP signal (upper panel) or GFP and DAPI signal in a merged image (middle panel) are shown. Cells were also transfected with GFPRem expression vector and either LK0.1 or LKΔHP but without reporter vectors (lower panel).

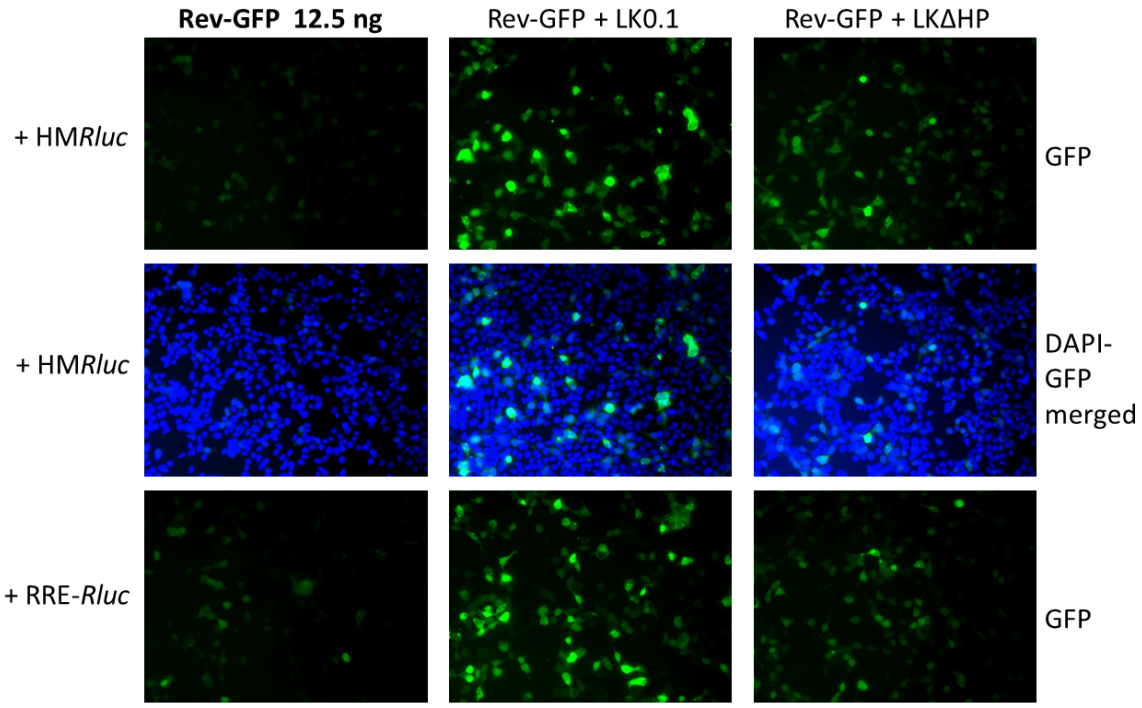

Figure 3.28: LK0.1 and LKΔHP increase the GFP signal intensity of Rev-GFP.

Transfection of 293 cells was performed with pHM*Rluc* and 12.5 ng of Rev-GFP expression plasmid in the absence and presence of 5 μg of LK0.1 or LKΔHP. After 48h, cells were treated with DAPI for nuclear straining and observed under a fluorescence microscope. GFP signal (upper panel) or GFP and DAPI signal in a merged image (middle panel) are shown. Cells were transfected with Rev, pRRE-*Rluc* and either LK0.1 or LKΔHP (lower panel).

To determine whether LK0.1 has a similar effect on non Rev-like proteins, 100 ng of a GFP-expressing vector, EGFPN3 (Clontech), was co-transfected with 1 μg or 4 μg of LK0.1 into 293 cells. The cell extracts were then harvested for Western blotting with GFP-specific antibody. As shown in Figure 3.29A (lanes 3 and 4), the expression level of GFP was increased with the addition of LK0.1. Using the actin levels from the same blot as an indication of loading quantification, the increase in GFP expression is dependent on the amount of co-transfected LK0.1.

A red fluorescent protein construct, ER-mCherry, was also tested. ER-mCherry (200 ng) was co-transfected with either LK0.1 or LKΔHP in 293 cells, and the RFP signal was observed with a fluorescence microscope (Figure 3.29B). Cells co-transfected with ER-mCherry and LK0.1 showed a greatly increased RFP signal over cells transfected with ER-mCherry alone (lower left panel). Co-transfection of ER-mCherry with LKΔHP showed a slight increase in RFP signal (lower right panel). Therefore, LK0.1 induced expression levels of both GFP and RFP in transfected cells.

Since the total protein levels in the cell extracts resulting from the co-transfection of Rem and LK0.1 do not show any dramatic changes (data not shown), the levels of endogenous proteins are not affected by LK0.1. Therefore, LK0.1 affects the expression levels of exogenous DNAs introduced into cells.

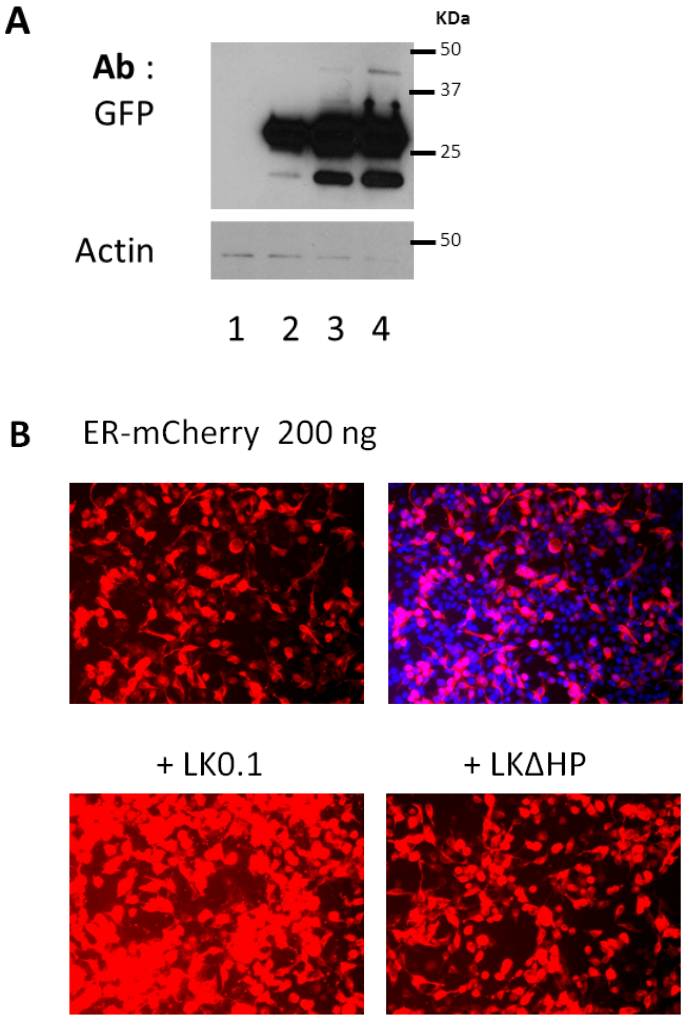

Figure 3.29: LK0.1 and LKΔHP increase the expression levels of GFP and ER-mCherry.

(A) Co-transfection of 293 cells with 100 ng of EGFPN3, a GFP-encoding vector, and 1 μg or 4 μg of LK0.1; Lane 1, an empty vector (pcDNA3) alone; lane 2, 100 ng of EGFPN3; lane 3, 100 ng of EGFPN3 with 1 μg of LK0.1; lane 4, 100 ng of EGFPN3 with 4 μg of LK0.1 (B) The ER-mCherry construct (200 ng) was co-transfected with 5 μg of LK0.1 or LKΔHP in 293 cells. After 48 h, cells were treated with DAPI for nuclear staining and observed using a fluorescence microscope. Upper panel shows cells transfected with 200 ng of ER-mCherry alone (left) and the merged image of mCherry (red) signal with DAPI (blue) (right). Lower panels show ER-mCherry co-transfected with LK0.1 or LKΔHP.

3.3.6 A NON-LENTIVIRAL SHRNA VECTOR DOES NOT INDUCE ADDITIONAL REM ACTIVITY

LK0.1 is a lentiviral vector containing part of the HIV genome, including the 5' LTR, the 5'-end of the *gag* gene, the RRE, part of the *env* gene and the 3' LTR (Figure 3.20A). To test whether the lentiviral backbone is responsible for the super-induction of Rem activity, a non-lentiviral shRNA expression vector was used to compare Rem activation with that of LK0.1. pCEP4 (Invitrogen) is an episomal mammalian expression vector that does not contain lentiviral elements (Figure 3.30A). An shRNA vector based on pCEP4 was developed by inserting a histone H1 polymerase III promoter followed by a hairpin into the pCEP4 vector. The pCEP4 control vector and two of the pCEP4-based hairpin-containing vectors, E6AP-3 and HPV18E6 (kindly provided by the Huibregtse laboratory), were co-transfected with GFPRem expression plasmids into 293 cells. LK0.1 was independently co-transfected with GFPRem as a control. As shown in Figure 3.30B, the normalized luciferase activity values verified that none of the pCEP4-based vectors induced additional Rem activity, whereas LK0.1 caused a 4-fold increase. Surprisingly, pCEP4 and E6AP-3 decreased both firefly and *Renilla* lucifierase values significantly in the absence and in the presence of Rem (Figure 3.31). However, the HPV18E6 hairpin-containing vector did not decrease firefly values.

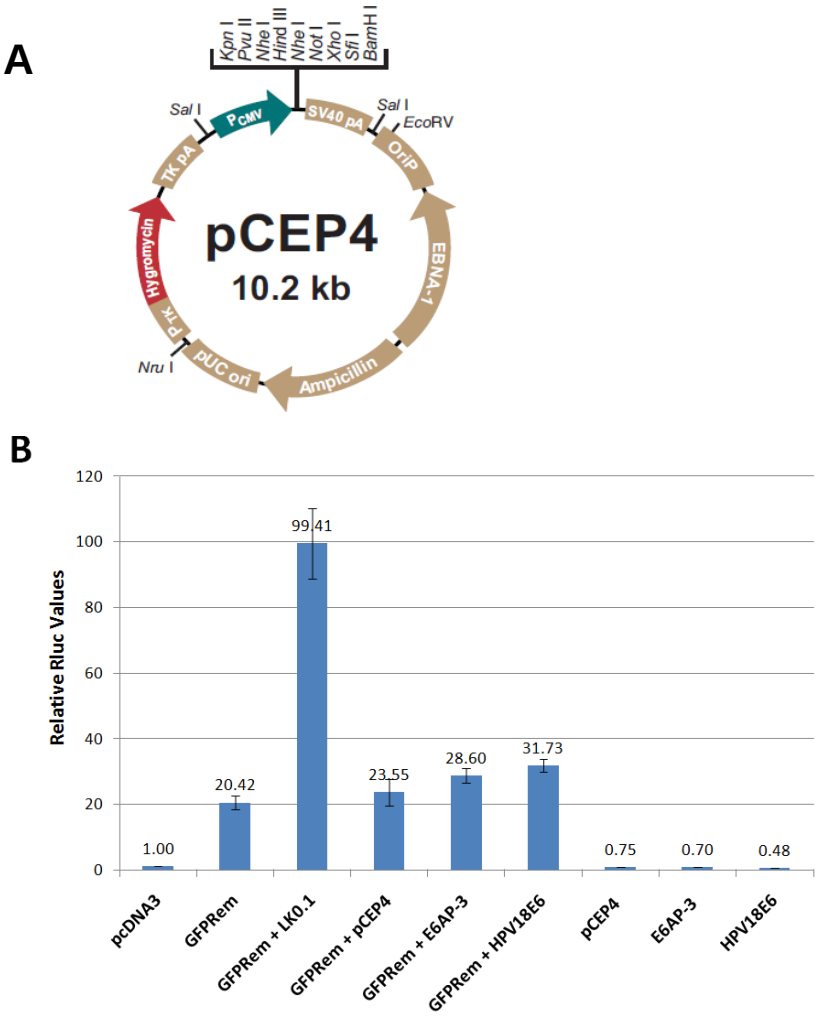

Figure 3.30: Non-lentiviral pCEP4-based shRNA expression vector does not induce additional Rem activity.

(A) Map of pCEP4 vector. (B) Luciferase activity of 293 cells transfected with 12.5 ng of GFPRem expression plasmid in the presence of 4 µg of LK0.1 or pCEP4-based specific shRNA-expressing vectors. Cells also were transfected with pCEP4 or pCEP4-based shRNA-expression vector alone. The average luciferase value of the pHM*Rluc* reporter vector with pcDNA3 was set to 1 as described in Figure 3.2. Co-transfection of Rem and each shRNA-expression vector was performed in triplicate, with the exception that the pCEP4-based shRNA vector transfection was based on one sample.

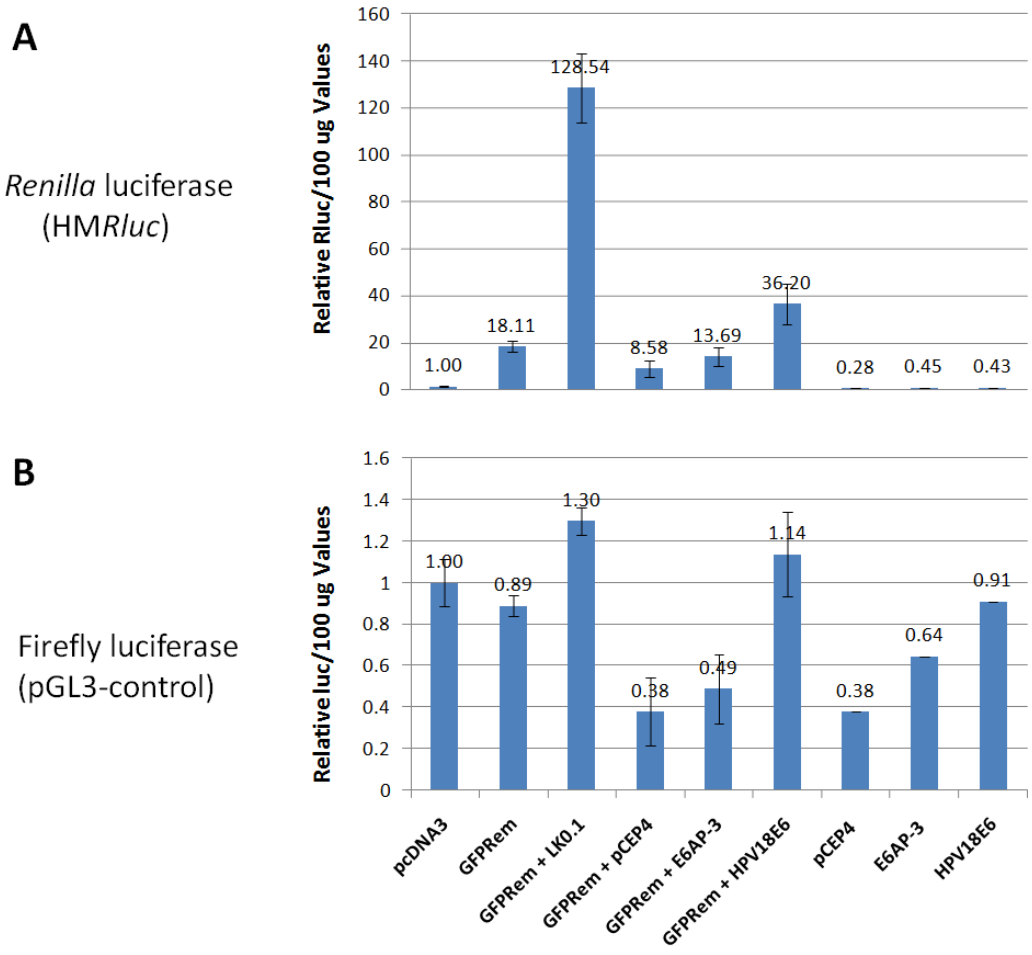

Figure 3.31: pCEP4 and pCEP4-based shRNA vector E6AP-3 decrease individual luciferase values in the same experiment described in Figure 3.30B.

(A) *Renilla* luciferase values of triplicate transfections (+/- standard deviations) are reported without normalization for effects on expression of the non-Rem responsive pGL3-control vector. The average *Renilla* activity of the reporter in the presence of pcDNA3 only was assigned a value of 1. (B) Firefly luciferase values of triplicate transfections (+/- standard deviations) are shown for the pGL3-control vector.

3.3.7 LENTIVIRAL ELEMENT OF LK0.1 AFFECTS THE INDUCTION OF PROTEIN EXPRESSION LEVELS.

Since the pCEP4 non-lentiviral vector revealed firefly luciferase activity different from LK0.1, the lentiviral elements were deleted from LK0.1 to define their potential effect on activity compared to full-length LK0.1. Two deletion mutants were prepared using PCR-based site-directed mutagenesis. The U6, pol III promoter, and the LK0.1 hairpin were removed in the LKΔU6 mutant. For the LKΔPsi mutant, most of the *gag-env* fusion (*Psi* (Ψ) to the hairpin) was removed (Figure 3.32).

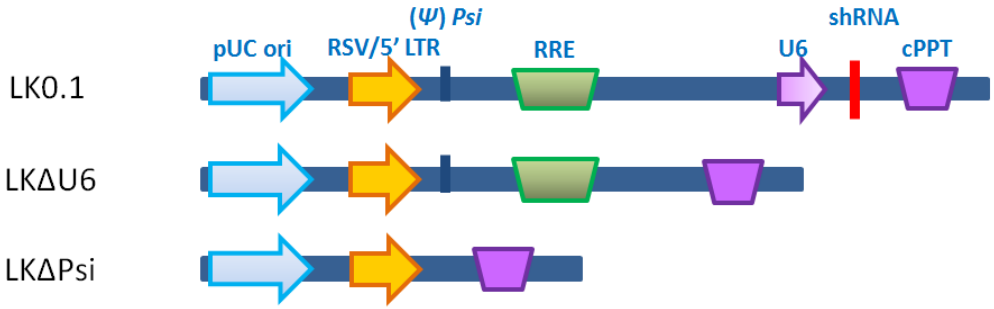

Figure 3.32: Diagrams of deletion mutants of the LK0.1 vector.

The LKΔU6 construct was made by removing the U6 polIII promoter and the hairpin structure from LK0.1. The LKΔPsi was prepared by introducing a deletion encompassing the Psi HIV packaging signal through the hairpin structure.

To determine whether the deletion of the lentiviral elements from LK0.1 leads to the loss of its capability to induce Rem activity and expression levels, 293 cells were transiently co-transfected with 5 μg of the deletion mutants of LK0.1 in the presence and the absence of 12.5 ng of the GFPRem expression construct. The same amount of LK0.1 and LKΔHP were co-transfected with the GFPRem expression plasmid separately for comparison of their activity with that of the deletion mutants. As shown in Figure 3.33A, none of the LK0.1 deletion mutants leads to super-induction, but a slight increase in Rem activity was evident when the luciferase values were normalized. The LKΔU6 and LKΔPsi mutants had the same effect on activity as the LKΔHP mutant. Nevertheless, LKΔPsi behaved differently than LKΔHP and LKΔU6 after examination of the two luciferase values independently (Figure 3.33B). LKΔHP and LKΔU6 induced both the pHM*Rluc* (*Renilla* luciferase) reporter and the pGL3-control (firefly) reporter vector slightly, comparable to elevation observed with LK0.1. The LKΔPsi increased *Renilla* values in the presence or absence of Rem, but did not increase the firefly luciferase value. In a repeated experiment, LKΔPsi again displayed this different effect on the individual luciferase values compared to the other deletion mutants (data not shown).

The LKΔU6 and LKΔPsi mutants also increased the expression levels of Rem. Increased Rem levels were observed when GFPRem expression vector was co-transfected with either LK0.1 or the deletion mutants, as observed in Western blotting of the cell extracts from the same transfection (Figure 3.34A). LKΔPsi co-transfection had the least effect on Rem levels compared to the other LK0.1-based plasmids, but it was still higher than Rem alone. LKΔHP and LKΔU6 had similar effects on Rem protein levels. This observation confirms that the lentiviral element of LK0.1 (tested using LKΔPsi) affects

Rem activity and expression levels to some degree, but does not abolish super-induction completely.

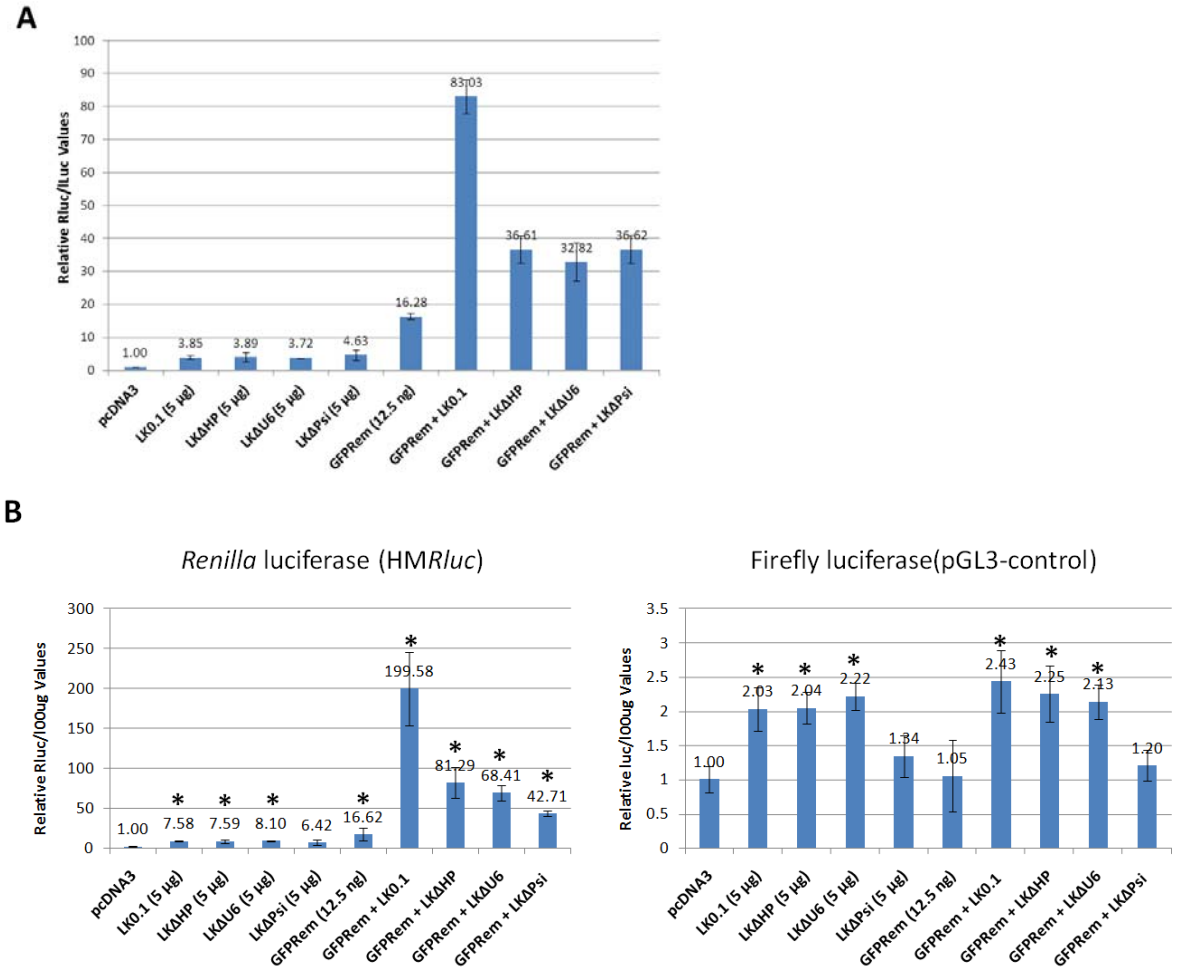

Figure 3.33: Deletion of the lentiviral element from LK0.1 affects Rem activity.

(A) Normalized luciferase activity of 293 cells transfected with 5 µg of LK0.1 and LK0.1 deletion mutants with and without 12.5 ng of the GFPRem expression vector. The average luciferase value of the reporter vector with pcDNA3 was assigned a value of 1 as described in Figure 3.2. (B) Individual *Renilla* and firefly luciferase activity values from the transfection. The * indicates significantly induced *Renilla* or firefly luciferase values ($P<0.05$) of LK0.1 and the deletion mutants relative to that of reporter vector with an empty vector, pcDNA3.

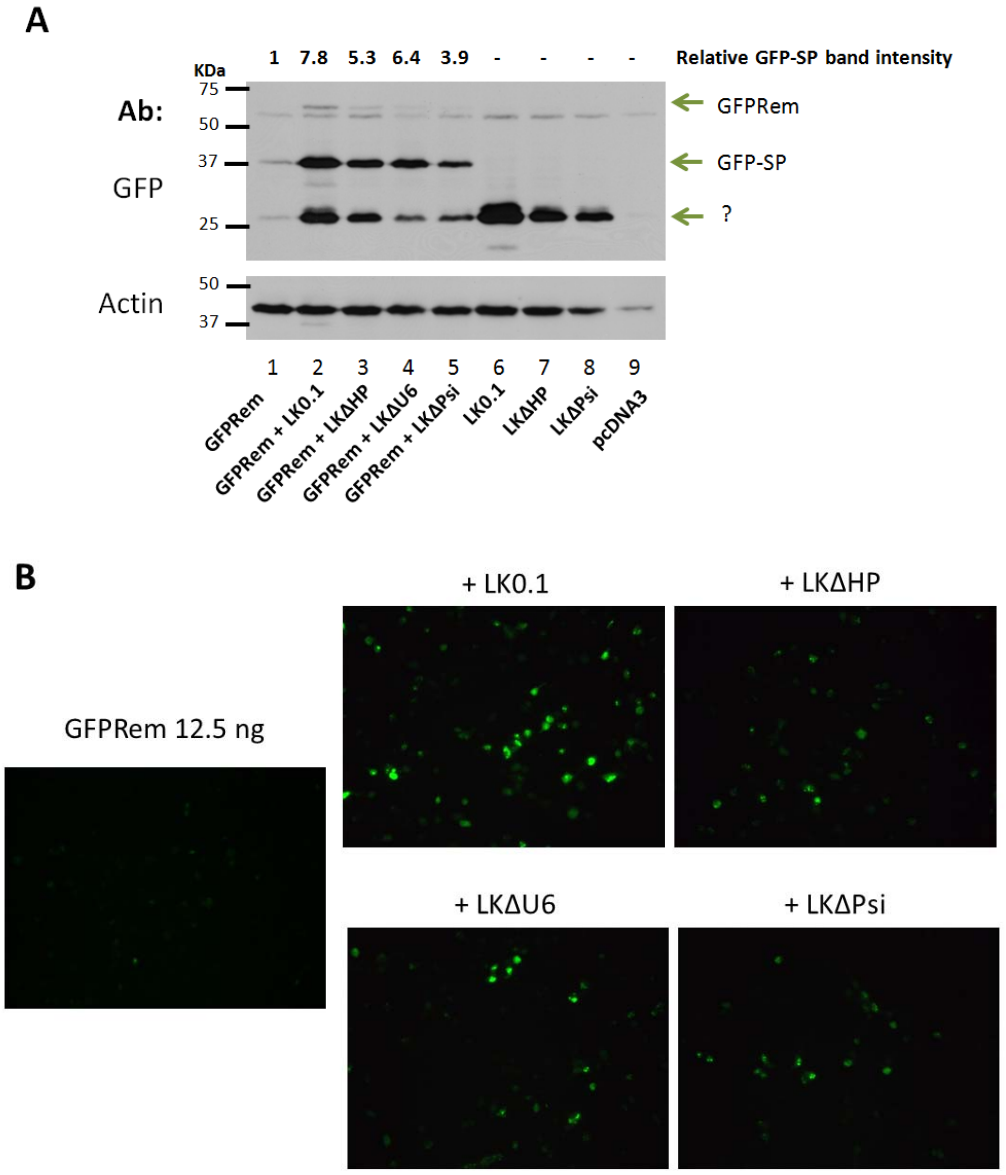

Figure 3.34: Deletion of the lentiviral elements from LK0.1 affects Rem activity.

(A) Western blotting of 293 cell extracts from the same transfection shown in Figure 3.33. GFP-specific antibody was used to detect GFPRem, GFP-SP and another band of unknown origin. Blotting with actin-specific antibody confirmed equal protein loading. The intensity of the GFP-SP band was normalized to the intensity of the actin band of each lane and the normalized value of lane 1 was set to 1. (B) Cells were transfected with 12.5 ng of GFPRem expression construct in the absence and presence of 5 μg of LK0.1 and LK0.1 deletion mutants. After 48 h, cells were observed under a fluorescence microscope.

Cells from the same transfection were observed under a fluorescence microscope (Figure 3.34B). Co-transfection of the GFPRem expression construct with all of the LK0.1 deletion mutants revealed an increased GFP signal intensity compared to the GFPRem construct alone, but the intensity was less than that of the co-transfection of the GFPRem plasmid with LK0.1.

3.3.8 LK0.1 AND REM DO NOT INDUCE PHOSPHORYLATION OF EIF2A OR THE INTERFERON PATHWAY.

Since LK0.1 significantly induced both the expression level of Rem and Rem activity, it is possible that LK0.1 affects the translation machinery. When cells undergo environmental stress or viral infection, cells regulate translation to reduce stress or arrest the viral infection. One mechanism to regulate translation is to phosphorylate eIF2α, leading to reduced translation. Therefore, to determine whether transfection of LK0.1 affects the levels of phosphorylated eIF2α in transfected cells, Western blotting was conducted with 293 cell extracts co-transfected with the GFPRem expression construct and LK0.1. As shown in Figure 3.35, some induction of phosphorylated eIF2α was observed after the transfection of pcDNA3 control vector. No difference was observed between individual transfectants. Therefore, neither Rem nor LK0.1 induces phosphorylation of eIF2α.

The deletion of the hairpin structure from LK0.1 greatly reduced Rem super-induction and expression levels, indicating that the hairpin structure is important for LK0.1-mediated Rem super-induction. The hairpin in the shRNA expression vector is thought to be processed by the RNA interference system to produce siRNA [168]. However, some shRNA expression vectors are reported to elevate expression of

interferon (IFN)-inducible genes [25]. Also, the hairpin contains a dsRNA portion which could induce an immune response due to the dsRNA in the cells. To check whether the IFN-related pathway is induced by either Rem or LK0.1, a Western blot was performed to detect RIG-G, an IFN-inducible protein. As positive controls, IFN-treated and untreated HeLa and A549 cell extracts were used (supplied by Dr. Larissa Durfee from the laboratory of Dr. Jon Huibregtse). Although RIG-G protein was detected in the IFN-treated control cell extracts (HeLa and A549), none of the extracts of co-transfected GFPRem and LK0.1 revealed RIG-G expression (data not shown). Therefore, neither eIF2α nor the IFN-related pathways correlated with the LK0.1-mediated Rem super-induction and increased Rem expression.

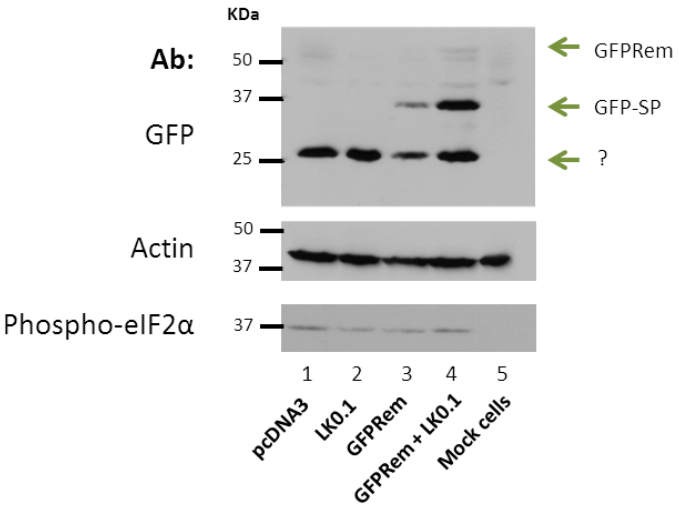

Figure 3.35: Rem and LK0.1 do not induce phosphorylation of eIF2α.

Western blotting of 293 cell extracts transfected with GFPRem expression plasmid and LK0.1. GFP-specific antibody was used to detect GFP-SP and actin-specific antibody was used to confirm equal protein loading. To detect phospho-eIF2α, a specific antibody was used. To compare the effect of transfection on the level of phospho-eIF2α, an untransfected (Mock) cell extract was loaded.

3.3.9 LK0.1 REDUCES STRESS GRANULES.

Recently White *et al*. have shown that poliovirus inhibits the formation of stress granules (SGs) in infected cells [228]. Stress granules are cytoplasmic foci consisting of silenced mRNA-protein particles (mRNPs) that are formed to regulate mRNA metabolism during stress [5, 6]. To determine whether either Rem or LK0.1 affects the formation of cellular stress granules, 293 cells were transiently co-transfected with 12.5 ng of GFPRem expression plasmid and 5 μg of LK0.1. After 48 h, cells were fixed and permeabilized. Cells were then incubated with RasGAP-SH3-binding protein (G3BP)-specific antibody. G3BP is one of the RNA-binding proteins assembled in stress granules [218]. Interestingly, no stress granules were observed in uninfected mock cells, but a dramatic induction was caused by the transfection. As we had observed in a prior experiment where transfection resulted in increased phosphorylated eIF2α (Figure 3.35), the transfection process itself induces a cellular stress reaction. Even transfection of the empty vector, pcDNA3, induced stress granules (Figure 3.36). Transfections of GFPRem expression plasmid alone yield a response similar to that of pcDNA3. However, when LK0.1 was introduced, the number of cells containing stress granules was significantly decreased (Figure 3.37). Co-transfection with GFPRem and LK0.1 plasmids showed a similar number of cells containing stress granules as transfection of LK0.1 alone. This result suggests that LK0.1 decreases formation of stress granules, which may contribute to increased Rem activity and expression levels.

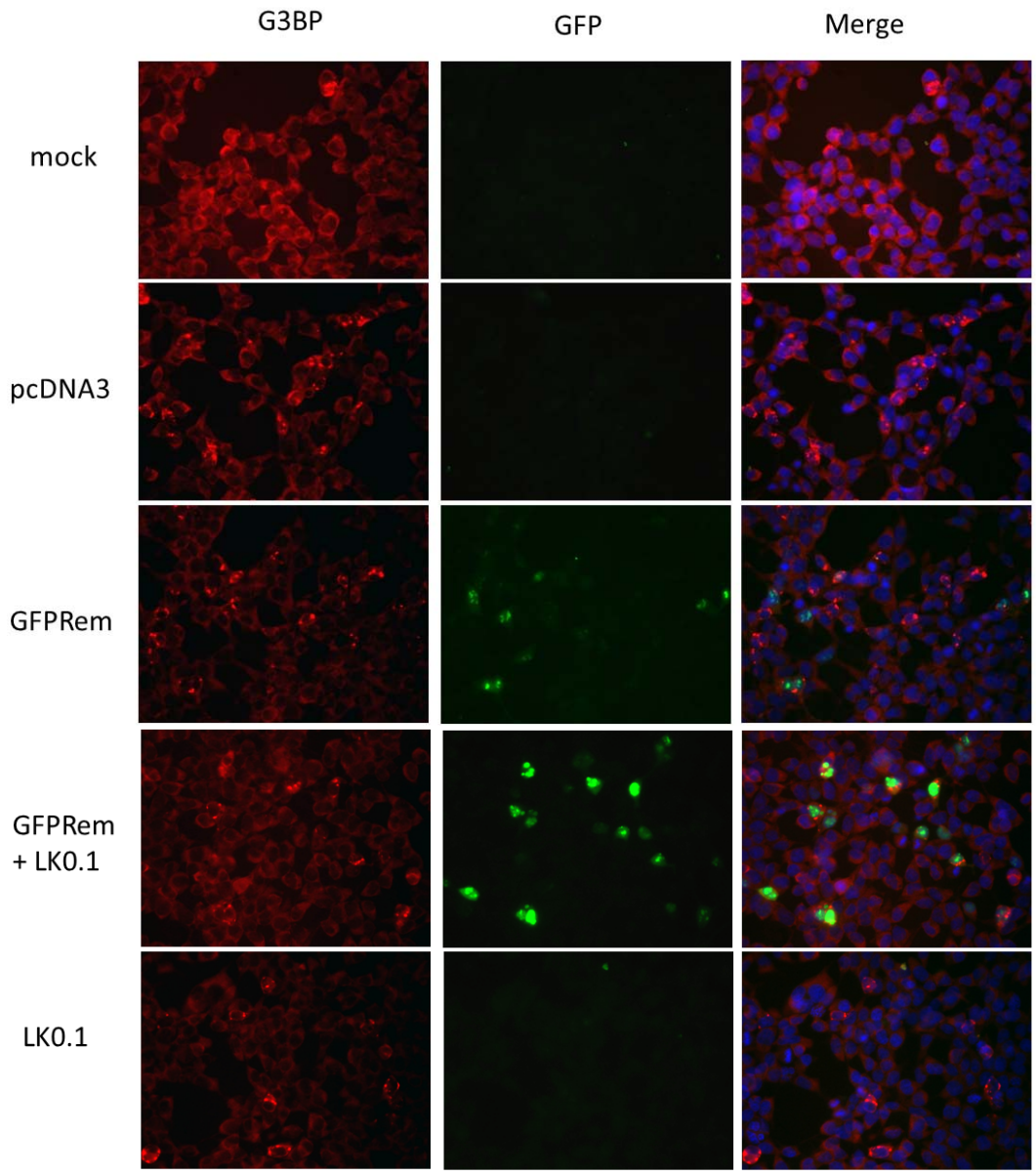

Figure 3.36: LK0.1 decreases the formation of stress granules.

GFPRem expression vector (12.5 ng) and LK0.1 (5 µg) were co-transfected into 293 cells. Both GFPRem expression plasmid and LK0.1 were transfected independently as controls. Mock cells were included as a control for stress due to the transfection process. After 48 h, fixed and permeabilized cells were incubated with G3BP-specific antibody. Alexafluor 594-conjugated rabbit antibody was used to detect the G3BP-bound primary antibody. Cells were stained with DAPI for nuclear visualization.

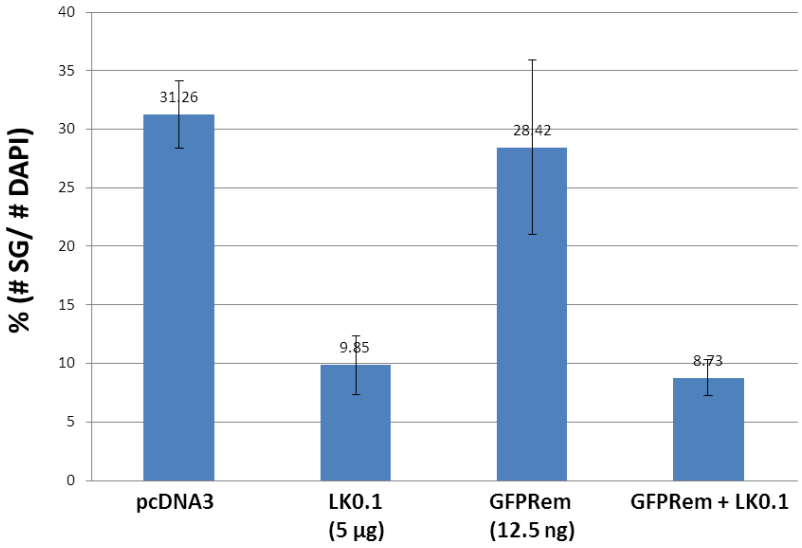

Figure 3.37: LK0.1 significantly decreases the formation of stress granules.

Co-transfection of GFPRem expression vector (12.5 ng) and LK0.1 (5 µg) into 293 cells was repeated to detect the formation of stress granules as described in Figure 3.36. For quantification, the percentage of cells containing stress granules out of the total number of cells (DAPI+ cells) was determined. Cells were counted in four random fields.

4. DISCUSSION

4.1 THE RmRE IS A 476-nt SEGMENT LOCATED AT THE JUNCTION OF THE MMTV *ENV* GENE AND THE 3' LTR.

The regulation of cellular nuclear export, which allows only fully spliced mRNAs to be transported to the cytoplasm, is a key checkpoint to generate only functional proteins necessary for cell activity. Retroviruses package their intron-containing genomic RNA in the cytoplasm and utilize unspliced RNAs to produce functional viral proteins. Complex retroviruses encode a viral export protein and contain export protein-binding sites in the viral genome. Both components are needed to directly regulate the nuclear export and expression of retroviral unspliced RNAs. Like other complex retroviruses, MMTV encodes a regulatory protein, Rem, to allow efficient nuclear export of its unspliced RNAs. Mertz *et al.* have shown that Rem is generated from a doubly spliced viral RNA lacking introns, similar to the HIV-encoded Rev protein [142]. Assays for Rem function used pHM*Rluc*, a reporter vector designed to measure Rem export function [142]. Although pHM*Rluc* appears to measure a post-export function of Rem, suggesting that Rem may have more than one MMTV RNA-binding site, the data presented here indicate a potential Rem-responsive element (RmRE) located at the junction of the *env* gene and the 3' LTR [140].

Previous studies have shown that the substitution of the MMTV 3' LTR with the the SV40 polyadenylation site eliminates the Rem response in the vector pHMeLTR*luc* [142]. Insertion of a 496-nt BglII/ScaI fragment encompassing the end of the MMTV *env* gene and the 3' LTR in the HM*Rluc* vector upstream of the SV40 polyadenylation site in pHMeLTR*luc* elicits the same level of Rem response as the entire 3'-end of the

MMTV genome found in pHM*Rluc* [140]. To determine the minimum size of the RmRE, a series of deletions were introduced into the BglII/ScaI fragment in pHMeLTR*luc*, and the Rem responsiveness of these mutants was measured in transient transfections. Mutants with deletions of 20 nt from the 5'-end did not affect responsiveness. However, deletion of more than 30 nt from the 5'-end revealed a partial response, whereas deletion of more than 40 nt abolished Rem responsiveness. Deletions from the 3'-end showed a partial responsiveness (Figure 3.2 and Table 3.1). Therefore, the minimal RmRE is a 479-bp segment located at the junction of the *env* gene and the 3' LTR. Since deletion of more than 20 nt from the 5'-end of the RmRE abolished Rem responsiveness, the first 20 nt of the RmRE may be a critical determinant of a structurally functional element.

Four sequence differences were found between the Rem cDNA sequence isolated by our lab and the consensus sequences of several MMTV isolates. Each of the differences was replaced individually with the sequence for the Rem consensus amino acid. Only the substitution at position 71 from a proline to a consensus leucine (RemP71L) resulted in increased activity and cleavage to SP (Figure 3.3A). Despite a significant change in activity, Rem containing a leucine at position 71 recognizes the same RmRE boundaries. This minimal RmRE was cell-type independent since the same limits of the element were defined in both HC11 mouse cells and Jurkat human T cells (Figure 3.3C).

Retroviruses all contain a *cis*-acting element that functions in RNA export and expression. Simple retroviruses contain an extended stem-loop structure, the CTE, which is recognized by cellular export factors, whereas complex retroviruses typically require multiple stem-loop structures for recognition by viral export proteins. The viral export

factors then act as adapters between the response element of the viral RNA and the cellular export machinery [36, 152].

To determine the most likely structure of the MMTV Rem-responsive element at the 3'-end of the genome, nuclease mapping experiments were conducted using RNases T1, A, and V1. The positions of either double stranded or single stranded RNA located in the RmRE were entered as constraints for Mfold, a web-based RNA secondary structure prediction program. The suggested RmRE structure includes multiple stem-loops and many single-stranded regions (Figure 3.4) [140]. This extensive and complex structure is similar to *cis*-acting elements of other complex retroviruses, such as HIV-1 RRE and HTLV-1 Rex. Mertz *et al.* additionally determined that the nuclear export of unspliced RNA by Rem is dependent on the cellular factor Crm1, which is commonly involved in the nuclear export of genomic RNAs associated with other complex retroviruses [142].

Müllner *et al.* have reported an RmRE of 490 nt at a region that largely overlaps with the region defined by Mertz *et al.* The structure predicted by Müllner *et al.* consists mostly of an extended double stranded stem, which is very similar to a CTE structure, connected to a branched stem-loop structure [149]. The branched stem-loop structure was located mostly in the overlapping sequences. The discrepancy between the two suggested structures may be due to the Mullner prediction being based on sequence rather than the combination of software predictions and RNase mapping as utilized by Mertz *et al.* In addition, covariation analysis of sequences among different infectious MMTV strains supports the tenet that the patterns of base pairing predicted by the Mertz model (Fig. 3.4) were conserved, even with variations in nucleotides. This pattern matches the complex stem-loop model, not the extended hairpin model.

HIV-1 Rev and its response element, the RRE, have been the most extensively studied among many retroviruses. Rev is generated from fully spliced *env* mRNA and is exported to the cytoplasm by the cellular export system. The RRE is located within an intron of the *env* gene, and all unspliced and partially spliced HIV RNAs contain the RRE. Therefore, Rev can selectively bind to viral intron-containing RNAs to facilitate their export. However, not all response elements of complex retroviruses are located in introns. The HTLV-1 RxRE and HERV-K RcRE are located at the 3' LTR [276, 132]. Since all viral mRNAs terminate at the R/U5 border of the 3' LTR, these response elements are included in all viral mRNAs. The RmRE appears at the junction of the *env* gene and the 3' LTR (Figure 3.5). Therefore, Rem may not selectively bind to unspliced RNAs as Rev does. It is intriguing that MMTV maintains a less selective response element than HIV. Most retroviral gene products translated from unspliced or partially spliced RNAs are structural proteins that are required for virion production in host cells. The production of these MMTV structural proteins is highly dependent on Rem. Since Rem and Sag proteins are generated from fully spliced RNAs, their nuclear export is independent of Rem. Therefore, the existence of the RmRE at the 3' LTR may increase the levels of Rem and Sag early in the infectious cycle prior to the production of structural proteins. Then, more SP is available to participate in the export of unspliced RNA to the cytoplasm, thus facilitating more rapid viral production. SP, one of the cleavage products of Rem, has been shown to have the same activity as full-length Rem [142], and the same SP can be produced by Env. The fact that SP can be generated from both Rem and Env suggests that MMTV is highly dependent on SP function prior to Env production. Alternatively, the C-terminal product of Rem [29, 48] may be required early

in virus replication. Sag is also important for viral transmission from dendritic cells to T and B lymphocytes and dissemination within the mammary gland [62, 186].

Indik *et al.* found that the Crm1 inhibitor, leptomycin B, selectively affected genomic MMTV RNA export, but not other viral RNAs, such as envelope mRNA [95], indicating that export function of Rem is selective. It is therefore possible that MMTV contains an additional RmRE within the 5' portion of the genome for selective nuclear export of viral unspliced RNA, whereas the RmRE at the 3'-end is utilized for other functions. MMTV contains a packaging signal at the 5'-end of the MMTV genome [182, 193]. The packaging signal, *Psi* (ψ), is the site where Gag protein binds to genomic RNA to encapsidate the RNA genome. Generally, it is composed of stem-loop structures. The packaging signal of HIV-1 is known to be cloverleaf-shaped with four stem-loops. Murine leukemia virus (MuLV), a simple retrovirus, is known to utilize its highly structured packaging signal as a *cis*-acting element to support nuclear export of unspliced RNA [205]. Therefore, SP may either bind to the MMTV packaging signal itself or another RmRE located in proximity to the packaging signal. Mutant hybrid proviral clones with deletion mutations in the potential packaging signal site (kindly provided by Dr. Tahir Rizvi) were used to verify the existence of a potential RmRE near the 5'-end of the MMTV genome. Preliminary analysis of stable cell lines expressing these mutant viruses indicates the presence of unstable viral RNAs and poor Gag production (data not shown). Although firm conclusions from these data are not possible, a complex structure at the 5' end of the MMTV genome seems to be critical for RNA stability.

The RxRE is located within the 3' LTR, and all HTLV-1 mRNAs contain the RxRE [2, 76, 219]. The RxRE is required for Rex function as well as for relieving an intrinsic structural HTLV-1 problem; the structural conformation of RxRE results in the

close association of the elements required for polyadenylation at the 3'-end of viral mRNAs [2, 211]. These elements are otherwise physically separated within the unusually long R region at the HTLV-1 3' LTR. Other possible activities of the RxRE and Rex may be related to additional functions proposed for Rem. Retroviral export proteins have been reported to exhibit additional functions such as translational upregulation, pre-mRNA stabilization, and splicing regulation [65, 96].

Previous studies from our lab using RNA fractionation experiments and transfection of the reporter plasmid pHM*Rluc* imply additional functions of Rem [141]. The *Renilla* luciferase gene is located between the splice donor and splice acceptor sites in the *env* gene within the pHM*Rluc* vector to measure Rem activity on unspliced RNA containing the reporter. Whereas HERV-K Rec did not induce the pHM*Rluc* vector, Rem, Rex and Rev all induce luciferase activity of the pHM*Rluc* vector, although the effects of Rex and Rev are minimal compared to Rem [141]. However, there was no difference in the nuclear and cytoplasmic mRNA levels of the *Renilla* gene in the presence or absence of Rem, Rex, or Rev. Therefore, increased luciferase activity is not a result of the nuclear export function of these export proteins, indicating a post-export event, such as translational regulation. Rev has been shown to lead to the cytoplasmic accumulation of CAT mRNA of the HIV-based reporter vector, pDM128. One possible reason for the failure of Rev to increase export of *Renilla* mRNA from pHM*Rluc* might be that the RmRE is localized outside an intron, unlike the position of the RRE in the HIV genome.

In summary, SP is a common factor generated from *rem* and *env* mRNAs and contains RNA-binding motifs similar to other Rev-like proteins. SP recognizes the RmRE at the junction of the end of the *env* gene and the 3' LTR. The RmRE contains an extensive, complex secondary RNA structure similar to those found in the HIV and

HTLV genomes. The RmRE at the 3'-end of the MMTV genome is located in all mRNAs, which may imply additional functions of SP.

4.2 REM IS PROCESSED BY SIGNAL PEPTIDASE IN THE ENDOPLASMIC RETICULUM AND IS RETROTRANSLOCATED FOR NUCLEAR FUNCTION.

Unlike Rev and Rex, Rem consists of a SP and a C-terminus [29, 142]. SP contains Rev-like functional motifs, such as an NLS, NES, NoLS and ARM, as well as hydrophobic residues to which signal recognition particles can bind. Rem and Env share the same reading frame, including the SP. SP directs Rem and Env to the ER where cleavage occurs. GFP-tagged SP is observed mainly in nucleoli [142]. Dultz *et al.* have shown that SP is generated in the presence of microsomal membranes and released from them [48]. Therefore, SP has a dual function, and SP has to be retrotranslocated from the ER for its nuclear activity.

Western blotting with cell extracts of MMTV-infected cells (GR-B2 cells and MMTV-infected HC11 cells) showed that SP is the dominant form of Rem (Figure 3.6). SP can be generated from both Rem and Env (Figure 3.7). The Dultz lab has shown that the inhibitor of signal peptide peptidase (SPP), an intramembrane protease which cleaves ER signal peptides, does not affect SP cleavage. To test the involvement of ER signal peptidase in Rem processing, substitution mutations were introduced in the consensus cleavage site. SP was not generated from cleavage site mutants. Both a single mutant (G98R) and a double mutant (V96RG98R) in either *rem* or *env* cDNA lost activity in the reporter assay. Therefore, cleavage by ER signal peptidase is critical for SP function. An additional interesting observation was that these SP cleavage mutants were highly

unstable (Figure 3.10A). To visualize the GFP-tagged SP cleavage mutants under a fluorescence microscope, a 20-fold increase in the amount of DNA was introduced to obtain comparable expression. Although expression levels of GFP-tagged Rem/SP and cleavage site mutants were similar by Western blotting (Figure 3.10C), the intensity of the GFP signal from cleavage site mutants was significantly weaker (Figure 3.10A and B). This result suggests that these cleavage site mutants may be unfolded or misfolded. Both mutant proteins in Western blotting revealed additional bands that had lower mobility than the mutant full-length protein (Figure 3.10C). These bands possibly represent glycosylated forms of the mutants, implying that mutant proteins remain in the ER membrane, where N-glycosylation happens [48]. Confocal images of the cleavage site mutants showed that both mutants are absent from nucleoli, unlike Rem. Their final localization was difficult to determine because of their low level expression and fluorescence (Figure 3.11).

The ER is a cellular organelle where the folding of secretory and membrane proteins occurs. For proteins to be fully functional, proper folding of proteins is crucial, yet the folding process is highly error-prone. A number of chaperones and enzymes reside in the ER to facilitate protein folding [8, 72, 222]. Only properly folded proteins can be transported to the Golgi apparatus [72]. ER chaperones and enzymes retain terminally misfolded proteins in the ER to re-fold them, but if target proteins remain folding-defective, they are degraded via the ERAD pathway [151, 222].

SP cleavage site mutants may be retained longer in the ER or ER membrane because they are misfolded or unfolded. Most mutant proteins are probably degraded as noted from their low steady-state expression level. It is possible that full-length wild type Rem is recognized as being folding-defective prior to ER signal peptidase cleavage.

Cleaved SP may fold quickly once retrotranslocated to the cytoplasm. The cleaved C-terminus also may acquire proper folding in the ER lumen and then be transported to either the membrane or the extracellular space. The A1 chain of cholera toxin, a bacterial AB toxin, becomes unfolded in the ER, but once retrotranslocated, it is quickly folded and becomes functional [79, 183, 227].

The 26S proteasome is a central component of the ERAD pathway. Since proteasomes are localized in the cytoplasm, retrotranslocation of terminally misfolded proteins is required for their ultimate degradation [8, 73]. Two inhibitors of the 26S proteasome function, lactacystin and MG132, revealed that Rem processing is greatly affected by inhibition of the 26S proteasome. The accumulation of full-length GFPRem (see Figure 3.12) may result from either inhibition of Rem processing or inhibition of the degradation of full-length Rem before cleavage. A slight accumulation of SP was also observed, indicating that some SP is degraded in the 26S proteasome. This accumulation was directly related to an increase in the functional assay (Figure 3.13).

The retrotranslocation of SP is dependent on the ERAD pathway since Rem or SP co-transfection with p97QQ, which is a dominant-negative form of p97/VCP, inhibited Rem function (Figures 3.14 and 3.16). p97/VCP is a cytoplasmic AAA ATPase that functions in the retrotranslocation of ERAD substrates [8, 222]. Since DN p97/VCP did not affect the processing of Rem to SP, retrotranslocation primarily happens after SP cleavage takes place. Therefore, Rem uses a unique trafficking mechanism by actively utilizing the host ERAD pathway. Rem moves to the ER co-translationally and is recognized by chaperones and enzymes in the ER, perhaps as a misfolded protein. Once SP is cleaved from Rem, SP is retrotranslocated by p97/VCP and may quickly acquire proper folding or interact with other cellular factors, leading to dissociation from ERAD

factors in the cytoplasm. Recognition of the SP NLS then allows transport into the nucleus where it functions in nuclear export of viral RNAs.

To understand the details of Rem processing, there are many questions still to be answered. Various proteins are involved in the series of steps involved in the ERAD pathway: proteins that recognize ERAD substrate proteins, E3 ligases and proteins involved in retrotranslocation steps. Rem must interact with ER chaperones and folding enzymes. SP must associate with retrotranslocon-related proteins, possibly E3 ligases and cytoplasmic factors. Which proteins are involved in Rem processing and retrotranslocation? The Derlin family is known to associate with ERAD substrates and to be involved in retrotranslocation. It is not clear yet whether Derlin is a retrotranslocon [73, 222]. Derlin-1 and Derlin-2 usually have different substrate specificities, and Rem function was shown to be dependent on Derlin-1, not Derlin-2 (Figure 3.18). Nevertheless, SP is independent of Derlin-1, indicating SP and Derlin-1 association happens before SP is cleaved. Derlin could recruit p97/VCP either directly or via VCP-interacting membrane protein (VIMP) [240, 241]. To understand how Derlin-1 participates in Rem processing and SP retrotranslocation, immunoprecipitation and further functional assay experiments are ongoing.

Other retroviruses also encode functional proteins from the envelope signal peptides. Like MMTV Rem, HERV-K Rec protein and JSRV Rej contain signal peptides that function as nuclear export proteins [132, 237]. Their trafficking patterns have not been reported yet, but it is possible that their SP-containing nuclear factors utilize the ERAD pathway.

A remaining question is why MMTV encodes Rem even though Env SP can provide the same function. As mentioned above, SP might be a multifunctional protein

and different levels may be required early and late during MMTV replication or transmission. Another possibility is that the C-terminus of Rem might have a unique function. Published results indicate that the Rem C-terminus (RemCT) is a glycoprotein [29, 48]. Corroborating experiments from our laboratory have detected RemCT after Western blotting of whole cell extracts from transfections with constructs expressing C-terminally tagged Rem. However, the localization pattern of RemCT has not been determined yet. Since Rem does not contain an ER retention signal, folded RemCT may be transported to either the cell membrane or the extracellular space for an immune modulatory function. Alternatively, RemCT may assist in functions of Env proteins, which are viral membrane proteins.

In summary, the SP of Rem functions as an ER signal sequence and as a nuclear export protein. Rem is directed to the ER co-translationally and cleaved by ER signal peptidase. Cleaved SP is retrotranslocated into the cytoplasm by p97/VCP but it evades degradation in the 26S proteasome. Derlin-1 is involved in Rem recognition, but does not appear to be required if the Rem C-terminus is removed.

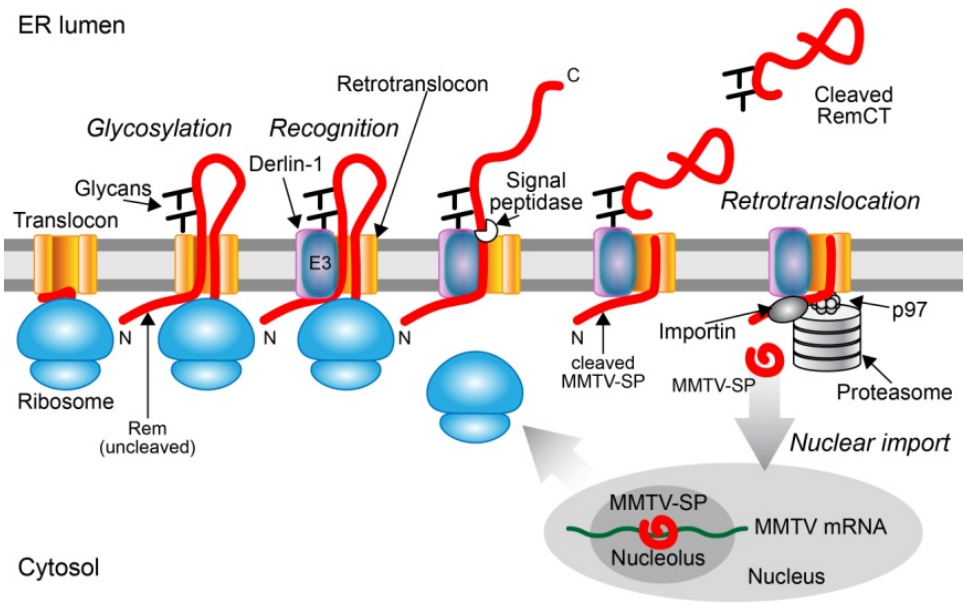

Figure 4.1: Proposed model for Rem processing and trafficking using ERAD.

Rem is directed to the ER co-translationally, where it is glycosylated and recognized by Derlin-1 or E3 ubiquitin ligases. Rem is then cleaved by signal peptidase. Cleaved SP is retrotranslocated via the ERAD system but evades proteasomal degradation. The SP of Rem functions as an ER signal sequence and as a nuclear export protein.

4.3 LENTIVIRAL shRNA EXPRESSION VECTORS CAUSE SUPER-INDUCTION OF REM ACTIVITY AND INCREASED REM EXPRESSION.

Small interfering RNAs have proven to be a powerful tool in biology. siRNAs targeting specific mRNAs are produced from precursor RNAs that are processed by a series of cellular enzymes including the RNase III enzyme, Dicer. Many siRNAs ultimately lead to the degradation of the target mRNA [168]. shRNAs contain the potential siRNA sequence in a hairpin structure retained after expression from an appropriate vector. This shRNA expression vector is processed in the nucleus by another cellular RNase III, Drosha, and exported to the cytoplasm where further processing occurs to generate specific siRNAs [168]. Various types of shRNA expression vectors have been developed. pLK0.1-puro (LK0.1) is a commercially available (Sigma) shRNA expression vector. It contains part of the HIV-1 genome sequence, including the HIV-1 packaging signal and the RRE. Insertion of a part of the HIV-1 genome enables the shRNA vector to be packaged and used for infections for efficient and stable expression of siRNAs in mammalian cells.

Interestingly, experiments involving co-transfection of constructs expressing GFPRem and LK0.1 containing the specific siRNA sequence to target cellular protein p97/VCP yielded unexpected data. Prior results from experiments with dominant-negative p97 expression constructs indicate that SP function is dependent on wild-type p97. Therefore, a decrease of Rem activity was expected after the knock down of p97/VCP by the siRNA. In contrast, every shRNA expressed from the LK0.1 backbone caused super-induction of Rem activity. Since even LK0.1, which is a control vector containing non-human and mouse specific sequences, induced Rem activity, Rem super-

induction was caused by the shRNA vector itself and was not a specific effect of gene knock-down by the siRNA.

To understand the mechanism of Rem super-induction, a series of experiments with LK0.1 were performed. LK0.1 induced the individual luciferase activities of both reporter vectors, pHM*Rluc* and pGL3-control, by about two fold. The pHM*Rluc* vector is responsive to Rem due to the presence of the RmRE, whereas pGL3-control vector lacks Rem responsiveness and is used to normalize for differences in transfection and expression efficiency. The induction of Rem-specific activity is much higher only in the presence of the RmRE (Figures 3.20 and 3.21). Western blotting of transfected cell extracts verified that Rem expression levels also were highly induced (Figure 3.22B). In most cases, the increase in Rem expression caused by LK0.1 was correlated with the level of Rem super-induction, but not in all cases (Figure 3.23). The same super-induction effect of LK0.1 was observed in co-transfections with Rev and Rex (Figure 3.24).

siRNAs contain dsRNA portions, which are effective factors in triggering host immune responses, since dsRNA is recognized as an indication of viral infection [104]. Various responses are induced upon dsRNA recognition, such as gene silencing, reduced translation, and induction of cytokines to activate the immune system [104]. To determine whether the LK0.1 hairpin structure itself is a key factor, the hairpin was deleted from LK0.1, resulting in a vector labeled LKΔHP. Surprisingly, the deletion of the hairpin led a lower super-induction of Rem activity, as well as Rev and Rex activity (Figure 3.25). However, LKΔHP did not abolish an increase in Rem activity. Also, deletion of the hairpin from LK0.1 still induced the Rem levels as determined by Western

blotting (Figure 3.26B) and enhanced the GFP signal from GFPRem when visualized under a fluorescence microscope (Figures 3.27 and 3.28).

Results from the co-transfection of LK0.1 or LKΔHP with EGFPN1, an enhanced GFP expression vector, or ER-mCherry, a RFP-expressing ER marker, suggested that induction by LK0.1 is not limited to Rev-like proteins (Figure 3.29). However, transfection of LK0.1 did not affect the levels of endogenous cellular proteins as determined by Coomassie Blue staining of total transfected cell extracts (data not shown). Therefore, these data suggest that the primary effect of LK0.1 is on the expression or activity of newly introduced genes.

To characterize the potential effector sequences in the LK0.1 plasmid, the non-lentiviral expression vectors, E6AP-3 and HPV18E6, were employed in transfections to compare their effects with LK0.1 (Figures 3.30 and 3.31). Interestingly, neither of these pCEP4-based shRNA expressing vectors caused super-induction of Rem activity. Therefore, the lentiviral element in LK0.1 may cooperate with a hairpin structure. Two additional LK0.1 deletion mutants were designed: one with a deletion from the hairpin to the pol III promoter U6 (LKΔU6) and a second with a deletion encompassing the *Psi* packaging signal (LKΔPsi) (Figure 3.30). Whereas LKΔU6 behaved like LKΔHP, LKΔPsi further decreased Rem protein expression levels (Figure 3.32A). No difference in GFP signal intensity was detectable under a fluorescence microscope (Figure 3.32B). Normalized Rem activity also was unchanged (Figure 3.31). LKΔPsi slightly decreased firefly luciferase values from a control vector. These experiments suggested that lentiviral sequences within the HIV genome, including the untranslated packaging region, influence expression of co-transfected genes.

An additional factor that may affect Rem super-induction by LK0.1 is the transfection process itself, which introduces some level of cellular stress. When cells are exposed to stress, stress-sensing kinases phosphorylate the α subunit of eukaryotic translation initiation factor eIF2, leading to the inhibition of translation. Western blotting with cell extracts of transfected cells revealed that all transfected cells had a marked increase in the level of phosphorylated-eIF2α (Figure 3.33). Also, a dramatic increase in the cellular production of stress granules was observed in transfected cells. Surprisingly, the transfection of LK0.1 decreased the number of cells inducing stress granules, implying that LK0.1 can relieve cellular stress or affect granule formation to some degree (Figure 3.34). Stress granules are formed under various unfavorable conditions, resulting in transient storage of mRNAs and inhibition of translation of housekeeping proteins. The net effect is enhancement of the translation of chaperone and repair proteins to relieve stress and assist in cellular maintenance [5, 6]. By relieving stress levels, LK0.1 may be able to stimulate translation of newly synthesized mRNA.

LK0.1, therefore, has the potential to induce several cellular reactions: an siRNA signaling pathway, the interferon response, and cellular stress. The cellular response to the hairpin structure of LK0.1 leads to the super-induction of Rem activity. Recently, Bridge *et al*. have shown that an shRNA-expressing vector induced the IFN-inducible gene, OAS [25]. However, shRNA-induced upregulation of the IFN pathway was not observed after co-transfections with LK0.1 as detected by Western blotting for RIG-G or ISG15 (data not shown). It is possible that unknown cellular partners of Rem or Rev-like proteins are recruited by the hairpin and then mediate super-induction. The expression level of B23, a known Rem and Rev-binding protein localized to the nucleolus, showed no differences in levels by Western blotting after cell transfections with LK0.1 (data not

shown). Other potential partners can be tested. The decrease of stress granules due to LK0.1 might activate translation, leading to the increased expression levels of *rem* or other newly introduced genes. To determine whether the effect of LK0.1 on stress granules is correlated with Rem super-induction, the effect on stress granules by LKΔHP can be compared to that of LK0.1.

An additional intriguing observation is that protein bands of about 27 kDa were observed in Western blotting using extracts of cells transfected with LK0.1 (Figures 3.22 and 3.26). These unidentified bands are detected with GFP-specific antibody even when no GFP-expression constructs are introduced. In some cases, the transfection process itself can induce a 27 kDa band, but when LK0.1 was transfected, double bands were observed. The higher molecular band could be a post-translationally modified form of the 27 kDa protein, perhaps due to phosphorylation. Since the 27 kDa protein primarily appeared when LK0.1 was introduced, LK0.1 may lead to the induction of these proteins, which are possibly responsible for the LK0.1-driven cellular response and super-induction of Rem activity. If LK0.1 has an effect on the cellular stress response, these bands could represent a stress response protein, such as heat shock protein 27. Hsp27 is one of the most universal chaperones and can be induced by various stresses, such as heat, irradiation, and oxidative stress [114]. This possibility is currently being tested.

In summary, the commercially available shRNA expression vector, LK0.1, unexpectedly induces additional Rem activity and increases Rem expression levels. The increase in the expression level is not always directly correlated with the super-induction of Rem activity. Experiments with a series of deletion mutants suggest that the hairpin structure may be the factor that primarily causes super-induction of Rem activity. Nevertheless, sequences within the HIV genome also appear to contribute to increased

Rem activity. LK0.1 transfection reduced the formation of stress granules. The reduction of stress granules may release sequestered cellular mRNAs that are involved in increased Rem expression levels and the levels of co-transfected genes. LK0.1 transfection also induces one or more unknown 27 kDa proteins. Characterization of these proteins may provide mechanistic insight into the LK0.1-related phenomenon.

4.4 FURTHER STUDIES.

Further studies are needed to understand the details of Rem processing and the SP retrotranslocation processes. To identify cellular partner proteins, utilization of dominant-negative proteins, RNA interference and immunoprecipitation of Rem/SP-associated protein complexes can be used. These experiments will help our understanding of strategies utilized by MMTV and related viruses to establish efficient viral replication. Expansion of our knowledge of the ERAD pathway is necessary. Also, to understand the mechanism of LK0.1-driven Rem super-induction, the effect of LK0.1 on the cellular stress response will be further analyzed.

Appendix

List of abbreviations

ARM	arginine-rich motif
ATP	adenosine triphosphate
ASV/ALV	avian sarcoma/leukemia virus
CA	capsid
Crm1	chromosome region maintenance 1 protein
CT	cholera toxin
CTE	constitutive transport element
Cux1	CCAAT displacement protein 1
Da	daltons
DMEM	dulbecco's modified Eagles medium
DNA	deoxyribonucleic acid
dNTP	deoxyribonucleotide triphosphate
DR	direct repeats
DTT	dithiothreitol
DU	dUTPase
EDTA	ethylenediamine tetraacetate
EGF	epidermal growth factor
eIF2	eukaryotic initiation factor 2
EJC	exon junction complex
Env	envelope
ER	Endoplasmic reticulum
ERAD	Endoplasmic reticulum-associated protein degradation
ERQC	Endoplasmic reticulum quality control
Gag	group-specific antigen
GAPDH	glyceraldehyde-3-phosphate dehydrogenase
GTP	guanosine triphosphate
HERV	human endogenous retrovirus
HIV	human immunodeficiency virus
HPV	human papillomavirus
HRE	hormone-responsive element
HTLV	human T-cell leukemia virus
IFN	interferon
IL	interleukin
IN	integrase
IRE1	inositol-requiring enzyme 1
ISG	interferon-stimulating gene
LTR	long terminal repeat
LUC	luciferase
MA	matrix

MG	mammary gland
MGE	mammary gland enhancer
MMTV	mouse mammary tumor virus
MPMV	Mason-Pfizer monkey virus
MuLV	murine leukemia virus
NC	nucleocapsid
NES	nuclear export sequence
NFX1	nuclear export family 1
NHK	null Hong Kong
NLS	nuclear localization signal
NoLS	nucleolar localization signal
NRE	negative regulatory element
OAS	oligoadenylate synthase
PB	processing body
PCR	polymerase chain reaction
PDI	protein disulfide isomerase
PKR	double stranded RNA-activated protein kinase, protein kinase R
PQC	protein quality control
PR	protease
Rem	regulator of export of MMTV mRNAs
RmRE	Rem-responsive element
RNC	ribosome nascent chain complex
RRE	Rev response element
RxRE	Rex1 response element
RNA	ribonucleic acid
RPMI	Roswell park memorial institute
RSV	Rous sarcoma virus
RT	room temperature
RT-PCR	reverse transcription-polymerase chain reaction
Sag	superantigen
SATB1	special AT-rich binding protein 1
SDS	sodium dodecyl sulphate
SG	stress granule
SP	signal peptide
SRP	signal recognition particle
SU	surface glycoprotein
TAP	Tip-associated protein
TCR	T cell receptor
TGF	transforming growth factor
TLR	Toll-like receptor
TM	transmembrane
TNF	tumor necrosis factor
UPR	unfolded protein response

VCP	valosin-containing protein
VIMP	VCP-interating membrane protein
WCL	whole cell lysate
XBP-1	X-box binding protein-1

Bibliography

1. **Adachi, Y., T. D. Copeland, C. Takahashi, T. Nosaka, A. Ahmed, S. Oroszlan, and M. Hatanaka.** 1992. Phosphorylation of the Rex protein of human T-cell leukemia virus type I. J. Biol. Chem. **267**:21977-21981.

2. **Ahmed, Y. F., S. M. Hanly, M. H. Malim, B. R. Cullen, and W. C. Greene.** 1990. Structure-function analyses of the HTLV-I Rex and HIV-1 Rev RNA response elements: insights into the mechanism of Rex and Rev action. Genes. Dev. **4**: 1014-1022.

3. **Alcock, F., and E. Swanton.** 2009. Mammalian OS-9 is upregulated in response to endoplasmic reticulum stress and facilitates ubiquitination of misfolded glycoprotein. J. Mol. Biol. **385**: 1032-1042.

4. **Alexopoulou, L., A. C. Holt, R. Medzhitov, and R. A. Flavell.** 2001. Recognition of double-stranded RNA and activation of NF-κB by Toll-like receptor 3. Nature **413**: 732-738.

5. **Anderson, P. and N. Kedersha.** 2002. **Stressful initiations.** J. Cell. Sci. **115**: 3227-3234.

6. **Anderson, P. and N. Kedersha.** 2006. RNA granules. J. Cell Biol. **172**: 803-808.

7. **Ardavin, C., G. Waanders, I. Ferrero, F. Anjuere, H. Acha-Orbea and H. R. MacDonald.** 1996. Expression and presentation of endogenous mouse mammary tumor virus superantigens by thymic and splenic dendritic cells and B cells. J. Immunol. **157**:2789-2794.

8. **Bagola, K., M. Mehnert, E. Jarosch, and T. Sommer.** 2011. Protein dislocation from the ER. Biochim. Biophys. Acta. **1808**: 925-936.

9. **Ballar, P., Y. Shen, H. Yang, and S. Fang.** 2006. The role of a novel p97/valosin-containing protein-interacting motif of gp78 in endoplasmic reticulum-associated degradation. J. Biol. Chem. **281**: 35359-35368.

10. **Ballaun, C., G. K. Farrington, M. Dobrovnik, J. Rusche, J. Hauber, and E. Böhnlein.** 1991. Functional analysis of human T-cell leukemia virus type I *rex*-response element: direct RNA binding of Rex protein correlates with in vivo activity. J. Virol. **65**: 4408-4413.

11. **Barbulescu, M., G. Turner, M. I. Seaman, A. S. Deinard, K. K. Kidd, and J. Lenz.** 1999. Many human endogenous retrovirus K (HERV-K) proviruses are unique to humans. Curr. Biol. **9**: 861-868.

12. **Bashkirov, V. I., H. Scherthan, J. A. Solinger, J. M. Buerstedde, and W. D. Heyer.** 1997. A mouse cytoplasmic exoribonuclease (mXRN1p) with preference for G4 tetraplex substrates. J. Cell Biol. **136**: 761-773.

13. **Bernardi, K. M., M. L. Forster, W. I. Lencer, and B. Tsai.** 2008. Derlin-1 facilitates the retro-translocation of cholera toxin. Mol. Biol. Cell **19**: 877-884.

14. **Bernardi, K. M., J. M. Williams, M. Kikkert, S. van Voorden, E. K. Wiertz, Y. Ye, and B. Tsai.** 2010. The E3 ubiquitin ligases Hrd1 and gp78 bind to and promote cholera toxin retro-translocation. Mol. Biol. Cell **21**: 140-151.

15. **Bernasconi, R., T. Pertel, J. Luban, and M. Molinari.** 2008. A dual task for the Xbp1-responsive OS-9 variants in the mammalian endoplasmic reticulum: inhibiting secretion of misfolded protein conformers and enhancing their disposal. J. Biol. Chem. **283**: 16446-16454.

16. **Bernstein, E., A. A. Caudy, S. M. Hammond, and G. J. Hannon.** 2001. Role for a bidentate ribonuclease in the initiation step of RNA interference. Nature **409**: 363-366.

17. **Bhadra, S., M. M. Lozano, S. M. Payne, J. P. Dudley.** 2006. Endogenous MMTV proviruses induce susceptibility to both viral and bacterial pathogens. PLoS Pathog. **2**:e128.

18. **Bhattacharyya, S. N., R. Habermacher, U. Martine, E. I. Closs, and W. Filipowicz.** 2006. Relief of microRNA-mediated translational repression in human cells subjected to stress. Cell **125**: 1111-1124.

19. **Binette, J., M. Dubé, J. Mercier, D. Halawani, M. Latterich, and E. A. Cohen**. 2007. Requirements for the selective degradation of CD4 receptor molecules by the human immunodeficiency virus type 1 Vpu protein in the endoplasmic reticulum. Retrovirology **4**: 75.

20. **Bishop, J. M.** 1978. Retroviruses. Ann. Rev. Biochem. **47**: 35-89.

21. **Bittner, J. J.** 1936. Some possible effects of nursing on the mammary gland tumor incidence in mice. Science. **84:** 162.

22. **Borer, R. A., C. F. Lehner, H. M. Eppenberger, and E. A. Nigg.** 1989. Major nucleolar proteins shuttle between nucleus and cytoplasm. Cell **56**: 379-390.

23. **Braun, I. C., A. Herold, M. Rode, E. Conti, and E. Izaurralde.** 2001. Overexpression of TAP/p15 heterodimers bypasses nuclear retention and stimulates nuclear mRNA export. J. Biol. Chem**. 276**: 20536-20543.

24. **Brekelmans, P., P. van Soest, J. Voerman, P. P. Platenburg, P. J. Leenen, and W. van Ewijk.** 1994. Transferrin receptor expression as a marker of immature cycling thymocytes in the mouse. Cell. Immunol. **159**: 331-339.

25. **Bridge, A. J., S. Pebernard, A. Ducraux, A. Nicoulaz, and R. Iggo.** 2003. Induction of an interferon response by RNAi vectors in mammalian cells. Nat. Genet. **34**: 263-264.

26. **Briggs, J. A. G., B. E.Watson, B. E. Gowen, and S. D. Fuller**. 2004. Cryoelectron microscopy of mouse mammary tumor virus. J. Virol. **78**:2602-2608.

27. **Buchschacher, G. L.** 2001. Introduction to Retroviruses and retroviral vectors. Somat. Cell Mol. Genet. **26**: 1-11.

28. **Burzyn, D., J. C. Rassa, D. Kim, I. Nepomnaschy, S. R. Ross, and I. Piazzon.** 2004. Toll-like receptor 4-dependent activation of dendritic cells by a retrovirus. J. Virol. **78**: 576-584.

29. **Byun, H., N. Halani, J. A. Mertz, A. F. Ali, M. M. Lozano, and J. P. Dudley.** 2010. Retroviral Rem protein requires processing by signal peptidase and retrotranslocation for nuclear function. Proc. Natl. Acad. Sci. U.S.A. **107**: 12287-12292.

30. **Cai, H., C. Wang, and C. Tsou.** 1994. Chaperone-like activity of protein disulfide isomerase in the refolding of a protein with no disulfide bonds. J. Biol. Chem. **269**: 24550-24552.

31. **Caporale, M., F. Arnaud, M. Mura, M. Golder, C. Murgia, and M. Palmarini**. 2009. The signal peptide of a simple retrovirus envelope functions as a posttranscriptional regulator of viral gene expression. J. Virol. **83**: 4591-4604.

32. **Chawla-Sarkar, M., D. J. Lindner, Y.-F. Liu, B. R. Williams, G. C. Sen, R. H. Silverman, and E. C. Borden.** 2003. Apoptosis and interferons: Role of interferon-stimulated genes as mediators of apoptosis. Apoptosis **8**: 237-249.

33. **Choi, Y., J. W. Kappler, and P. Marrack.** 1991. A superantigen encoded in the open reading frame of the 3' long terminal repeat of mouse mammary tumour virus. Nature **350**: 203-207.

34. **Christianson, J. C., T. A. Shaler, R. E. Tyler, and R. R. Kopito.** 2008. OS-9 and GRP94 deliver mutant alpha1-antitrypsin to the Hrd1-SEL1L ubiquitin ligase complex for ERAD. Nat. Cell Biol. **10**: 272-282.

35. **Clemens, M. J. and A. Elia.** 1997. The double-stranded RNA-dependent protein kinase PKR: structure and function. J. Interferon Cytokine Res. **17**: 503-524.

36. **Cullen, B. R.** 2003. Nuclear mRNA export: insights from virology. Trends Biochem. Sci. **28**: 419-424.

37. **Cullinan, S. B., D. Zhang, M. Hannink, E. Arvisais, R. J. Kaufman, and J. A. Diehl.** 2003. Nrf2 is a direct PERK substrate and effector of PERK-dependent cell survival. Mol. Cell. **23**: 7198-7209.

38. **Cunnea, P. M., A. Miranda-Vizuete, G. Bertoli, T. Simmen, A. E. Damdimopoulos, S. Hermann, S. Leinonen, M. P. Huikko, J.-A. Gustafsson, R. Sitia, and G. Spyrou**. 2003. ERdj5, an endoplasmic reticulum (ER)-resident protein containing DnaJ and thioredoxin domains, is expressed in secretory cells or following ER stress. J. Biol. Chem. **278**: 1059-1066.

39. **Dayton, E. T., D. A. Konings, D. M. Powell, B. A. Shapiro, L. Butini, J. V. Maizel, and A. I. Dayton.** 1992. Extensive sequence-specific information throughout the CAR/RRE, the target sequence of the human immunodeficiency virus type 1 Rev protein. J. Virol. **66**:1139-1151.

40. **Dekaban, G. A., and J. K. Ball.** 1984. Integration of type B retroviral DNA in virus-induced primary murine thymic lymphomas. J. Virol. **52**: 784-792.

41. **Dollins, D. E., R. M. Immormino, and D. T. Gewirth.** 2005. Structure of unliganded GRP94, the endoplasmic reticulum Hsp90. Basis for nucleotide-induced conformational change. J. Biol. Chem. **280**: 30438-30447.
42. **Dauber, B., G. Heins, and T. Wolff.** 2004. The influenza B virus nonstructural NS1 protein is essential for efficient viral growth and antagonizes beta interferon induction. J. Virol. **78**: 1865-1872.

43. **Diebold, S. S., M. Montoya, H. Unger, L. Alexopoulou, P. Roy, L. E. Haswell, A. Al-Shamkhani, R. Flavell, P. Borrow, and C. Reis e Sousa.** 2003. Viral infection switches non-plasmacytoid dendritic cells into high interferon producers. Nature **424**: 324-328.

44. **Doudna, J. A. and R. T. Batey.** 2004. Structural insights into the signal recognition particle. Annu. Rev. Biochem. **73**: 539-557.

45. **Dougherty, J. D., J. P. White, and R. E. Lloyd.** 2011. Poliovirus-mediated disruption of cytoplasmic processing bodies. J. Virol. **85**: 64-75.

46. **Doyle, S. E., R. O'Connell, S. A. Vaidya, E. K. Chow, K. Yee, and G. Cheng.** 2003. Toll-like receptor 3 mediates a more potent antiviral response than Toll-like receptor 4. J. Immunol. **170**: 3565-3571.

47. **Dudley, J. P.** 1999. Mouse mammary tumor virus, Encyclopedia of Virology, R. G. Webster and A. Granoff. Academic Press Ltd., London, UK.

48. **Dultz, E., M. Hildenbeutel, B. Martoglio, J. Hochman, B. Dobberstein, and K. Kapp.** 2008. The signal peptide of the mouse mammary tumor virus Rem protein is released from the endoplasmic reticulum membrane and accumulates in nucleoli. J. Biol. Chem. **283**: 9966-9976.

49. **Ellgaard, L. and A. Helenius.** 2001. ER quality contol: towards an understanding at the molecular level. Curr. Opin. Cell Biol. **13**: 431-437.

50. **Ernst, R. K., M. Bray, D. Rekosh, and M. L. Hammarskjöld.** 1997. A structured retroviral RNA element that mediates nucleocytoplasmic export of intron-containing RNA. Mol. Cell. Biol. **17**: 135-144.

51. **Ernst, R. K., M. Bray, D. Rekosh, and M. L. Hammarskjöld**. 1997. Secondary structure and mutational analysis of the Mason-Pfizer monkey virus RNA constitutive transport element. RNA **3**: 210-222.

52. **Felber B. K.** 1997. *In:* mRNA Metabolism and Post-transcriptional Gene Regulation. *Morris D and Harford JB (eds)*. Wiley-Liss Inc.: New York, pp.323–340.

53. **Finley, D.** 2009. Recognition and processing of ubiquitin-protein conjugates by the proteasome. Annu. Rev. Biochem. **78**: 477-513.

54. **Frankhauser, C., E. Izaurralde, Y. Adachi, P. Wingfield, and U. R. Laemmli.** 1991. Specific complex of human immunodeficiency virus type 1 Rev and nucleolar B23 proteins: dissociation by the Rev response element. Mol. Cell. Biol. **11**:2567-2575.

55. **Fribourg, S., I. C. Braun, E. Izaurralde, and E. Conti.** 2001. Structural basis for the recognition of a nucleoporin FG repeat by the NTF2-like domain of the TAP/p15 mRNA nuclear export factor. Mol. Cell **8**: 645-656.

56. **Futran, J., J. D. Kemp, E. H. Field, A. Vora, and R. F. Ashman.** 1989. Transferrin receptor synthesis is an early event in B cell activation. J. Immunol. **143**: 787-792.

57. **Gallo, R., F. Wong-Staal, L. Montagnier, W. A. Haseltine, and M. Yoshida.** 1988. HIV/HTLV gene nomenclature. Nature **333**: 504.

58. **Geiss, G., G. Jin, J. Guo, R. Bumgarner, M. G. Katze, and G. C. Sen.** 2001. A complehensive view of regulation of gene expression by double-stranded RNA-mediated cell signaling. J. Biol. Chem. **276**: 30178-30182.

59. **Gessain, A., F. Barin, J. C. Vernant, O. Gout, L. Maurs, A. Calender, and G. de Thé.** 1985. Antibodies to human T-lymphotropic virus type-I in patients with tropical spastic paraparesis. Lancet **2**: 407-410.

60. **Ghaemmaghami, S., W. –K. Huh, K. Bower, R. W. Howson, A. Belle, N. Dephoure, E. K. O'Shea, and J. S. Weissman.** 2003. Global analysis of protein expression in yeast. Nature **425**: 737-741.

61. **Golovkina, T. V., A. Chervonsky, J. P. Dudley, S. R. Ross.** 1992. Transgenic mouse mammary tumor virus superantigen expression prevents viral infection. Cell **69**: 637-645.

62. **Golovkina, T. V., J. P. Dudley, and S. R. Ross.** 1998. B and T cells are required for mouse mammary tumor virus spread within the mammary gland. J. Immunol. **161**: 2375-2382.

63. **Golovkina, T. V**. 2000. A novel mechanism of resistance to mouse mammary tumor virus infection. J. Virol. **74**: 2752-2759.

64. **Groenendyk, J., P. K. Sreenivasaiah, D. H. Kim, L. B. Agellon, and M. Michalak.** 2010. Biology of endoplasmic reticulum stress in the heart. Circ. Res. **107**: 1185-1197.

65. **Gröne, M., C. Koch, and R. Grassmann**. 1996. The HTLV-1 Rex protein induces nuclear accumulation of unspliced viral RNA by avoiding intron excision and degradation. Virology. **218**: 316-325.

66. **Grudnik, P., G. Bange, and I. Sinning.** 2009. Protein targeting by the signal recognition particle. Biol. Chem. **390**: 775-782.

67. **Harding, H. P., Y. Zhang, and D. Ron D.** 1999. Protein translation and folding are coupled by an endoplasmic-reticulum-resident kinase. Nature **397**: 271-274.

68. **Hammarskjöld, M.** 1997. Regulation of retroviral RNA export. Semin. Cell Dev. Biol. **8**: 83-90.

69. **Haze, K., H. Yoshida, H. Yanagi, T. Yura, and K. Mori.** 1999. Mammalian transcription factor ATF6 is synthesized as a transmembrane protein and activated by proteolysis in response to endoplasmic reticulum stress. Mol. Biol. Cell **10**: 3787-3799.

70. **Hazes, B. and R. J. Read.** 1997. Accumulating evidence suggests that several AB-toxins subvert the endoplasmic reticulum-associated protein degradation pathway to enter target cells. **36**: 11051-11054.

71. **Heaphy, S., C. Dingwall, I. Ernberg, M. J. Gait, S, M. Green, J. Karn, A. D. Lowe, M. Singh, and M. A. Skinner.** 1990. HIV-1 regulator of virion expression (Rev) protein binds to an RNA stem-loop structure located within the Rev response element region. Cell **60**: 685-693.

72. **Hebert, D. N. and M. Molinari.** 2007. In and out of the ER: protein folding, quality control, degradation, and related human diseases. Physiol. Rev. **87**: 1377-1408.

73. **Hebert, D. N., R. Bernasconi, and M. Molinari.** 2010. ERAD substrates: which way out? Semin. Cell Dev. Biol. **21**: 526-532.

74. **Hegde, R. S. and H. D. Bernstein.** 2006. The surprising complexity of signal sequences. Trends Biochem. Sci. **31**: 583-571.

75. **Hegde, R. S. and H. L. Ploegh.** 2010. Quality and quantity control at the endoplasmic reticulum. Curr. Opin. Cell Biol. **22**: 437-446.

76. **Heger, P., O. Rosorius, C. Koch, G. Casari, R. Grassmann, and J. Hauber.** 1998. Multimer formation is not essential for nuclear export of human T-cell leukemia virus type 1 Rex *trans*-activator protein. J. Virol. **72**: 8659-8668.

77. **Heger, P., O. Rosorius, J. Hauber and R. H. Stauber.** 1999. Titration of cellular export factors, but not heteromultimerization, is the molecular mechanism of *trans*-dominant HTLV-1 Rex mutants. Oncogene. **18**: 4080-4090.

78. **Helenius, A. and M. Aebi.** 2004. Roles of N-linked glycans in the endoplasmic reticulum. Annu. Rev. Biochem. **73**: 1019-1049.

79. **Heiligenstein, S., K. Eisfeld, T. Sendzik, N. Jimenéz-Becker, F. Breinig, and M. J. Schmitt.** 2006. Retrotranslocation of a viral A/B toxin from the yeast endoplasmic reticulum is independent of ubiquitination and ERAD. EMBO J. **25**: 4717-4727.

80. **Held, W., G. A. Waanders, A. N. Shakhov, L. Scarpellino, H. Acha-Orbea, and H. R. MacDonald.** 1993. Superantigen-induced immune stimulation amplifies mouse mammary tumor virus infection and allows virus transmission. Cell **74**: 529-540.

81. **Hirsch, C., R. Gauss, S. C. Horn, O. Neuber, and T. Sommer.** 2009. The ubiquitylation machinery of the endoplamic reticulum. Nature. **458**: 453-460.

82. **Hizi, A., L. E. Henderson, T. D. Copeland, R. C. Sowder, C. V. Hixson and S. Oroszlan.** 1987. Characterization of mouse mammary tumor virus gag-pro gene products and the ribosomal frameshift site by protein sequencing. Proc. Natl. Acad. Sci. U.S.A. **84**:7041-7045.

83. **Hofacre, A., T. Nitta, and H. Fan.** 2009. Jaagsiekte sheep retrovirus encodes a regulatory factor, Rej, required for synthesis of Gag protein. J. Virol. **83**: 12483-12498.

84. **Hofer, L., I. Weichselbraun, S. Quick, G. K. Farrington, E. Böhnlein, and J. Hauber.** 1991. Mutational analysis of the human T-cell leukemia virus type I trans-acting rex gene product. J. Virol. **65**:3379-3383.

85. **Hope, T. J.** 1999. The ins and outs of HIV Rev. Arch. Biochem. Biophys. **365**: 186-191.

86. **Horn, S. C., J. Hanna, C. Hirsch, C. Volkwein, A. Schütz, U. Heinemann, T. Sommer, and E. Jarosch.** 2009. Usa1 functions as a scaffold of the HRD-ubiquitin ligase. Mol. Cell **36**: 782-793.

87. **Hoseki, J., R. Ushioda, and K. Nagata.** 2010. Mechanism and components of endoplasmic reticulum associated degradation. J. Biochem. **147**: 19-25.

88. **Hosoda, A., Y. Kimata, A. Tsuru, and K. Kohno.** 2003. JPDI, a novel endoplasmic reticulum-resident protein containing both a BiP-interacting J-domain and thioredoxin-like motifs. J. Biol. Chem. **278**: 2669-2676.

89. **Hosokawa, N., I. Wada, K. Nagasawa, T. Moriyama, K. Okawa, and K. Nagata.** 2008. Human XTP3-B forms an endoplasmic reticulum quality control scaffold with the HRD1-SEL1L ubiquitin ligase complex and BiP. J. Biol. Chem. **283**: 20914-20924.

90. **Howard, D. K. and J. Schlom.** 1980. Differential host ranges for in vitro infectivity of mouse mammary tumour viruses. J. Gen. Virol. **47**:439-448.

91. **Hüssy, P., H. Langen, J. Mous, and H. Jacobsen.** 1996. Hepatitis C virus core protein: carboxy-terminal boundaries of two processed species suggest cleavage by a signal peptide peptidase. Virology **224**: 93-104.

92. **Hutten, S. and R. H. Kehlenbach.** 2007. CRM1-mediated nuclear export: to the pore and beyond. Trends Cell Biol**. 17**: 193-201.

93. **Hwang, C., A. J. Sinskey, and H. F. Lodish.** 1992. Oxidized redox state of glutathione in the endoplasmic reticulum. Science **257**: 1496-1502.

94. **Immormino, R. M., D. E. Dollins, P. L. Shaffer, K. L. Soldano, M. A. Walker, and D. T. Gewirth.** 2004. Ligand-induced conformational shift in the N-terminal domain of GRP94, an Hsp90 chaperone. J. Biol. Chem. **279**: 46162-46171.

95. **Indik, S., W. H. Günzburg, B. Salmons, and F. Rouault.** 2005. A novel, mouse mammary tumor virus encoded protein with Rev-like properties. Virology **337**: 1-6.

96. **Inoue, J., M. Itoh, T. Akizawa, H. Toyoshima, and M. Yoshida**. 1991. HTLV-1 Rex protein accumulates unspliced RNA in the nucleus as well as in cytoplasm. Oncogene. **6**: 1753-1757.

97. **Jacks, T., K. Townsley, H. E. Varmus and J. Majors.** 1987. Two efficient ribosomal frameshifting events are required for synthesis of mouse mammary tumor virus gag-related polyproteins. Proc. Natl. Acad. Sci. U.S.A. **84**: 4298-4302.

98. **Janeway, C. A**. 1991. Selective elements for the Vβ region of the T cell receptor: MIs and the bacterial toxin mitogens. Adv. Immunol. **50**: 1-53.

99. **Jin, J., T. Sturgeon, C. Chen, S. C. Watkins, O. A. Weisz, and R. C. Montelaro.** 2007. Distinct Intracellular Trafficking of Equine Infectious Anemia Virus and Human Immunodeficiency Virus Type 1 Gag during Viral Assembly and Budding Revealed by Bimolecular Fluorescence Complementation Assays. J. Virol. **81**: 11226-11235.

100. **Jin, L., B. W. Guzik, Y. Bor, D. Rekosh, and M. -L. Hammarskjöld**. 2003. Tap and NXT promote translation of unspliced mRNA. Genes Dev**. 17**: 3075-3086.

101. **Joshi, B., A. L. Cai, B. D. Keiper, W. B. Minich, R. Mendez, C. M. Beach, J. Stepinski, R. Stolarski, E. Darzynkiewicz, and R. E. Rhoads.** 1995.

Phosphorylation of eukaryotic protein synthesis initiation factor 4E at Ser-209. J. Biol. Chem. **270**: 14597-14603.

102. **Kang, Y. and B. R. Cullen.** 1999. The human Tap protein is a nuclear mRNA export factor that contains novel RNA-binding and nucleocytoplasmic transport sequences. Genes Dev. **13**:1126-1139.

103. **Karapetian, O., A. N. Shakhov, J. P. Kraehenbuhl and H. Acha-Orbea.** 1994. Retroviral infection of neonatal Peyers patch lymphocytes: the mouse mammary tumor virus model. J. Exp. Med. **180**: 1511-1516.

104. **Karpala, A. J., T. K. Doran, and A. G. D. Bean.** 2005. Immune responses to dsRNA: implications for gene silencing technologies. Immunol. Cell Biol. **83**: 211-216.

105. **Katahira, J., K. Strässer, A. Podtelejnikov, M. Mann, J. U. Jung, and E. Hurt.** 1999. The Mex67p-mediated nuclear mRNA export pathway is conserved from yeast to human. EMBO J. **18**: 2593-2609.

106. **Katz, E., M. H. Lareef, J. C. Rassa, S. M. Grande, L. B. King, J. Russo, S. R. Ross and J. G. Monroe.** 2005. MMTV Env encodes an ITAM responsible for transformation of mammary epithelial cells in three-dimensional culture. J. Exp. Med. **201**: 431-439.

107. **Kaufmann, S., M. Sauter, M. Schmitt, B. Baumert, B. Best, A. Boese, K. Roemer, and N. Mueller-Lantzsch.** 2010. Human endogenous retrovirus protein Rec interacts with the testicular zinc-finger protein and androgen receptor. J. Gen. Virol. **91**: 1494-1502.

108. **Kedersha, N., G. Stoecklin, M. Ayodele, P. Yacono, J. Lykke-Andersen, M. J. Fritzler, D. Scheuner, R. J. Kaufman, D. E. Golan, and P. Anderson**. 2005. Stress granules and processing bodies are dynamically linked sites of mRNP remodeling. J. Cell Biol. **169**: 871-884.

109. **Kimball, S. R., R. L. Horetsky, D. Ron, L. S. Jefferson, and H. P. Harding.** 2003. Mammalian stress granules represent sites of accumulation of stalled translation initiation complexes. Am. J. Physiol., Cell Physiol. **284**: C273-284.

110. **Klionsky, D. J.** 2005. The molecular machinery of autophagy: unanswered questions. J. Cell. Sci. **118**: 7-18.

111. **Kothe, M., Y. Ye, J. S. Wagner, H. E. De Luca, E. Kern, T. A. Rapoport, and W. I. Lencer.** 2005. Role of p97 AAA-ATPase in the retrotranslocation of the cholera toxin A1 chain, a non-ubiquitinated substrate. J. Biol. Chem. **280**: 28127-28132.

112. **Kohno, K.** 2010. Stress-sensing mechanisms in the unfolded protein response: similarities and differences between yeast and mammals. J. Biochem. **147**: 27-33.

113. **Korman, A. J., P. Bourgarel, T. Meo and G. E. Rieckhof.** 1992. The mouse mammary tumour virus long terminal repeat encodes a type II transmembrane glycoprotein. EMBO J. **11**:1901-1905.

114. **Kostenko, S. and U. Moens**. 2009. Heat shock protein 27 phosphorylation: kinases, phosphatases, functions and pathology. Cell. Mol. Life Sci. **66**: 3289-3307.

115. **Kozak, C., G. Peters, R. Pauley, V. Morris, R. Michalides, J. Dudley, M. Green, M. Davisson, O. Prakash, A. Vaidya, J. Hilgers, A. Verstraeten, N. Hynes, H. Diggelmann, D. Peterson, J. C. Cohen, C. Dickson, N. Sarkar, R. Nusse, H. Varmus and R. Callahan.** 1987. A standardized nomenclature for endogenous mouse mammary tumor viruses. J. Virol. **61**:1651-1654.

116. **Lander, E. S., L. M. Linton, B. Birren, C. Nusbaum, M. C. Zody, J. Baldwin, K. Devon, K. Dewar, M. Doyle, and other authors.** 2001. Initial sequencing and analysis of the human genome. Nature **409**: 860-921.

117. **Lass, A., E. McConnell, K. Fleck, A. Palamarchuk, and C. Wójcik.** 2008. Analysis of Npl4 deletion mutants in mammalian cells unravels new Ufd1-interacting motifs and suggests a regulatory role of Npl4 in ERAD. Exp. Cell Res. **314**: 2715-2723.

118. **LeBlanc, J. J., S. Uddowla, B. Abraham, S. Clatterbuck, and K. L. Beemon.** 2007. Tap and Dbp5, but not Gag, are involved in DR-mediated nuclear export of unspliced Rous sarcoma virus RNA. Virology **363**: 376-386.

119. **Lee, A. S.** 2001. The glucose-regulated proteins: stress induction and clinical applications. Trends Biochem. Sci. **26**: 504-510.

120. **Lee, A., N. N. Iwakoshi, and L. H. Glimcher.** 2003. XBP-1 regulates a subset of endoplasmic reticulum resident chaperone genes in the unfolded protein response. Mol. Cell. Biol. **23**: 7448-7459.

121. **Lencer, W. I.** 2001. Microbes and microbial Toxins: paradigms for microbial-mucosal toxins. V. Cholera: invasion of the intestinal epithelial barrier by a stably folded protein toxin. Am. J. Physiol. Gastrointest. Liver Physiol. **280**: G781-786.

122. **Li, W., S. Schulman, D. Boyd, K. Erlandson, J. Beckwith, T. A. Rapoport.** 2007. The plug domain of the SecY protein stabilizes the closed state of the translocation channel and maintains a membrane seal. Mol. Cell **26**: 511-521.

123. **Lièvremont, J. P., R. Rizzuto, L. Hendershot, and J. Meldolesi.** 1997. BiP, a major chaperone protein of the endoplasmic reticulum lumen, plays a direct and important role in the storage of the rapidly exchanging pool of Ca2+. J. Biol. Chem. **272**: 30873-30879.

124. **Lilley, B. N., J. M. Gilbert, H. L. Ploegh, and T. L. Benjamin.** 2006. Murine polyomavirus requires the endoplasmic reticulum protein Derlin-2 to initiate infection. J. Virol. **80**: 8739-8744.

125. **Lilley, B. N., H. L. Ploegh.** 2004. A membrane protein required for dislocation of misfolded proteins from the ER. Nature **429**: 834-840.

126. **Lim, P. J., R. Danner, J. Liang, H. Doong, C. Harman, D. Srinivasan, C. Rothenberg, H. Wang, Y. Ye, S. Fang, and M. J. Monteiro.** 2009. Ubiquilin and p97/VCP bind erasin, forming a complex involved in ERAD. J. Cell Biol. **187**: 201-217.

127. **Lima, W. F., H. Wu, J. G. Nichols, H. Sun, H. M. Murray, and S. T. Crooke.** 2009. Binding and cleavage specificities of human Argonaute2. J. Biol. Chem. **284**: 26017-26028.

128. **Lindsay, M. A.** 2008. microRNAs and the immune response. Trends Immunol. **29**: 343-351.

129. **Liu, J., D. Bramblett, Q. Zhu, M. M. Lozano, R. Kobayashi, S. R. Ross, and J. P. Dudley.** 1997. The matrix attachment region-binding protein SATB1 participates in negative regulation of tissue-specific gene expression. Mol. Cell. Biol. **17**:5275-5287.

130. **Liu, Y., P. Choudhury, C. M. Cabral, and R. N. Sifers.** 1997. Intracellular disposal of incompletely folded human alpha1-antitrypsin involves release from calnexin and post-translational trimming of asparagine-linked oligosaccharides. J. Biol. Chem. **272**: 7946-7951.

131. **Ma, Y., J. W. Brewer, J. A. Diehl, and L. M. Hendershot.** 2002. Two distinct stress signaling pathways converge upon the CHOP promoter during the mammalian unfolded protein response. J. Mol. Biol. **318**: 1351-1365.

132. **Magin, C., R. Löwer, and J. Löwer.** 1999. cORF and RcRE, the Rev/Rex and RRE/RxRE homologues of the human endogenous retrovirus family HTDV/HERV-K. J. Virol. **73**: 9496-9507.

133. **Maitra, U., J. Seo, M. M. Lozano, and J. P. Dudley.** 2006. Differentiation-induced cleavage of Cutl1/CDP generates a novel dominant-negative isoform that regulates mammary gene expression. Mol. Cell. Biol. **26**:7466-7478.

134. **Malim, M. H., L. S. Tiley, D. F. McCarn, J. R. Rusche, J. Hauber, and B. R. Cullen**. 1990. HIV-1 structural gene expression requires binding of the Rev trans-activator to its RNA target sequence. Cell **60**: 675-683.

135. **Marin, O., S. Sarno, M. Boschetti, M. A. Pagano, F. Meggio, V. Ciminale, D. M. D'Agostino, and L. A. Pinna.** 2000. Unique features of HIV-1 Rev protein phosphorylation by protein kinase CK2 ('casein kinase-2'). FEBS Lett. **481**:63-67.

136. **Marrack, P., E. Kushnir and J. Kappler.** 1991. A maternally inherited superantigen encoded by a mammary tumour virus. Nature **349**:524-526.

137. **Matlack, K. E., B. Misselwitz, K. Plath, and T. A. Rapoport.** 1999. BiP acts as a molecular ratchet during posttranslational transport of prepro-alpha factor across the ER membrane. Cell **97**: 553-564.

138. **McCracken, A. A. and J. L. Brodsky**. 1996. Assembly of ER-associated protein degradation in vitro: dependence on cytosol, calnexin, and ATP. J. Cell Biol. **132**: 291-298.

139. **Melnick, J., J. L. Dul, and Y. Argon.** 1994. Sequential interaction of the chaperones BiP and GRP94 with immunoglobulin chains in the endoplasmic reticulum. Nature **370**: 373-375.

140. **Mertz, J. A., A. B. Chadee, H. Byun, R. Russell, and J. P. Dudley.** 2009. Mapping of the functional boundaries and secondary structure of the mouse mammary tumor virus Rem-responsive element. J. Biol. Chem. **284**: 25642-25652.

141. **Mertz, J. A., M. M. Lozano, and J. P. Dudley**. 2009. Rev and Rex proteins of human complex retroviruses function with the MMTV Rem-responsive element. Retrovirology.**6**: 10.

142. **Mertz, J. A., M. S. Simper, M. M. Lozano, S. M. Payne, and J. P. Dudley.** 2005. Mouse mammary tumor virus encodes a self-regulatory RNA export protein and is a complex retrovirus. J. Virol. **79**: 14737-14747.

143. **Meyer, H. H, J. G. Shorter, J. Seemann, D. Pappin, and G. Warren.** 2000. A complex of mammalian ufd1 and npl4 links the AAA-ATPase, p97, to ubiquitin and nuclear transport pathways. EMBO J. **19**: 2181-2192.

144. **Michalides R, E. Wagenaar, J. Hilkens, J. Hilgers, B. Groner, and N. E. Hynes**. 1982. Acquisition of proviral DNA of mouse mammary tumor virus in thymic leukemia cells from GR mice. J. Virol. **43**: 819-829.

145. **Mok E, T. V. Golovkina, S. R. Ross.** 1992. A mouse mammary tumor virus mammary gland enhancer confers tissue-specific but not lactation-dependent expression in transgenic mice. J. Virol. **66**: 7529-7532.

146. **Mori, K., W. Ma, M. J. Gething, and J. Sambrook.** 1993. A transmembrane protein with a cdc2+/CDC28-related kinase activity is required for signaling from the ER to the nucleus. Cell **74**: 743-756.

147. **Mueller, B., E. J. Klemm, E. Spooner, J. H. Claessen, and H. L. Ploegh.** 2008. SEL1L nucleates a protein complex required for dislocation of misfolded glycoproteins. Proc. Natl. Acad. Sci. U.S.A. **105**: 12325-12330.

148. **Mueller, B., B. N. Lilley, and H. L. Ploegh.** 2006. SEL1L, the homologue of yeast Hrd3p, is involved in protein dislocation from the mammalian ER. J. Cell Biol. **175**: 261-270.

149. **Müllner, M., B. Salmons, W. H. Günzburg, and S. Indik**. 2008. Identification of the Rem-response element of mouse mammary tumor virus. Nucleic Acids Res. **36**: 6284-6294.

150. **Munro, S.** 2001. The MRH domain suggests a shared ancestry for the mannose 6-phosphate receptors and other N-glycan-recognising proteins. Curr. Biol. **11**: R499-501.

151. **Nakatsukasa, K. and J. L. Brodsky.** 2008. The recognition and retrotranslocation of misfolded proteins from the endoplasmic reticulum. Traffic. **9**: 861-870.

152. **Nakielny, S. and G. Dreyfuss.** 1999. Transport of proteins and RNAs in and out of the nucleus. Cell **99**: 677-690.

153. **Nakielny, S., U. Fischer, W. M. Michael, and G. Dreyfuss**. 1997. RNA transport. Annu. Rev. Neurosci **20**: 269-301.

154. **Nandi, S. and C. M. McGrath.** 1973. Mammary Neoplasia in Mice. Adv. Cancer Res. **17**: 353-414.

155. **Nguyen, T., P. J. Sherratt, and C. B. Pickett.** 2003. Regulatory mechanisms controlling gene expression mediated by the antioxidant response element. Annu. Rev. Pharmacol. Toxicol. **43**: 233-260.

156. **Nitta, T., A. Hofacre, S. Hull, and H. Fan.** 2009. Identification and mutational analysis of a Rej response element in Jaagsiekte sheep retrovirus RNA. J. Virol. **83**: 12499-12511.

157. **Nover, L., K. Scharf, and D. Neumann.** 1989. Cytoplasmic heat shock granules are formed from precursor particles and are associated with a specific set of mRNAs. Mol. Cell. Biol. **9**: 1298-1308.

158. **Oda, Y., T. Okada, H. Yoshida, R. J. Kaufman, K. Nagata, and K. Mori.** 2006. Derlin-2 and Derlin-3 are regulated by the mammalian unfolded protein response and are required for ER-associated degradation. J. Cell Biol. **172**: 383-393.

159. **Ogert, R. A., L. H. Lee, and K. L. Beemon.** 1996. Avian retroviral RNA element promotes unspliced RNA accumulation in the cytoplasm. J. Virol **70**: 3834-3843.

160. **Okuda-Shimizu, Y. and L. M. Hendershot**. 2007. Characterization of an ERAD pathway for nonglycosylated BiP substrates, which require Herp. Mol. Cell **28**: 544-554.

161. **Ono, M.** 1986. Molecular cloning and long terminal repeat sequences of human endogenous retrovirus genes related to types A and B retrovirus genes. J. Virol. **58**: 937-944.

162. **Ono, M., T. Yasunaga, T. Miyata, and H. Ushikubo.** 1986. Nucleotide sequence of human endogenous retrovirus genome related to the mouse mammary tumor virus genome. J. Virol. **60**: 589-598.

163. **Osame, M., K. Usuku, S. Izumo, N. Ijichi, H. Amitani, A. Igata, M. Matsumoto, and M. Tara.** 1986. HTLV-I associated myelopathy, a new clinical entity. Lancet **1**: 1031-1032.

164. **Paca, R. E., R. A. Ogert, C. S. Hibbert, E. Izaurralde, and K. L. Beemon.** 2000. Rous sarcoma virus DR posttranscriptional elements use a novel RNA export pathway. J. Virol **74**: 9507-9514.

165. **Payne, S. L. and J. H. Elder.** 2001. The role of retroviral dUTPases in replication and virulence. Curr. Protein Pept. Sci. **2**:381-388.

166. **Pena, F., A. Jansens, G. van Zadelhoff, and I. Braakman.** 2010. Calcium as a crucial cofactor for low density lipoprotein receptor folding in the endoplasmic reticulum. J. Biol. Chem. **285**: 8656-8664.

167. **Perlmutter, D. H.** 2006. The role of autophagy in alpha-1-antitrypsin deficiency: a specific cellular response in genetic diseases associated with aggregation-prone proteins. Autophagy **2**: 258-263.

168. **Perron, M. P. and P. Provost.** 2009. Protein components of the microRNA pathway and human diseases. Methods Mol. Biol. **487**: 369-385.

169. **Peters, G. and C. Glover.** 1980. tRNAs and priming of RNA-directed DNA synthesis in mouse mammary tumor virus. J. Virol. **35**:31-40.

170. **Pilon, M., R. Schekman, and K. Römisch.** 1997. Sec61p mediates export of a misfolded secretory protein from the endoplasmic reticulum to the cytosol for degradation. EMBO J. **16**: 4540-4548.

171. **Pindel, A. and A. Sadler.** 2011. The role of protein kinase R in the interferon response. J. Interferon cytokine Res. **31**: 59-70.

172. **Player, M. R., P. F. Torrence.** 1998. The 2-5A system: modulation of viral and cellular processes through acceleration of RNA degradation. Pharmacol. Ther. **78**: 55-113.

173. **Plemper, R. K., S. Böhmler, J. Bordallo, T. Sommer, and D. H. Wolf.** 1997. Mutant analysis links the translocon and BiP to retrograde protein transport for ER degradation. Nature **388**: 891-895.

174. **Pollard, V. W. and M. H. Malim.** 1998. The HIV-1 Rev protein. Annu. Rev. Microbiol**. 52**: 491-532.

175. **Pond, S. J. K., W.K Ridgeway, R. Robertson, J. Wang, and D. P. Millar.** 2009. HIV-1 Rev protein assembles on viral RNA one molecule at a time. Proc. Natl. Acad. Sci. U.S.A. **106**: 1404-1408.

176. **Quan, H., G. Fan, and C. C. Wang.** 1995. Independence of the chaperone activity of protein disulfide isomerase from its thioredoxin-like active site. J. Biol. Chem. **270**: 17078-17080.

177. **Randow, F. and B. Seed**. 2001. Endoplasmic reticulum chaperone gp96 is required for innate immunity but not cell viability. Nat. Cell Biol. **3**: 891-896.

178. **Rapoport, T. A., B. Jungnickel, and U. Kutay.** 1996. Protein transport across the eukaryotic endoplasmic reticulum and bacterial inner membranes. Annu. Rev. Biochem. **65**: 271-303.

179. **Raven, J. F. and A. E. Koromilas.** 2008. PERK and PKR. Cell Cycle. **7**: 1146-1150.

180. **Reuss, F. U. and J. M. Coffin.** 1995. Stimulation of mouse mammary tumor virus superantigen expression by an intragenic enhancer. Proc. Natl. Acad. Sci. U.S.A **92**: 9293-9297.

181. **Richly, H., M. Rape, S. Braun, S. Rumpf, C. Hoege, and S. Jentsch.** 2005. A series of ubiquitin binding factors connects CDC48/p97 to substrate multiubiquitylation and proteasomal targeting. Cell **120**: 73-84.

182. **Rizvi, T. A., J. Ali, P. S. Phillip, A. Ghazawi, P. Jayanth, and F. Mustafa.** 2009. Role of a heterologous retroviral transport element in the development of genetic complementation assay for mouse mammary tumor virus (MMTV) replication. Virology **385**: 464-472.

183. **Rodighiero, C., B. Tsai, T. A. Rapoport, and W. I. Lencer.** 2002. Role of ubiquitination in retro-translocation of cholera toxin and excape of cytosolic degradation. EMBO Rep. **3**: 1222-1227.

184. **Ross, C. A. and M. A. Poirier MA.** 2005. Opinion: What is the role of protein aggregation in neurodegeneration? Nat. Rev. Mol. Cell Biol. **6**: 891-898.

185. **Ross, S. R.** 2000. Using genetics to probe host-virus interactions; the mouse mammary tumor virus model. Microbes Infect. **2**:1215-1223.

186. **Ross, S. R.** 2008. MMTV infectious cycle and the contribution of virus-encoded proteins to transformation of mammary tissue. J. Mammary Gland Biol. Neoplasia. **13**:299-307.

187. **Ross S. R., J. J. Schofield, C. J. Farr, and M. Bucan.** 2002. Mouse transferrin receptor 1 is the cell entry receptor for mouse mammary tumor virus. Proc. Natl. Acad. Sci. U.S.A. **99**:12386-12390.

188. **Ross, S. R., J. W. Schmidt, E. Katz, L. Cappelli, S. Hultine, P. Gimotty, and J. G. Monroe.** 2006. An immunoreceptor tyrosine activation motif in the mouse mammary tumor virus envelope protein plays a role in virus-induced mammary tumors. J. Virol. **80**: 9000-9008.

189. **Rumpf, S. and S. Jentsch.** 2006. Functional division of substrate processing cofactors of the ubiquitin-selective Cdc48 chaperone. Mol. Cell **21**: 261-269.

190. **Rutkevich, L. A., M. F. Cohen-Doyle, U. Brockmeier, and D. B. Williams.** 2010. Functional relationship between protein disulfide isomerase family members during the oxidative folding of human secretory proteins. Mol. Biol. Cell **21**: 3093-3105.

191. **Ruvolo, V. R., S. M. Kurinna, K. B. Karanjeet, T. F. Schuster, A. M. Martelli, J. A. McCubrey, and P. P. Ruvolo.** 2008. PKR regulates B56(alpha)-mediated BCL2 phosphatase activity in acute lymphoblastic leukemia-derived REH cells. J. Biol. Chem. **283**: 35474-35485.

192. **Saito, A., K. Ochiai, S. Kondo, K. Tsumagari, T. Murakami, D. R. Cavener, and K. Imaizumi**. 2011. Endoplasmic reticulum stress response mediated by the PERK-eIF2(alpha)-ATF4 pathway is involved in osteoblast differentiation induced by BMP2. J. Biol. Chem. **286**:4809-4818.

193. **Salmons, B., S. Moritz-Legrand, I. Garcha, and W. H. Günzburg**. 1989. Construction and characterization of a packaging cell line for MMTV-based conditional retroviral vectors. Biochem. Biophys. Res. Commun. **159**: 1191-1198.

194. **Samuel, C. E.** 2001. Antiviral actions of interferons. Clin. Microbiol. Rev. **14**: 778-809.

195. **Sarkar, N. H. and D. H. Moore.** 1974. Surface structure of mouse mammary tumor virus. Virology **61**:38-55.

196. **Sarkar, N. H., E. S. Whittington, J. Racevskis and S. L. Marcus.** 1978. Phosphoproteins of the murine mammary tumor virus. Virology **91**:407-422.

197. **Schlom, J., D. Colcher, S. Spiegelman, S. Gillespie and D. Gillespie.** 1973. Quantitation of RNA tumor viruses and virus like particles in human milk by hybridization to polyadenylic acid sequences. Science **179**:696-698.

198. **Schmitz, A., H. Herrgen, A. Winkeler, and V. Herzog.** 2000. Cholera toxin is exported from microsomes by the Sec61p complex. J. Cell Biol. **148**: 1203-1212.

199. **Schröder, M. and R. J. Kaufman**. 2005. The mammalian unfolded protein response. Annu. Rev. Biochem. **74**: 739-789.

200. **Schulman, H. M., P. Ponka, A. Wilczynska, Y. Gauthier, and G. Shyamala.** 1989. Transferrin receptor and ferritin levels during murine mammary gland development. Biochim. Biophys. Acta. **1010**:1-6.

201. **Sen, G. C. and S. N. Sarkar**. 2005. Transcriptional signaling by double-stranded RNA: role of TLR3. Cytokine Growth Factor Rev. **16**: 1-14.

202. **Shen, Y., and L. M. Hendershot.** 2007. Identification of ERdj3 and OBF-1/BOB-1/OCA-B as direct targets of XBP-1 during plasma cell differentiation. J. Immunol. **179**: 2969-2978.

203. **Shiu, R. P., J. Pouyssegur, and I. Pastan.** 1977. Glucose depletion accounts for the induction of two transformation-sensitive membrane proteinsin Rous sarcoma virus-transformed chick embryo fibroblasts. Proc. Natl. Acad. Sci. U.S.A. **74**: 3840-3844.

204. **Siednienko, J. and S. M. Miggin.** 2009. Expression analysis of the Toll-like receptors in human peripheral blood mononuclear cells. Methods Mol. Biol. **517**: 3-14.

205. **Smagulova, F., S. Maurel, Z. Morichaud, C. Devaux, M. Mougel and L. Houzet**. 2005. The highly structured encapsidation signal of MuLV RNA is involved in the nuclear export of its unspliced RNA. J. Mol. Biol. **354**: 1118-1128.

206. **Soldano, K. L., A. Jivan, C. V. Nicchitta, D. T. Gewirth.** 2003. Structure of the N-terminal domain of GRP94. Basis for ligand specificity and regulation. J. Biol. Chem. **278**: 48330-48338.

207. **Stamminger, T.** 2008. Interactions of human cytomegalovirus proteins with the nuclear transport machinery. Curr. Top. Microbiol. Immunol. **325**:167-185.

208. **Stutz, F. and E. Izaurralde.** 2003. The interplay of nuclear mRNP assembly, mRNA surveillance and export. Trends Cell Biol. **13**: 319-327.

209. **Suhasini, M. and T. R. Reddy.** 2009. Cellular proteins and HIV-1 Rev function. Curr. HIV Res. **7**: 91-100.

210. **Surjit, M., S. Jameel, and S. K. Lal.** 2007. Cytoplasmic localization of the ORF2 protein of hepatitis E virus is dependent on its ability to undergo retrotranslocation from the endoplasmic reticulum. J. Virol. **81**: 3339-3345.

211. **Susova, O. Y. and V. E. Gurtsevich.** 2003. The role of region pX in the life cycle of HTLV-1 and incarcinogenesis. Mol. Biol. **37**: 334-344.

212. **Suzuki, T., H. Park, M. A. Kwofie, and W. J. Lennarz.** 2001. Rad23 provides a link between the Png1 deglycosylating enzyme and the 26 S proteasome in yeast. J. Biol. Chem. **276**: 21601-21607.

213. **Tang, H. and F. Wong-Staal.** 2000. Specific interaction between RNA helicase A and Tap, two cellular proteins that bind to the constitutive transport element of type D retrovirus. J. Biol. Chem. **275**:32694-32700.

214. **Tang, H., Y. Xu, and F. Wong-Staal.** 1997. Identification and purification of cellular proteins that specifically interact with the RNA constitutive transport elements from retrovirus D. Virology **228**:333-339.

215. **Tange, T. Ø., A. Nott, and M. J. Moore.** 2004. The ever-increasing complexities of the exon junction complex. Curr. Opin. Cell Biol **16**: 279-284.

216. **Teixeira, D., U. Sheth, M. A. Valencia-Sanchez, M. Brengues, and R. Parker.** 2005. Processing bodies require RNA for assembly and contain nontranslating mRNAs. RNA **11**: 371-382.

217. **Threadgill, D. S., W. K. Steagall, M. T. Flaherty, F. J. Fuller, S. T. Perry, K. E. Rushlow, S. F. Le Grice and S. L. Payne.** 1993. Characterization of equine infectious anemia virus dUTPase: growth properties of a dUTPasedeficient mutant. J. Virol. **67**:2592-2600.

218. **Tourrière, H., K. Chebli, L. Zekri, B. Courselaud, J. M. Blanchard, E. Bertrand, and J. Tazi.** 2003. The RasGAP-associated endoribonuclease G3BP assembles stress granules. J. Cell Biol. **160**: 823-831.

219. **Toyoshima, H., M. Itoh, J. Inoue, M. Seiki, F. Takaku, and M. Yoshida.** 1990. Secondary structure of the human T-cell leukemia virus type 1 rex-responsive element is essential for rex regulation of RNA processing and transport of unspliced RNAs. J. Virol. **64**: 2825-2832.

220. **Tsai, B., C. Rodighiero, W. I. Lencer, and T. A. Rapoport.** 2001. Protein disulfide isomerase acts as a redox-dependent chaperone to unfold cholera toxin. Cell **104**: 937-948.

221. **Vattem, K. M. and R. C. Wek.** 2004. Reinitiation involving upstream ORFs regulates ATF4 mRNA translation in mammalian cells. Proc. Natl. Acad. Sci. U.S.A. **101**: 11269-11274.

222. **Vembar, S. S. and J. L. Brodsky.** 2008. One step at a time: endoplasmic reticulum-assocaited degradation. Nat. Rev. Mol. Cell Biol. **9**: 944-957.

223. **Von Heijne, G.** 1985. Signal sequences. The limits of variation. J. Mol. Biol. **184**: 99-105.

224. **Ward, A. M., D. Rekosh, and M. Hammarskjold**. 2009. Trafficking through the Rev/RRE pathway is essential for efficient inhibition of human immunodeficiency virus type 1 by an antisense RNA derived from the envelope gene. J. Virol. **83**: 940-952.

225. **Weihl, C. C., S. Dalal, A. Pestronk, and P. I. Hanson.** 2006. Inclusion body myopathy-associated mutations in p97/VCP impair endoplasmic reticulum-associated degradation. Hum. Mol. Genet. **15**: 189-199.

226. **Wek, R. C., H. –Y. Jiang, and T. G. Anthony.** 2006. Coping with stress: eIF2 kinases and translational control. Biochem. Soc. Trans. **34**: 7-11.

227. **Wernick, N. L. B., H. D. Luca, W. R. Kam, and W. I. Lencer.** 2010. N-terminal extension of the cholera toxin A1-chain causes rapid degradation after retrotranslocation form endoplasmic reticulum to cytosol. J. Biol. Chem. **285**: 6145-6152.

228. **White, J. P., A. M. Cardenas, W. E. Marissen, and R. E. Lloyd.** 2007. Inhibition of cytoplasmic mRNA stress granule formation by a viral proteinase. Cell Host Microbe. **2**: 295-305.

229. **Wiertz, E. J., T. R. Jones, L. Sun, M. Bogyo, H. J. Geuze, H. L. Ploegh.** 1996. The human cytomegalovirus US11 gene product dislocates MHC class I heavy chains from the endoplasmic reticulum to the cytosol. Cell **84**: 769-779.

230. **Wilczynska, A., C. Aigueperse, M. Kress, F. Dautry, and D. Weil.** 2005. The translational regulator CPEB1 provides a link between dcp1 bodies and stress granules. J. Cell. Sci. **118**: 981-992.

231. **Wolff, B., G. Cohen, J. Hauber, D. Meshcheryakova, and C. Rabeck.** 1995. Nucleocytoplasmic transport of the Rev protein of human immunodeficiency virus type 1 is dependent on the activation domain of the protein. Exp. Cell Res. **217**: 31-41.

232. **Wreschner, D. H., T. C. James, R. H. Silverman, and I. M. Kerr**. 1981. Ribosomal RNA cleavage, nuclease activation and 2-5A(ppp(A2'p)nA) in interferon-treated cells. Nucleic Acids Res. **9**: 1571-1581.

233. **Xu, L., T. J. Wrona and J. P. Dudley.** 1996. Exogenous mouse mammary tumor virus (MMTV) infection induces endogenous MMTV sag expression. Virology **215**:113-123.

234. **Xu, L., T. J. Wrona and J. P. Dudley.** 1997. Strain-specific expression of spliced MMTV RNAs containing the superantigen gene. Virology **236**: 54-65.

235. **Xu, Z., and B. R. Williams.** 2000. The B56alpha regulatory subunit of protein phosphatase 2A is a target for regulation by double-stranded RNA-dependent protein kinase PKR. Mol. Cell. Biol. **20**: 5285-5299.

236. **Yang, J. and B. R. Cullen.** 1999. Structural and functional anaylsis of the avian leukemia virus constitutive transport element. RNA. **5**: 1645-1655.

237. **Yang, J., H. P. Bogerd, S. Peng, H. Wiegand, R. Truant, and B. R. Cullen**. 1999. An ancient family of human endogenous retroviruses encoded a functional homolog of the HIV-1 Rev protein. Proc. Natl. Acad. Sci. U.S.A. **96**: 13404-13408.

238. **Ye, J., R. B. Rawson, R. Komuro, X. Chen, U. P. Davé, R. Prywes, M. S. Brown, and J. L. Goldstein.** 2000. ER stress induces cleavage of membrane-bound ATF6 by the same proteases that process SREBPs. Mol. Cell **6**: 1355-1364.

239. **Ye, Y., H. H. Meyer, and T. A. Rapoport.** 2003. Function of the p97-Ufd1-Npl4 complex in retrotranslocation from the ER to the cytosol: dual recognition of nonubiquitinated polypeptide segments and polyubiquitin chains. J. Cell Biol. **162**: 71-84.

240. **Ye, Y., Y. Shibata, C. Yun, D. Ron, and T. A. Rapoport.** 2004. A membrane protein complex mediates retro-translocation from the ER lumen into the cytosol. Nature **429**: 841-847.

241. **Ye, Y., Y. Shibata, M. Kikkert, S. van Voorden, E. Wiertz, and T. A. Rapoport.** 2005. Recruitment of the p97 ATPase and ubiquitin ligases to the site of

retrotranslocation at the endoplasmic reticulum membrane. Proc. Natl. Acad. Sci. U.S.A. **102**: 14132-14138.

242. **Yedavalli, V. S. R. K., C. Neuveut, Y. -H. Chi, L. Kleiman, and K. -T. Jeang.** 2004. Requirement of DDX3 DEAD box RNA helicase for HIV-1 Rev-RRE export function. Cell **119**:381-392.

243. **Yi, R., H. P. Bogerd, and B. R. Cullen.** 2002. Recruitment of the Crm1 nuclear export factor is sufficient to induce cytoplasmic expression of incompletely spliced human immunodeficiency virus mRNAs. J. Virol **76**:2036-2042.

244. **Yoneyama, M., M. Kikuchi, T. Natsukawa, N. Shinobu, T. Imaizumi, M. Miyagishi, K. Taira, S. Akira, and T. Fujita.** 2004. The RNA helicase RIG-I has an essential function in double-stranded RNA-induced innate antiviral responses. Nat. Immunol. **5**: 730-737.

245. **Yoshida, Y., T. Chiba, F. Tokunaga, H. Kawasaki, K. Iwai, T. Suzuki, Y. Ito, K. Matsuoka, M. Yoshida, K. Tanaka, and T. Tai.** 2002. E3 ubiquitin ligase that recognizes sugar chains. Nature **418**: 438-442.

246. **Yoshida, H., T. Matsui, A. Yamamoto, T. Okada, and K. Mori.** 2001. XBP1 mRNA is induced by ATF6 and spliced by IRE1 in response to ER stress to produce a highly active transcription factor. Cell **107**: 881-891.

247. **Yoshida, Y and K. Tanaka.** 2010. Lectin-like ERAD players in ER and cytosol. Biochim. Biophys. Acta. **1800**: 172-180.

248. **Zamanian-Daryoush, M., S. D. Der, and B. R. Williams.** 1999. Cell cycle regulation of the double stranded RNA activated protein kinase, PKR. Oncogene 18: 315-326.

249. **Zhu, Q., U. Maitra, D. Johnston, M. M. Lozano, and J. P. Dudley.** 2004. The Homeodomain Protein CDP Regulates Mammary-Specific Gene Transcription and Tumorigenesis. Mol. Cell. Biol. **24**:4810-4823.

Vita

Hyewon Byun was born in Busan, Korea on September 04, 1977, the daughter of Deoksu Byun and Malsun Lee. After completing her high school education in Busan, Korea in 1995, she entered the Department of Biological Sciences at the Korea Advanced Institute of Science and Technology (KAIST), Daejeon, Korea. In 1999, she graduated with a Bachelor of Science degree in Biological Sciences. She joined the Department of Biological Sciences at The KAIST, Daejeon, Korea in 1999 and got her Master of Science degree in 2001. The same year, she entered the Daeduk R&D Center of the SK Corporation in Daejeon, Korea, as a research scientist until 2004. She worked as a research scientist in the Laboratory of Cellular Signal Transduction of Ewha Woman University, Seoul, Korea until 2005. She entered the Institute for Cell and Molecular Biology Ph.D. program at The University of Texas at Austin and started her work in Dr. Jaquelin Dudley's lab in June, 2006.

Permanent address: 11624 Jollyville Rd. Apt 1223

Austin, TX 78759

This dissertation was typed by the author.